THE STUDY OF EXOSOMES AND MICROVESICLES SECRETED FROM BREAST CANCER CELL LINES

Ying Zheng

A Thesis Submitted for the Degree of PhD
at the
University of St Andrews

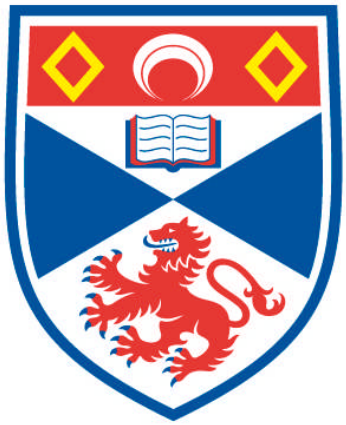

2012

The Study of Exosomes and Microvesicles Secreted From Breast Cancer Cell Lines

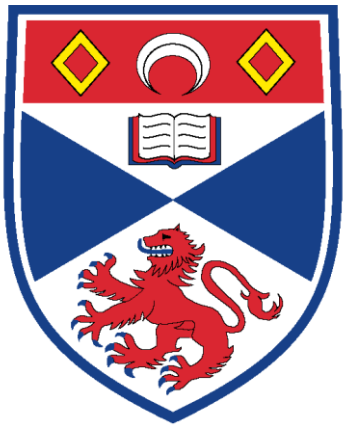

Ying Zheng

Thesis submitted in partial fulfillment of the requirements for the degree of Doctor of Philosophy

University of St Andrews

School of Medicine

October 2012

Declaration

I, Ying Zheng, hereby certify that this thesis, which is approximately 37, 000 words in length, has been written by me, that it is the record of work carried out by me and that it has not been submitted in any previous application for a higher degree.

I was admitted as a research student in October, 2009, and as a candidate for the degree of Ph.D in October 2009; the higher study for which this is a record was carried out in the University of St Andrews between 2009 and 2012.

Date: 2012 Signature of Candidate:

I hereby certify that the candidate has fulfilled the conditions of the Resolution and Regulations appropriate for the degree of Ph.D in the University of St Andrews and that the candidate is qualified to submit this thesis in application for that degree.

Date: 2012 Signature of Supervisor:

In submitting this thesis to the University of St Andrews I understand that I am giving permission for it to be made available for use in accordance with the regulations of the University Library for the time being in force, subject to any copyright vested in the work not being affected thereby. I also understand that the title and the abstract will be published, and that a copy of the work may be made and supplied to any bona fide library or research worker, that my thesis will be electronically accessible for personal or research use unless exempt by award of an embargo as requested below, and that the library has the right to migrate my thesis into new electronic forms as required to ensure continued access to the thesis. I have obtained any third-party copyright permissions that may be required in order to allow such access and migration, or have requested the appropriate embargo below.

The following is an agreed request by candidate and supervisor regarding the electronic publication of this thesis:

Embargo on both all of printed copy and electronic copy for the same fixed period of 3 years on the following ground:

publication would preclude future publication

Date 2012

Signature of Candidate: Signature of Supervisor:

Acknowledgements

First of all I would like to thank my supervisors Dr Simon Powis and Professor Andrew Riches. Without their guidance and support I would not have completed this project. Their wide knowledge and their logical way of thinking have been of great value for me. Their understanding, encouraging and personal guidance have provided a good basis for the present thesis. I would also like to thank Elaine for always being there to help and giving me untiring help during my difficult moments.

I would also like to thank Mary and everyone in the lab that has helped me along the way.

Special thanks go to my loving mum and aunty who travelled to the UK in turns to look after my son so that I could concentrate on completing my PhD, and thanks to my dad who has been giving me wise and invaluable advice.

I would like to thank my husband Tim for all his support during the last few years. Thanks for always believing in me and supporting me.

Finally, I would like to thank my dearest son Lee for all his kisses and hugs when I come home to him, which relieves all my stress.

Abstract

Exosomes are small secreted vesicles of endocytic origin with a size range of 50-150 nm. They are secreted by many cell types and display multiple biological functions including immune-activation, immune-suppression, antigen presentation, and the shuttling of mRNA and miRNA, as well as other cargo. We have characterised the exosomes secreted from two breast cancer cell lines, MDA-MB-231 and MCF7. Exosomes secreted from both cell lines display typical markers including ALIX, Tsg101, CD9 and CD63, and were capable of inducing apoptosis of the Jurkat T cell line, indicating the potential immune-suppressive function of such tumour-derived exosomes. To further investigate the biological potential of exosomes, we loaded purified exosomes with gene specific siRNAs using electroporation, and observed the targeted inhibition of both a known component of the exosome pathway, Rab27a, and also the arthritis associated gene ERAP1, demonstrating the potential novel use of exosomes as therapeutic gene delivery vectors. We have also shown that exosomes derived from MDA-MB-231 cells and the parental cells have different lipid composition, as analysed by lipidomics study.

Nanoparticle tracking analysis (NTA), which allows the rapid detection of size and concentration of nanoparticles within the size range 10 nm-1000 nm was tested for its ability to accurately measure size and concentration of exosomes and microvesicles under different conditions. NTA was capable of detecting apoptotic vesicles induced by Taxol and Curcumin treatment. Immunodepletion was used to determine the percentage of CD9 and CD63 positive vesicles. Our data suggest that NTA is a useful technique for measuring size and concentration of exosomes and microvesicles. We hypothesized that

NTA could assist in the screening of agents that interfere or promote exosome release. NTA was therefore used to detect increases in exosomes secretion induced by Tamoxifen and Thimerosal treatment, and to monitor the inhibition of exosome secretion from MDA-MB-231 breast cancer cells expressing inhibitory RNA targeted for Rab27a, a component of the exosome pathway. Increases in exosome release induced by Tamoxifen and Thimerosal was detected by NTA and a significant reduction in the release of exosomes by inhibition of Rab27a expression was also observed. Treatment with the known exosomal pathway inhibitor DMA also reduced exosome release, establishing the principle of NTA as a screening technique. We further compared the siRNA targeted cells for their ability to migrate, invade and form anchorage-independent colonies, which were all significantly reduced. Supplementation with MDA-MB-231 derived exosomes restored the ability to form colonies, suggesting exosomes may contribute to metastatic lesion formation. These data suggest that the exosomal pathway is a valid target to disrupt the behaviour of tumour cells and NTA can be used to monitor its activity.

List of figures and tables

Chapter I: Introduction

Chapter II: Materials and methods

Chapter III: Studying of Microvesicles using Flow Cytometry and Western Blot

Chapter IV: Nanoparticle tracking analysis with Nanosight.

Chapter V: Rab27a and its effects on exosome release

Abbreviations

AchR	Nicotinic acetylcholine receptor
ADAPT™	Adaptive dialysis-like affinity platform technology
AIDS	Acquired Immune Deficiency Syndrome
APS	Ammonium persulphate
APCs	Antigen presenting cells
ARTS1/ERAP1	Aminopeptidase reugulator of TNFR1 shedding/endoplasmic reticulum aminopeptidase1
BACE1	Beta-site APP cleaving enzyme 1
BAT3	HLA-B-associated transcript 3
BMDCs	Bone marrow-derived cells
BRCA1 or *2*	Breast cancer gene 1 or 2
BSA	Bovine serum albumin
cDNA	Complementary DNA
CEA	Carcinoembryonic antigen
CFSE	Carboxyfluorescein succinimidyl ester
CTLs	Cytotoxic T lymphocytes
DAPI	4’6-diamidino-2-phenylindole
DCs	Dendritic cells
DMA	Dimethyl amiloride
DMEM	Dulbecco’s Modified Eagle’s medium
DMSO	Dimethyl sulfoxide
DNA	Deoxyribonucleic acid
dNTP	Deoxynucleoside triphosphates
EBV	Epstein-Barr virus
ECL	Enhanced chemi-luminescence
E. coli	*Eschericia coli*
EDTA	Ethylenediaminetetraacetic acid
EEA1	Eukaryotic elongation factor
EGFR	Epidermal growth factor receptor
EIF4	Eukaryotic initiation factors
ER	Estrogen receptor
ESCRT	Endosomal sorting complex required for transport
FCS	Foetal calf serum
FITC	Fluorescein isothiocyanate
GAPDH	Glyceraldehyde 3-phosphate dehydrogenase
GPI	Glycosylphosphatidylinositol-anchored proteins
GM-CSF	Granulocyte-macrophages colony-stimulating factor
GPLs	Glycopeptidolipids
HER2	Human Epidermal Growth Factor Receptor 2
HCl	Hydrogen chloride
HCV	Hepatitis C virus
HIV	Human immunodeficiency virus
HRT	Hormone replacement therapy
HMGA2	High-mobility group AT-hook 2

ICAM	Intercellular adhesion molecule 1
IFN	Interferon
Ig	Immunoglobulin
IGF- II	Insulin-like growth factor-II
IL	Interleukin
KCl	Potassium chloride
LAMP2	Lysosomal-associated membrane protein 2
LB	Luria broth
LBPA	Lysobisphosphatidic acid
LFA-1	Leukocyte function associated antigen-1
LTC4	Leukotriene C4
MAGE	Melanoma-associated antigen
MAPK	Mitogen-activated protein kinase
MART1	Melanoma antigen recognized by T-cells 1
MDSC	Myeloid-derived suppressor cells
MFGE8	Milk fat globule-EGF factor 8 protein
MHC	Major Histocompatibility complex
MIC	MHC class I polypeptide-related sequence
MMP9	Matrix metallopeptidase 9
mRNA	Messenger RNA
MVB	Multivesicular bodies
MVE	Multivesicular endosomes
myD88	Myeloid differentiation primary response gene 88
Nef	Negative factor
NEM	N-ethylmaleimide
NCR3	Natural cytotoxicity receptor
NK cells	Natural killer cells
NP40	Nonidet P-40
NRSB	Non-reducing sample buffer
NaCl	Sodium chloride
NTA	Nanoparticle Tracking Analysis
OVA	Ovalbumin
PBS	Phosphate-buffered saline
PBST	Phosphate-buffered saline and Tween 20
PC	Phosphatidylcholine
PCR	Polymerase chain reaction
PE	Phosphatidylethanolamine
PEI	Polyethylenimine
PG	Phosphatidylglycerol
PGE2	Prostaglandin E2
PI	Phosphatidylinositol
PI	Propidium iodide
PMSF	Phenylmethylsulfonyl fluoride
PR	Progestorone receptor
PrPc	Cellular prion protein
PrPscr	Prion protein scrapie
PS	Phosphatidylserine
PSG	Penicillin-Streptomycin-Glutamine

RSB	Reducing sample buffer
RT-PCR	Reverse transcriptase-polymerase chain reaction
RVG	Rabies Virus Glycoprotein
TGF	Transforming growth factor
RNA	Ribonucleic acid
ROS	Reactive oxygen species
rpm	Rotations per minute
RPMI-1640	Roswell Park Memorial Institute medium
RT	Reverse transcriptase
SC1	Scaffold protein 1
SCID	Severe combined immunodeficiency
SDS	Sodium dodecyl sulphate
SDS-PAGE	SDS-polyacrylamide gel electrophoresis
shRNA	Short hairpin RNA
siRNA	Short inhibitory RNA
SM	Sphingomyelin
Stat3	Signal transducer and activator of transcription 3
TAE	Tris acetate EDTA
TEMED	N,N,N’,N’-tetramethylethylenediamine
Tim	T cell Ig mucin
TLR2	Toll-like receptor 2
TNF	Tumor necrosis factor
TNFR	Tumor necrosis factor receptor
TRAIL	Tumour necrosis factor-related apoptosis-inducing ligand
TSAP6	Tumour suppressor-activated pathway 6
ULBP	UL-16 binding protein

Chapter I. Introduction

One basic way of cell communication is by releasing extracellular molecules such as nucleotides, lipids and proteins into the environment, where these molecules will then bind to receptors on surrounding cells, leading to intracellular signalling and modification of the recipient cell (Bobrie et al., 2011). However, cells also contain and secrete more complicated structures in the form of membrane vesicles, with the cell type and compartment they are derived from determining their biological functions. These vesicles can contain numerous proteins, lipids and nucleic acids, and the way they interact and affect the recipient cell is complex. Exosomes, among the several different types of secreted vesicles, are probably the most studied. Exosomes are formed by inward budding of endosomal compartments called multivesicular bodies (MVBs). Although they have been known for decades, they were initially characterised as cell debris and signs of cell death. They were first described by the two research groups of Stahl and Johnstone, who reported that instead of fusing with lysosomes and being degraded, multivesicular endosomes in reticulocytes could fuse with the plasma membrane and release the contents *in vitro* (Harding et al., 1983; Pan et al., 1985). Johnstones's group used electron microscopy to demonstrate that multivesicular bodies fused with the plasma membrane and released their contents including '50 nm bodies' (Pan et al., 1985). The term 'Exosome' was proposed in 1987 by the same group to describe these vesicles (Johnstone et al., 1987). Nevertheless, this area did not receive much attention for the next 10 years until Raposo et al. reported that exosomes secreted from Epstein-Barr virus (EBV)-transformed B lymphocytes bear functional MHC molecules and could present MHC-antigenic peptide complexes to specific T cells

(Raposo et al., 1996). Two years later, it was discovered that dendritic cells also secrete exosomes bearing functional MHC-peptide complexes, which could induce antitumour immune responses in mice *in vivo* (Zitvogel et al., 1998).

Studies then started to show that exosomes secreted from one cell could be captured by another cell to allow information to be transferred to the recipient. Such information could include antigens to increase the number of antigen-presenting cells and improve immune responses (Thery et al., 2002). The discovery that exosomes can deliver mRNA and microRNA has sparked interest even more (Valadi et al., 2007), with evidence being presented that mRNA contained in exosomes can be translated into functional protein, indicating that exosomes can directly transfer genetic information that may modify recipient cell behaviour. Studies have also now shown that exosomes can act as delivery vectors for siRNA. Specially engineered exosomes successfully carried siRNA into the brain and knocked down a therapeutic target gene for Alzheimer's disease (Alvarez-Erviti et al., 2011), and plasma exosomes have been shown to be able to transfer siRNA into monocytes and lymphocytes (Wahlgren et al., 2012).

Types of membrane vesicles

Microvesicles including exosomes.

Microvesicle terminology often includes exosomes and shedding vesicles (cell surface membrane-derived particles). Exosomes are characterised as membrane vesicles with a size range of 50-150 nm. They are from endosomal origin and are secreted by most cell

types, such as haematopoietic, lymphocytes, dendritic cells, epithelial (van Niel et al., 2001), reticulocytes (Johnstone et al., 1987) and many tumour cells. Exosomes are limited by a lipid bilayer and are formed through inward budding of endosomal membranes, giving rise to intracellular multivesicular bodies (MVB) or multivesicular endosomes (MVE) that either fuse with the plasma membrane, releasing the exosomes to the extracellular environment, or are degraded by fusion with lysosomes. After exosomes reach their destinations, they can enter a target cell either by entering the cell's endocytic pathway, through ligand-receptor binding, or by fusing with the target cell's plasma membrane and releasing the contents into the cytoplasm of the target cell directly.

Figure 1.1 shows how exosomes are formed, possible molecules that are associated with the formation and secretion of exosomes, and how viruses hijack the pathway. It has been reported that ESCRT (endosomal sorting complex required for transport) machinery is required for the formation of internal vesicles of multivesicular bodies (MVB)/late endosomes. In 2001, two members of the ESCRT family, Alix and Tsg101, were shown to be involved in exosomes secretion in dendritic cells (Thery et al., 2001). It has been suggested that ESCRT-I and ESCRT-II together contribute to the budding processes and that ESCRT-III could be responsible for cleaving the buds to form intraluminal vesicles (Wollert and Hurley, 2010). A very recent study showed that syndecans (single transmembrane domain proteins, also known as SDC1-4) have a short, evolutionarily conserved cytoplasmic domain, which binds cytosolic factors such as the small PDZ scaffolding protein syntenin (also known as SDCBP) (Grootjans et al., 1997). The interaction of the syndecans with syntenin, and through syntenin with ALIX has

been suggested to support the biogenesis of intraluminal vesicles and exosomes, and the sorting of signalling cargo to these vesicles (Baietti et al., 2012).

It has been hypothesized that there are two distinct pathways for lysosome degradation and exosome secretion. The first pathway was found to be active in immature dendritic cells and sorted MHC II to intraluminal vesicles for degradation by lysosomes. The second pathway sorted MHC II together with a tetraspanin CD9 to intraluminal vesicles which were then secreted as exosomes (Buschow et al., 2009). An alternative pathway for sorting cargo into MVEs has been reported in oligodendroglial cells, suggesting that secretion of the myelin proteolipid protein (PLP) in association with exosomes was independent of the ESCRT machinery, but required the sphingolipid ceramide. Purified exosomes were enriched in ceramide, and inhibition of neutral sphingomyelinases (which help synthesise ceramide), reduced the release of exosomes (Trajkovic et al., 2008). Another lipid, lysobisphosphatidic acid (LBPA), has been shown to allow formation of intraluminal vesicles of MVBs for degradation by lysosomes, but it is unknown whether it also plays a role in exosome formation (Matsuo et al., 2004). In conclusion, these findings suggest that by using different intracellular machinery, subpopulations of MVBs can be formed which may also lead to different types of exosomes (Bobrie et al., 2011).

MVBs need to fuse with the plasma membrane to release exosomes. Small GTPases of the Rab family are classical proteins responsible for intracellular trafficking. Different Rab proteins have been reported to be responsible for exosome secretion in different cell types. Rab11 promotes docking and fusion of MVBs with the plasma membrane in

a calcium-dependent manner in human erythroleukemic K562 cells (Savina et al., 2005). In oligodendroglial cells, Rab35 is involved in secretion of exosomes that are enriched with PLP (Hsu et al., 2010). Rab27a and Rab27b play important roles in spontaneous secretion of MHC class II-containing exosomes secreted by HeLa cells (Ostrowski et al., 2010). Furthermore, fusion of MVB with plasma membrane may involve some specific SNARE proteins, although it has not been confirmed which SNARE proteins are responsible for this process.

Studies have shown monensin (a Na+/H+ exchanger) treatment results in the accumulation of intracellular Ca^{2+} as well as increased exosome release, indicating that exosomes secretion can be affected by changes in intracellular Ca^{2+} levels (Savina et al., 2003). Merendino et al supported the importance of intracellular Ca^{2+} levels by demonstrating that treatment with dimethyl amiloride (DMA, a blocker of Na+/H+ exchange) inhibited exosome secretion (Merendino et al., 2010). In addition, nutrient starvation, stress, rapamycin and hormone treatment induce autophagy, which then inhibit exosome release by redirecting the MVBs towards autophagic pathway and lysosome degradation. In this condition, fusion of MVBs with autophagosomes forms hybrid organelle-amphisomes and makes MVBs appear enlarged (Fader and Colombo, 2009; Fader et al., 2008).

In addition, intracellular and intercellular pH has also been shown to affect exosome release. When the microenvironment pH is low, exosome secretion and uptake increases. Of particular note the core mass of many tumours usually has low pH, caused by limited vascularization, nutrient and oxygen supplies. It has also been demonstrated

that p53 regulates the production of exosomes by regulating tumour suppressor-activated pathway 6 (TSAP6) under stressed conditions (Yu et al., 2006). This supports the importance of both exosomes and tumour pH as future anti-cancer strategies (Parolini et al., 2009).

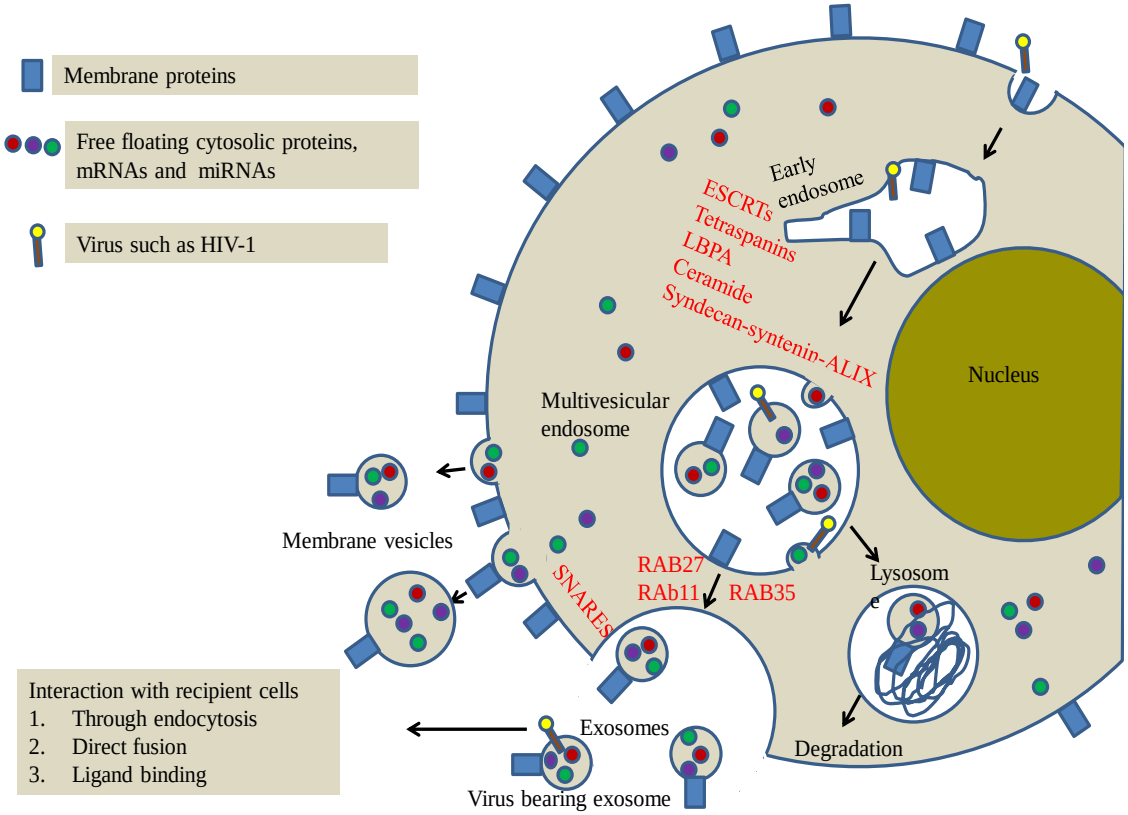

Figure 1.1: Exosome biogenesis and secretion and molecules involved, and the 'Trojan horse hypothesis'. Exosomes are formed by inward budding from the limiting membrane of the endosomes to form multivesicular endosomes/bodies (ESCRTs, tetraspaninins, LBPA, ceramide and Syndecan/syntenin might be involved in this process). These multivesicular endosomes/bodies can either be degraded by lysosomes or fuse with the plasma membrane and release the exosomes into the extracellular environment. The targeting of the MVE towards the plasma membrane may be regulated by some Rab family proteins such as Rab27, Rab11 and Rab35. Finally, the fusion of the MVEs with the plasma membrane may require SNARE proteins.

Shedding vesicles/membrane vesicles

Shedding vesicles bud directly from the plasma membrane and are then secreted directly into the extracellular environment. They can be of similar sizes to exosomes (50-150 nm) or can be larger than exosomes (over 150 nm and could be up to 1 μm) (Figure 1.1). Since they bud from the plasma membrane, it was expected that their composition would be comparable with the membrane composition of the originating cells. However, the targeting of proteins into shedding vesicles is selective and specific proteins are included or excluded. Increasing intracellular Ca^{2+} has been shown to increase the release of membrane vesicles (Salzer et al., 2002). It is unknown how the targeting is regulated and their function on distant tissue is not clear. Ectosomes are shedding vesicles of neutrophils and monocytes (Stein and Luzio, 1991). Microparticles are referred to as shedding vesicles from platelets and monocytes (Cocucci et al., 2009). To add to the confusion, sometimes these names are used interchangeably by different groups, and the literature on all such vesicles must be read with care.

Vesicles released from apoptotic cells

Dying and/or apoptotic cells will also release membrane vesicles that are different from vesicles released from healthy cells. They vary in size between 50-500 nm and are relatively heterogeneous. They contain very abundant histones (Thery et al., 2001), float at a higher sucrose density (1.24-1.28 g/ml) compared to exosomes and do not have the characteristic cup shape that exosomes have, when visualised by electron microscopy.

Apoptotic vesicles have been reported to have immune-activating functions. One study suggested that apoptotic vesicles from mycobacteria-infected macrophages contained TB-derived antigens, and uptake of these apoptotic vesicles by dendritic cells and the subsequent migration of these cells to the lymph nodes stimulated $CD8^+$ T cells in lymphatic tissues, indicating a possible role of apoptotic vesicles derived from dying infected cells in immunological regulation (Winau et al., 2006).

Exosome-like vesicles

There might be other types of microvesicles, some of which are exosome-like. Some of the differences between exosomes and these exosomes-like vesicles include their lipid composition, with lipid rafts present on exosomes but not on exosome-like vesicles; and their main protein markers (tetraspanins, Alix and Tsg101 for exosomes and TNFR1 for exosome-like vesicles (Thery et al., 2006).

Overall, the classification of the multiple vesicles secreted by cells has not been officially identified and a standard terminology on secreted vesicles should ideally be achieved. Most of the studies published have focused on exosomes, so not much is known about the function and composition of other types of vesicles. With more and more groups starting to study other types of vesicles, their function should become more clearly defined in the near future.

Composition of exosomes

The composition of exosomes is variable depending on what cells they were secreted from. Different techniques including immunoblotting, fluorescence activated cell sorting, mass spectrometry, electron microscopy and atomic force microscopy have been used to study the contents of exosomes.

The first "proteomic" analyses of the protein composition of exosomes were performed in late 1990s using mass spectrometry and the exosomes used were secreted from dendritic cells (Thery et al., 2001). More recently, an academic website that gathers all the analysis of exosomal protein, RNA and lipid content has been established to encourage participation of the scientific community (http://exocarta.ludwig.edu.au).

Protein composition

Some proteins are common to exosomes from almost any cell type, but also some proteins are cell type specific. One class of cytosolic proteins commonly seen in exosomes include the Rabs, the largest family of small GTPases, which regulate exosome docking and membrane fusion. A search for Rab proteins in Exocarta revealed more than 40 Rab proteins identified in different exosome studies. Exosomes are also rich in annexin, which play a role in membrane trafficking and fusion. Exosomes contain abundant transmembrane tetraspanins (CD9, CD63, CD81 and CD82) and heat shock proteins (HSP60, HSP70 and HSP90) which can facilitate peptide loading onto major histocompatibility complex (MHC) I and II (Gastpar et al., 2005; Graner et al.,

2009). Other transmembrane molecules include MHC class I and II molecules, integrins (various alpha and beta chains), surface peptidases (CD13 and CD26, and GPI-anchored molecules (CD55 and CD59), etc.

In their lumen, exosomes contain molecules associated with the internal side of membranes (clathrin, annexins, GTPases of the Rab family proteins), and also various cytosolic proteins: ESCRT proteins (Tsg 101, Alix) cytoskeleton proteins (moesin,tubulin, actin and actin-binding molecules), signal transduction molecules (protein kinases, heterodimeric G proteins, 14-3-3 proteins and syntenin), chaperone molecules (Hsc70 and Hsp90 and cyclophilin A), metabolic enzymes (GAPDH, enolase, pyruvate and phosphoglycerate kinases and aldolase), and translation initiation or elongation factors (EIF4 and EEF1) (Chaput and Thery, 2011).

Some proteins are cell type specific, including MHC class II, co-stimulatory proteins (CD80 and CD86) on antigen presenting cell-derived exosomes, integrin CD41a and Von Willebrand factor on platelet-derived exosomes, perforin and granzyme on cytotoxic T-lymphocyte derived exosomes, MFGE8/ lactadherin on immature dendritic cells derived exosomes (Veron et al., 2005), B cell receptor on B cell derived exosomes and CD11c (a specific marker for DCs) on DC-derived exosomes, etc (Janiszewski et al., 2004; Muntasell et al., 2007; Wolfers et al., 2001).

Lipid Composition

In addition to proteins, exosomes also obviously contain lipids as part of their membrane structure. Erythrocyte-secreted exosomes display similar lipid composition

to the plasma membrane of the erythrocytes (Vidal et al., 1989), whereas exosomes secreted from other cells such as dendritic cells, B cells and mast cells are enriched in sphingomyelin in comparison with the cells they were secreted from (Laulagnier et al., 2004; Subra et al., 2007; Wubbolts et al., 2003). B cells secreted exosomes are also enriched in cholesterol. LBPA, which has been identified for its involvement in the formation of internal vesicles in multivesicular endosomes, was unexpectedly found to be very low or undetectable in B cell and mastocyte exosomes (Buschow et al., 2009; Subra et al., 2007). Ceramide, a lipid which has been proposed to also be involved in the formation of the internal vesicles in MVEs that are finally released as exosomes, was found to be enriched in oligodendroglial exosomes (Trajkovic et al., 2008)

RNA composition

Exosomes have been reported to contain very abundant mRNA, miRNA and also non-coding RNA. Some studies have reported that certain RNAs are present at significantly different levels compare to the RNA content of the originating cell (Mittelbrunn et al., 2011; Skog et al., 2008; Zomer et al., 2010). There are also contradictory results which suggest that exosomal RNA contents were similar to their parental cells and exosomes could be potentially used as diagnostic markers (Rabinowits et al., 2009; Taylor and Gercel-Taylor, 2008). Thus, it still need to be determined if any RNA molecules can serve as reliable generic exosomal markers.

Interaction of exosomes with recipient cells.

How individual exosomes interact with recipient cell is still relatively unknown. It is possible exosomes bind to specific receptors at the cell surface, or enters the cell via endocytosis or fuse with plasma membrane (Figure 1.3).

1. ***Entry through Endocytosis***

The most effective way of exosome uptake is phagocytosis. Tian et al. showed that after exosomes from PC12 cells (a rat pheochromocytoma) were internalised through endocytosis they were actively transported by the cytoskeleton to the perinuclear region (Tian et al., 2010)

Escrevente et al. showed that SKOV3, an ovarian carcinoma cell line, used an energy dependent mechanism to internalize exosomes secreted from the same cell line. In their study, internalization of exosomes was inhibited when they treated the cells or exosomes with proteinase K indicating the requirement of proteins on exosomes and on cells. They suggested clathrin-dependent endocytosis to be implicated in the uptake of exosomes by SKOV3 cells but also that other endocytic pathways may be involved (Escrevente et al., 2011). Feng et al. have reported that phagocytic cells have a greater uptake of exosomes than nonphagocytic cells (Feng et al., 2010)

2. Entry through ligand-receptor binding

Second, exosomes could enter the recipient cell through ligand-receptor binding. The exosomal membrane contains phospholipids (e.g. phosphatidylserine) and proteins on their surface that can be captured by phosphatidylserine receptors such as the T cell immunoglobulin domain and mucin domain protein (TIM). Miyanishi et al. showed that TIM1 and TIM4 are phosphatidylserine-binding molecules and are expressed on the surface of activated lymphocytes or phagocytes, respectively. TIM1 and TIM4 also been shown to mediate exosomes uptake (Miyanishi et al., 2007).

It has been demonstrated that intercellular adhesion molecule 1 (ICAM1) is present on exosomes secreted from mature dendritic cells and can bind to leukocyte function associated antigen-1 (LFA-1, a ligand for ICAM1) expressed on the surface of dendritic cells (Segura et al., 2007) and activated T cells (Nolte-'t Hoen et al., 2009). Retroviruses such as HIV can hijack this mechanism to favour spreading. HIV-1 viruses budded from infected T cells bear host-derived ICAM1 and can interact with other T cells that express IFA1, thus helping with the spreading of the viruses (Fortin et al., 1998).

Furthermore, milk fat globule epidermal growth factor 8 protein (MFGE8) could play a role in the intake of exosomes into a neighbouring cell. MFGE8 has two domains: one binds to αvβ3 and αvβ5 integrins (expressed by human DCs and macrophages) and the other domain binds to phosphatidylserine-containing membranes (including exosomes). It has been shown to act as a bridge between apoptotic cells that express aminophospholipids and phagocytes that express integrins (Hanayama et al., 2002).

MFGE8 could bind to phosphatidylserine exposed on the surface of apoptotic cells through one domain, and the other domain of MFGE8 that is exposed on the surface of MFGE8-bearing apoptotic cells could bind to αvβ3 and αvβ5 integrins expressed on macrophages and promote the phagocytosis of these apoptotic cells by macrophages. It is possible that MFGE8 can also play a role in the capture of membrane vesicles by phagocytes that express αvβ3 or αvβ5 integrins (Andersen et al., 1997; Veron et al., 2005).

3. Entry through direct fusion

Exosomes can directly fuse with the plasma membrane and release the exosomal content into the cell cytoplasm. Parolini et al provided evidence that exosomes could fuse with the plasma membrane by showing that exosomes go across a lipid-dependent fusion process with plasma membrane, and this fusion is more efficient in an acidic microenvironment. (Parolini et al., 2009), suggesting that fusion of exosomes to cells is more frequent in the acidic environment found in a tumour compared to that in the surrounding normal tissue.

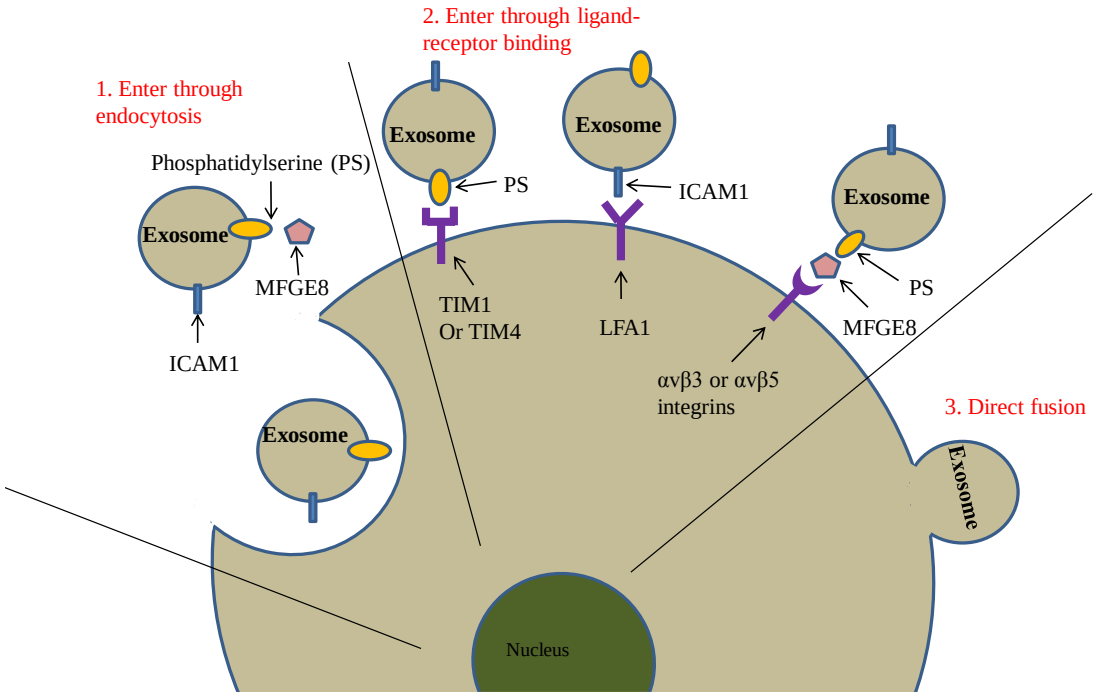

Figure 1.2: Three possible pathways exosomes utilise for communication with recipient cells. Exosomes may interact with neighbour cells via three different ways: 1. Exosomes may enter cell via endocytosis. 2. Certain phospholipids or proteins may bind to receptors on neighbour cells. 3. Direct fusion of exosomes with the plasma membrane of the target cell.

Function of exosomes

Exosomes can cause immune-activating responses *in vitro*

Exosomes secreted from antigen-presenting cells contain a range of immunostimulatory molecules that activate T cells, which suggest that they may have an important role in propagation of immune responses.

Dendritic cells-derived exosomes express high levels of functional MHC class-I and class-II peptide complexes together with CD86 molecules and it has been suggested that these exosomes may substitute for DCs to elicit MHC-class-I and class-II restricted T-cell responses and tumour rejection.

Mycobacteria-infected macrophages release exosomes containing glycopeptidolipids (GPLs) leading to the transfer of GPLs from infected to uninfected macrophages and can stimulate a proinflammatory response in resting macrophages (Bhatnagar and Schorey, 2007). Platelet-derived microparticles (PMPs) that are present at high concentration in the inflammatory areas could chemoattract immune cells such as NK cells, T and B lymphocytes as well as proliferation, survival and chemotaxis of haematopoietic cells (Baj-Krzyworzeka et al., 2002). Consistent with these results, it has also been reported that platelet-derived membrane vesicles may play an important role in inducing immune responses by acting as a vector for the CD154/CD40L (a ligand for CD40) which plays the role of a co-stimulatory molecule and is critical to the initiation and propagation of the adaptive immune response. It is mainly expressed on

activated T cells and also platelets. The delivery of CD154 by these microvesicles makes it possible for it to encounter the cells necessary to produce the antigen-specific response (Sprague et al., 2008). Fibroblasts obtained from the synovial fluid of patients with rheumatoid arthritis secrete exosomes that contain an active membrane-bound form of TNF, which binds to T cells and makes them resistant to activation induced cell death, thus potentially contributing to the development of this disease (Zhang et al., 2006)

Ligands that can bind to NK cell activating receptors have been shown to be present on exosomes and can activate NK cells *in vitro*. For example, HLA-B-associated transcript 3 (BAT3) has been identified as a ligand for natural cytotoxicity receptor 3 (NCR3)/NKp30 and has been shown to be present on exosomes secreted from heat-shocked dendritic cells and promote NK cell activation *in vitro* (Simhadri et al., 2008). Dendritic cell-derived exosomes from melanoma patients express NKG2D ligands (activatory signals for Natural Killer cells) MHC class I polypeptide-related sequence A (MICA) and MICB on their surface, that bind to NKG2D that are present on NK cells and lead to NK cell activation. IL-2 and trans-presentation of IL-15 and IL-15 receptor α chain (IL-15Rα) is required for NK cell survival, homeostasis and proliferation. The ability of exosomes derived from dendritic cells to promote NK cell proliferation was due to the simultaneous presence of IL-15Rα on these exosomes, which could bind to exogenous IL-15 and allow IFNγ secretion by NK cells thus induce NK cell proliferation. On the other hand, another ligand for NKG2D, ul16 binding protein 1 (ULBP1), was shown to be present on exosomes secreted from dendritic cells of normal volunteers (Viaud et al., 2009)

Tumour-derived exosomes can also have immune-activating properties. This mainly happens when the tumour cells are under stress conditions. The stress-inducible HSP 70 family is considered to function as an endogenous danger signal that can increase the immunogenicity of tumours and induce cytotoxic T lymphocytes (CTL) responses. They are a key part of the cell's mechanism for protein folding, and they help to protect cells from stress.

Under stress conditions, NKG2D ligands are up-regulated on tumour exosomes. Hsp70 also activates mouse NK cells that recognize stress-inducible NKG2D ligands on tumour cells. In the severe combined immunodeficiency (SCID) mice with Hsp70-overexpressing tumours, NK cells were activated so that they killed *ex vivo* tumour cells that expressed NKG2D ligands (Elsner et al., 2007). Tumour-derived microvesicles can activate monocytes to produce pro-inflammatory cytokines and Reactive oxygen intermediates (ROI) and result in enhanced cytotoxic/cytostatic potential of these monocytes both *in vitro* and *in vivo* (Baj-Krzyworzeka et al., 2007). Pancreatic tumour cells-derived exosomes have been shown to decrease tumour cell proliferation and induce apoptosis (Ristorcelli et al., 2008). However, most studies believe tumour-derived exosomes can prevent anti-tumour immune responses and promote tumour cell metastasize. This will be discussed in more details in the next section.

Antigen presentation by Exosomes

A study in 1996 showed that Epstein-Barr virus-transformed B lymphocytes, were able to secrete exosomes which exhibit abundant MHC class II molecules at their surface,

and can present antigenic peptides to T cells, suggesting their possible role in adaptive immune responses (Raposo et al., 1996). Two years later, it was reported that dendritic cells secrete exosomes that express functional MHC class I and class II, and T-cell costimulatory molecules, which eradicated or suppressed growth of established murine tumours in a T-lymphocyte-dependent manner in mice *in vivo* (Zitvogel et al., 1998).

Exosomes can present antigens directly or indirectly. Secreted membrane vesicles secreted by virtually any cell type bear MHC class I molecules that could potentially induce direct $CD8^+$ T cell activation. APC-derived exosomes also bear abundant MHC class II molecules, which are functional and can be recognised by $CD4^+$ T cells as allogeneic antigens (Peche et al., 2003). It has been reported that exosomes derived from dendritic cells induced activation of $CD8^+$ cytotoxic T lymphocytes clones, either alone (Admyre et al., 2006; Luketic et al., 2007), or with dendritic cells that express allogeneic MHC class I. These studies indicate that these exosomes bear functional preformed MHC-peptide complexes. Mature dendritic cells secrete exosomes that can induce T-cell activation more efficiently *in vitro* than exosomes secreted from immature dendritic cells (Admyre et al., 2006; Segura et al., 2007). In addition, Segura et al also reported only mature exosomes trigger effector T-cell responses *in vivo*, suggesting that exosomes derived from mature dendritic cells possess co-stimulating molecules that can help co-stimulate the T-cells (Admyre et al., 2006).

Exosomes secreted by peptide-pulsed DCs can transfer MHC II-peptide complexes to DCs that lack MHC class II to enable antigen-specific CD4 T cell activation (Segura et al., 2005; Thery et al., 2002). Exosomes bearing specific MHC II-peptide complexes

can activate primed CD4 T cells by themselves (Muntasell et al., 2007), but need to be captured by recipient DC to activate naive CD4 T cells (Muntasell et al., 2007; Segura et al., 2005; Thery et al., 2002). It was suggested that his difference may be due to the activated conformation of lymphocyte function-associated antigen (LFA-1) integrins that are only present at the surface of primed T lymphocytes, but not on naïve T lymphocytes, which allows efficient binding of exosomes that express intercellular adhesion Molecule-1 (ICAM1) to these primed T lymphocytes (Segura et al., 2007). Similar to $CD8^+$ T cells, exosomes derived from mature dentritic cells induce more effective $CD4^+$ T cell activation *in vitro* than exosomes derived from immature dendritic cells. Recipient DCs may also internalise and process MHC molecules from exosomes of allogeneic DCs as a source of peptides to load on their own MHC molecules (Montecalvo et al., 2008). Moreover, Mallegol et al reported that in intestinal epithelial cells that express MHC class II, peptides instead of MHC-peptide complexes, seem to be the major antigenic material transferred from exosomes to recipient DCs, and the transfer of antigenic peptides through exosomes to DCs is expressively more efficient than delivery of free peptide to DCs (Mallegol et al., 2007). Exosomes derived from endothelial cells infected with cytomegalovirus can transfer virus-derived antigen to DCs and thus indirectly activated $CD4^+$ T cells. Moreover, exosomes derived from macrophages infected with *Mycobacterium tuberculosis* or *Mycobacterium bovis*, which reside in endosomal compartments, contain pathogen-derived antigens and stimulate $CD4^+$ and $CD8^+$ T cells *in vitro* as well as induce naive T cell activation *in vivo* (Giri and Schorey, 2008).

Exosomes purified from cultured tumour cell lines (Wolfers et al., 2001) or from ascites

of patients (Caby et al., 2005) with tumours contain tumour antigens and can induce the activation of antigen-specific T cells *in vitro* only in the presence of recipient dendritic cells. It is possible this could be due to lack of co-stimulating molecules on tumours and tumour-derived exosomes (Thery et al., 2009). Antigens that are commonly present in tumour-derived exosomes are either cell surface transmembrane proteins such as human epidermal growth factor receptor 2 (EGFR2) and carcinoembryonic antigen (CEA), which are found in different types of carcinomas, or endosomal proteins from the endosome compartments of the donor cell (such as melanoma antigen recognized by T-cells 1 (MART 1) and glycoprotein 100 (gp100)).

A. Immune-activating function by professional-APC cells-derived exosomes

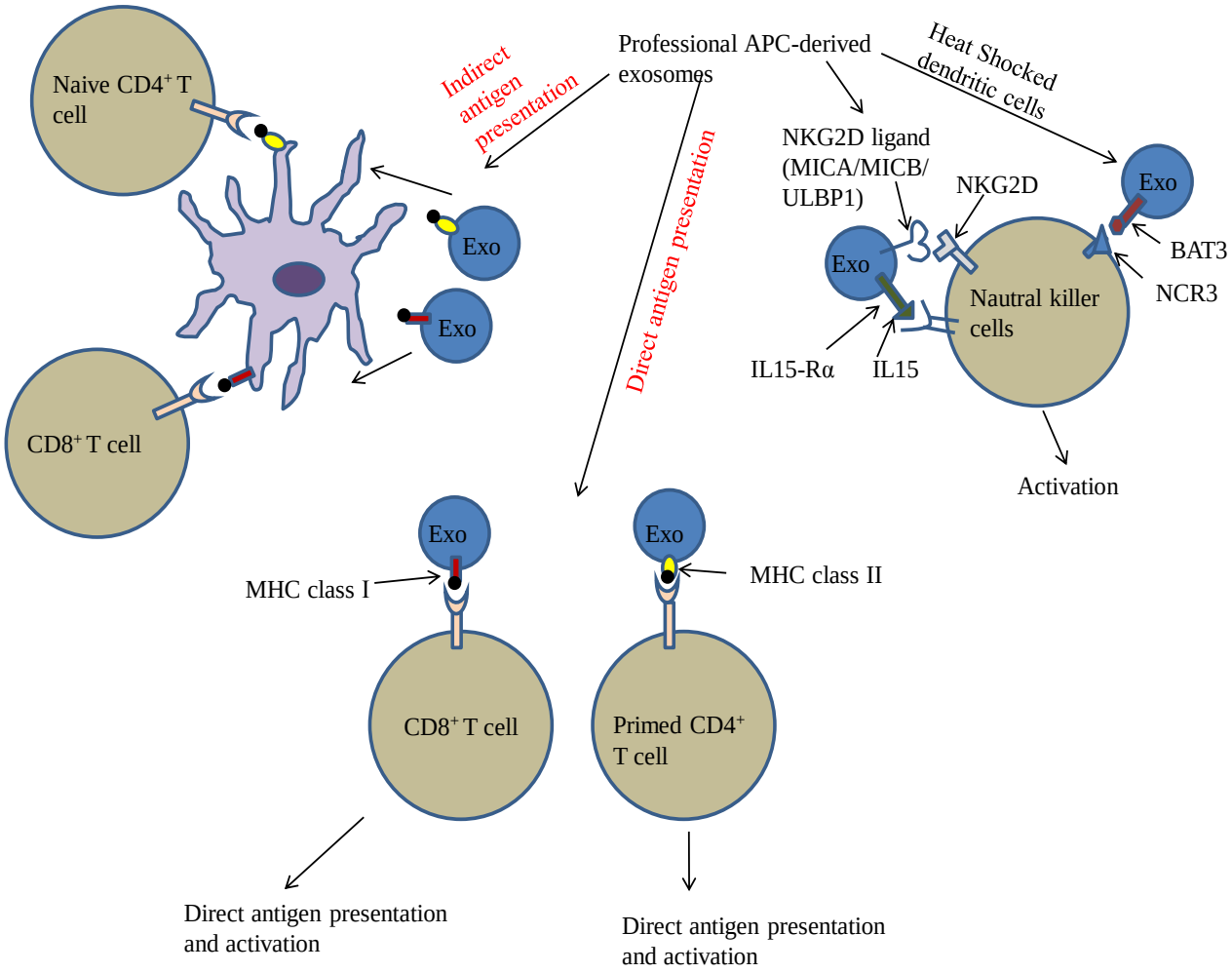

B. Immune-activating function of exosomes secreted from other cells.

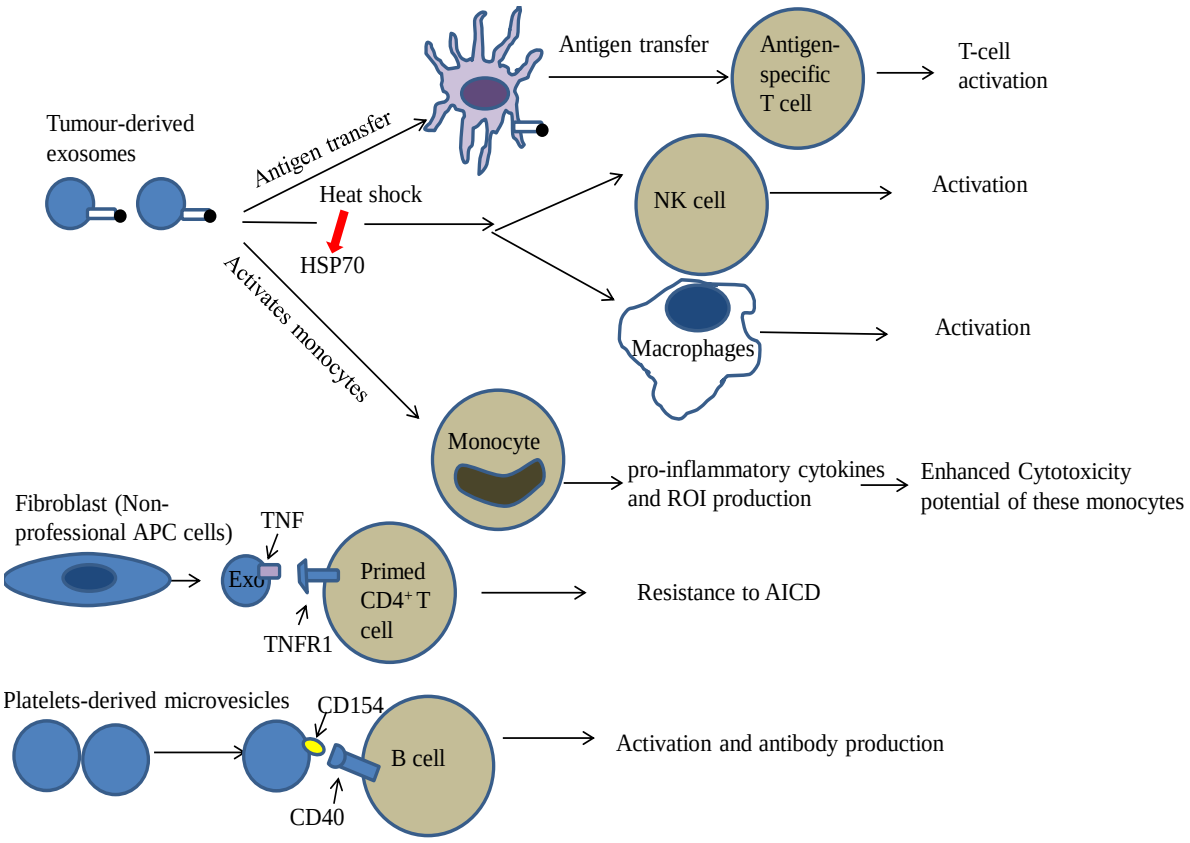

Figure 1.3: Immune-activating function of exosomes. A. Exosomes secreted from professional APC cells bear functional MHC complexes and can activate pre-activated $CD8^+$ and $CD4^+$ T cells, but will have to be transfer the antigen to dendritic cells to activate naive T cells. APC-derived exosomes also bear NKG2D ligands and can bind to NKG2D on NK cells leading to activation. Exosomes derived from heat-shocked dendritic cells bear BAT3, which will bind to NCR3 on NK cells leading to activation. **B**. Tumour derived exosomes can transfer antigens to specific T cells leading to activation; bear HSP70 under stress conditions and can activate macrophages and NK cells; activate monocytes to produce cytokines and ROI. Fibroblast-derived exosomes

can activate primed $CD4^+$ T cells and load to resistance to AICD. Platelets-derived exosomes can activate B cells.

Protumourigenic roles

Tumour-derived exosomes can have immunosuppressive properties

Immune evasion by tumour cells is a well-established mechanism wherein tumours avoid detection and elimination by the host immune system. Early reports indicate that tumour-derived membrane vesicles have immunosuppressive functions (Poutsiaka et al., 1985). Fas ligand (also known as CD95 ligand) is a type II transmembrane protein of the Tumour Necrosis factor (TNF) family. Exosomes derived from tumour cell lines bear Fas ligand that can induce T cell apoptosis leading to suppression of T-cell responses *in vitro* (Abusamra et al., 2005; Andreola et al., 2002). Addition of anti-FasL antibody blocked exosome-induced apoptosis (Abusamra et al., 2005).

In cancer patients, the loss of NKG2D, an activating receptor for NK cells, $CD8^+$ T cell and NKT cells, is a critical mechanism of cancer immune evasion. NKG2D down-modulation is due to direct exosomal delivery of membrane-bound transmembrane growth factor β1 (TGFβ1) to $CD8^+$ T cell or NK cell subsets (Clayton et al., 2008). Down-regulation of NKG2D is partly due to the presence of the expressed NKG2D ligand MICA. Clayton and colleagues demonstrated that other potential NKG2D ligands such as MICB may be present on the surface of tumour-derived exosomes, and may contribute to the down-regulation of NKG2D. On the other hand, some experiments

added combinations of other NKG2D-ligand specific antibodies and did not achieve a convincingly enhanced inhibitory effect, but this may be result of the poor blocking characteristics of the antibodies. In comparison, adding a TGFβ1-blocking antibody almost completely abrogated the reduction in surface NKG2D. These data suggest that down-regulation of NKG2D is mainly due to the presence of TGFβ1 and partly due to the presence of NKG2D ligands, but how precisely TGFβ1 and NKG2D ligands cooperate requires clarification.

Tumour-derived exosomes can also support the function of regulatory T cells (T_{reg}). Interleukin 2 (IL-2) is an important cytokine which not only supports expansion and differentiation of cytotoxic T cells and Natural Killer (NK) cells, but also supports T_{reg} cells and their suppressive functions (Clayton et al., 2007). Tumour exosomes inhibit IL-2 induced T cell proliferation by promoting the function of T_{reg} cells. Similarly, murine mammary carcinoma exosomes were shown to promote tumour growth, suppress the cytotoxic activity of NK cell function and inhibit IL-2-stimulated NK cell growth signalling (Liu et al., 2006). Tumour-derived exosomes were also reported to up-regulate the suppressive functions of human T_{reg} cells and make them more resistant to apoptosis through a TGF-β and IL-10 dependent pathway (Szajnik et al., 2010). Similarly, exosomes derived from the malignant effusion of cancer patients helped maintain the number and suppressive function of T_{reg} cells (Wada et al., 2010).

It was reported that galectin-9 containing exosomes were selectively detected in Epstein-Barr Virus (EBV) infected nasopharyngeal carcinoma and induced apoptosis of mature type 1 helper T cells when interacting with the membrane receptor Tim-3 (Klibi

et al., 2009). Nef (Negative factor), the HIV accessory protein, is one the most abundantly expressed viral proteins. It changes the host's cellular machinery and allows survival and replication of the virus. It was reported that HIV-infected cells export Nef in microvesicles, which caused activation-induced cell death of $CD4^+$ T cells, which is a hallmark of AIDS (Lenassi et al., 2010).

The expansion of Myeloid-derived suppressor cells (MDSCs) in a tumour bearing host leading to immune suppression has been recognized as an important mechanism tumour cells use to escape from the immune system. Tumour-derived exosomes are thought to be involved in this process. Tumour-derived exosomes can also target myeloid cells to modulate their differentiation and function. It has been reported that tumour exosomes mediated induction of IL-6 which plays a role in blocking bone marrow DC differentiation. The levels of IL-6 and phosphorylated Stat3 were elevated 12 hours after the tumour exosomes stimulation of murine myeloid precursors, and tumour exosomes were less efficient in inhibiting differentiation of bone marrow cells isolated from IL-6 knockout mice. It was suggested that bone marrow DC precursors capture tumour exosomes and subsequently induce the production of IL-6 and other cytokines, leading to the activation of Stat3. As a result, differentiation of bone marrow precursors into immature DC is blocked (Yu et al., 2007). Further work by the same group discovered that these myeloid cells were found to switch their differentiation pathway of these myeloid cells to the MDSC pathway and promote tumour growth, and the MDSC mediated promotion of tumour progression is dependent on prostaglandin E2 (PGE2) and TGF- β molecules present on tumour-derived exosomes (Xiang et al., 2009). Mice pre-treated with tumour-derived exosomes have an increase in recruitment of more

MDSCs in the lung which correlate significantly with tumour metastasis, and myD88 play an important role in this process (Liu et al., 2010). Similarly, Hsp72 present on tumour-derived exosomes was reported to trigger STAT3 activation in MDSCs through a Toll-like receptor 2(TLR2) /MyD88-dependent pathway (Chalmin et al., 2010).

Facilitation of Tumour Invasion and Metastasis

As described before, tumour-derived exosomes could potentially have immune-activating properties. As a contrast, most studies indicated that tumour derived exosomes facilitate tumour cell invasion and metastasis by promoting angiogenesis, modulating stromal cells and remodelling extracellular matrix, etc.

Mesothelioma cell-derived exosomes have strong angiogenic factors which increased vascular development in the neighbourhood of a tumour (Hegmans et al., 2004). Melanoma-derived exosomes were also capable of stimulating endothelial signalling that is important for endothelial angiogenesis. (Hood et al., 2009) It was also recently reported that melanoma exosomes injected locally preferentially travelled to sentinel lymph nodes and that this homing caused molecular signals that provoked melanoma cell recruitment, extracellular matrix deposition, and vascular proliferation in the lymph nodes (Hood et al., 2011). Tetraspanins, which are enriched in exosomes, have been reported to contribute to exosome-mediated angiogenesis. It was reported that exosomes secreted from a pancreatic tumour line that overexpress D6.1A (Human homologue CO-029, a tetraspanin associated with poor prognosis in patients with gastrointestinal

cancer), strongly encouraged tumour growth by its capacity to induce systematic angiogenesis in a rat model (Gesierich et al., 2006).

Tumour-derived exosomes can modulate the function of stromal cells such as fibroblasts. It was reported that exosomes derived from some cancer cells contain TGF-β, the delivery of which can drive the differentiation of fibroblasts towards the myofibroblasts phenotype, the enrichment of which in tumours indicate a different stroma which supports tumour growth, vascularization and metastasis (Webber et al., 2010).

Furthermore, exosomes shed by ovarian cancer and breast cancer cells were found to contain metalloproteinases with proteolytic activity. These exosomes can increase extracellular matrix degradation and increase the tumour's ability to invade into the stroma (Nieuwland et al., 2010; Runz et al., 2007; Stoeck et al., 2006)

Gastric cancer exosomes have been shown to promote cancer cell proliferation through activation of PI3K/Akt and MAPK/ERK pathway (Qu et al., 2009a). Exosomes can also be utilised by cancer cells to export anticancer drugs in order to develop drug resistance (Safaei et al., 2005). Moreover, transport of mRNAs and microRNAs, from tumour cells to neighbouring cells could have significant effects on tumorigenesis. This will be discussed in a later chapter. And a recent study has shown that exosomes derived from melanoma cells promoted metastatic niche formation and increased the metastatic behaviour of primary tumours by 'educating' bone marrow-derived cells

(BMDCs) toward a pro-metastatic and pro-vasculogenic phenotype through the receptor tyrosine kinase MET oncoprotein (Peinado et al., 2012)

Immune cells-derived exosomes can also be immune-suppressive

Immune cell-derived vesicles can also have immunosuppressive properties. PHA-activated T cells secrete exosomes bearing FasL and TNF-related apoptosis-inducing ligand (TRAIL). Activation with anti-CD59 antibody mainly triggered specific release of TRAIL-containing microvesicles/exosomes. FasL and TRAIL participate in activation-induced cell death (AICD) and eliminate over-activated T cells after a cellular immune response to prevent potential autoimmune damage (Monleon et al., 2001). Ectosomes derived from polymorphonuclear neutrophils inhibited the maturation of immature monocyte-derived dendritic cells by LPS (ligand for TLR4) and reduced capacity to activate T cells. After incubation with ectosomes, immature dendritic cells secreted TGF-β, which may be responsible for down-regulating of TLR4-mediated maturation of immature dendritic cells (Eken et al., 2008).

Stimulation of Fas receptor usually induces an apoptotic death signal, surprisingly the interaction between Fas and FASL in tumour cells does not necessarily always induce death, but could also promote proliferation and survival of tumour cells (Mitsiades et al., 2006). A very recent study reported that in the tumour environment, activated $CD8^+$ T cells were educated by tumour cells and secrete exosomes with FASL, which can not only induce dendritic cell apoptosis and inhibit their ability to stimulate $CD8^+$ CTL responses, but also promote melanoma and lung cancer cell invasion by increasing

upregulation of MMP9 expression via Fas signalling, providing a novel mechanism of tumour immune escape. Thus, $CD8^+$ CTL cells in the tumour environment were converted from a guard to an accessory of tumour progression by releasing FASL bearing exosomes (Cai et al., 2012).

Exosomes from body fluids could be immunosuppressive.

Vesicles purified from some body fluids can also have immunosuppressive activities. Exosomes from human breast milk *in vitro* inhibit T cell activation and increase the number of T_{reg} cells (Admyre et al., 2007). It was suggested that exosomes present in breast milk may have a role in the immune tolerance of the infant and may also protect the infant from allergy development.

It was recently reported that exosomes isolated from the plasma of mice bearing Ovalbumin (OVA)-expressing tumours were capable of suppressing OVA-specific immune responses. Depletion of vesicles positive for MHC class II from plasma-derived exosomes or using exosomes isolated from MHC class II deficient mice abolished the suppressive effect, indicating that host-derived circulating exosomes that bear MHC class II may be able to suppress tumour antigen specific immune responses (Yang et al., 2012).

MIC molecules are reported to be constitutively transcribed in human placenta throughout normal pregnancy and soluble MIC molecules are released from *in vitro* cultured placenta explants. Elevated levels of soluble MIC molecules are present in

pregnancy sera and are able to down-regulate the NKG2D receptor and impair the cytotoxic function of peripheral blood mononuclear cells from healthy donors. Taken together, these results suggest a novel mechanism for immune evasion of the fetal allograft through fetal MIC and maternal NKG2D interactions (Mincheva-Nilsson et al., 2006). A more recent study by the same group showed that the second family of human NKG2D ligands, ULBP, is also expressed by placenta. Isolated placenta exosomes carried ULBP1-5 and MIC on their surface and induced down-regulation of the NKG2D receptor on NK, $CD8^+$, and γδ T cells, leading to reduction of their *in vitro* cytotoxicity without affecting the perforin-mediated lytic pathway (Hedlund et al., 2009)

Shuttle for genetic and protein materials between cells

Exosomes have been shown to transfer protein material between cells. A study in 2008 has shown that glioblastomas cell-derived microvesicles expressed oncogenic EGF receptor EGFRvIII and can transfer it to cells that were EGFRvIII negative and induced EGFRvIII-dependent signalling pathway (Al-Nedawi et al., 2008). Larger particles have also been shown to mediate receptors transfer. Microparticles secreted by monocytes bear CCR-5, a chemokine receptor that is central to the transmission and propagation of HIV-1, and is the principal co-receptor for macrophage-tropic (M-tropic) HIV-1 strains. These microparticles could transfer this receptor to blood mononuclear cells that do not express CCR5. These cells thus became sensitive to infection by a macrophage-tropic HIV-1 (Mack et al., 2000).

A more recent advance in the field of exosome study has been the discovery that these vesicles can also contain, and deliver, species of RNA molecules that can be active in cells that take up the exosomes. In 2007, Valadi et al published in Nature Cell Biology demonstrating the presence of mRNA and microRNA in exosomes secreted by mast cells. They have also shown that some selected mRNA present in exosomes can be translated into proteins in target cells (Valadi et al., 2007). A study by Skog et al. also showed that exosomes derived from Glioblastoma cells are enriched in mRNA and miRNA. They showed that mRNA could be delivered into recipient normal cells and generate a functional protein, proving that the mRNA present was active and functional. These exosomes stimulated glioma cell proliferation and promoted tumour cell growth (Skog et al., 2008). The identification of RNA being present in exosomes supports the hypothesis that exosomes may be a delivery vehicle by which one cell communicates with another, actually delivering RNA and, in turn, modulating recipient-cell protein production. Not all mRNAs in a cell end up in exosomes. To understand the mechanism of mRNA targeting to these vesicles will provide us with a better understanding of the function of RNA delivery to secreted vesicles. Some groups are comparing RNA sequences in vesicles from normal and cancer cells, and also from biological fluids. Encapsulation into membrane vesicles protects extracellular RNAs from degradation, allowing efficient recovery from biological fluids such as plasma and urine (Thery, 2011). It should become clear whether exosomes can be used as biomarkers in the next few years.

Some miRNAs have a higher expression in exosomes compared to cells showing that microRNAs were uniquely packed into exosomes. In 2010, it was shown that EBV-

infected B cells release exosomes that bear EBV-encoded miRNAs, which can be transferred to non-infected cells and cause repression of target genes of these miRNAs (Pegtel et al., 2010). Moreover, Let-7 miRNAs, which play a tumour-suppressive role because they target oncogenes such as RAS and HMGA2, were released by AZ-P7a cells (gastric carcinoma cell line) via exosomes to the extracellular environment in order to maintain their tumourigenic and metastatic properties (Ohshima et al., 2010).

Use of exosomes as vehicles for delivery of drugs

Three main classes of delivery vehicles have been the centre of research on therapeutic RNAi: Viruses, polyethylenimine (PEI)-based nanoparticles and liposomes. Delivery of genetic material using all three types of methods have achieved some success, nevertheless, It is still extremely difficult to achieve clinically significant gene knock down in the target tissue without immune activation and toxicity.

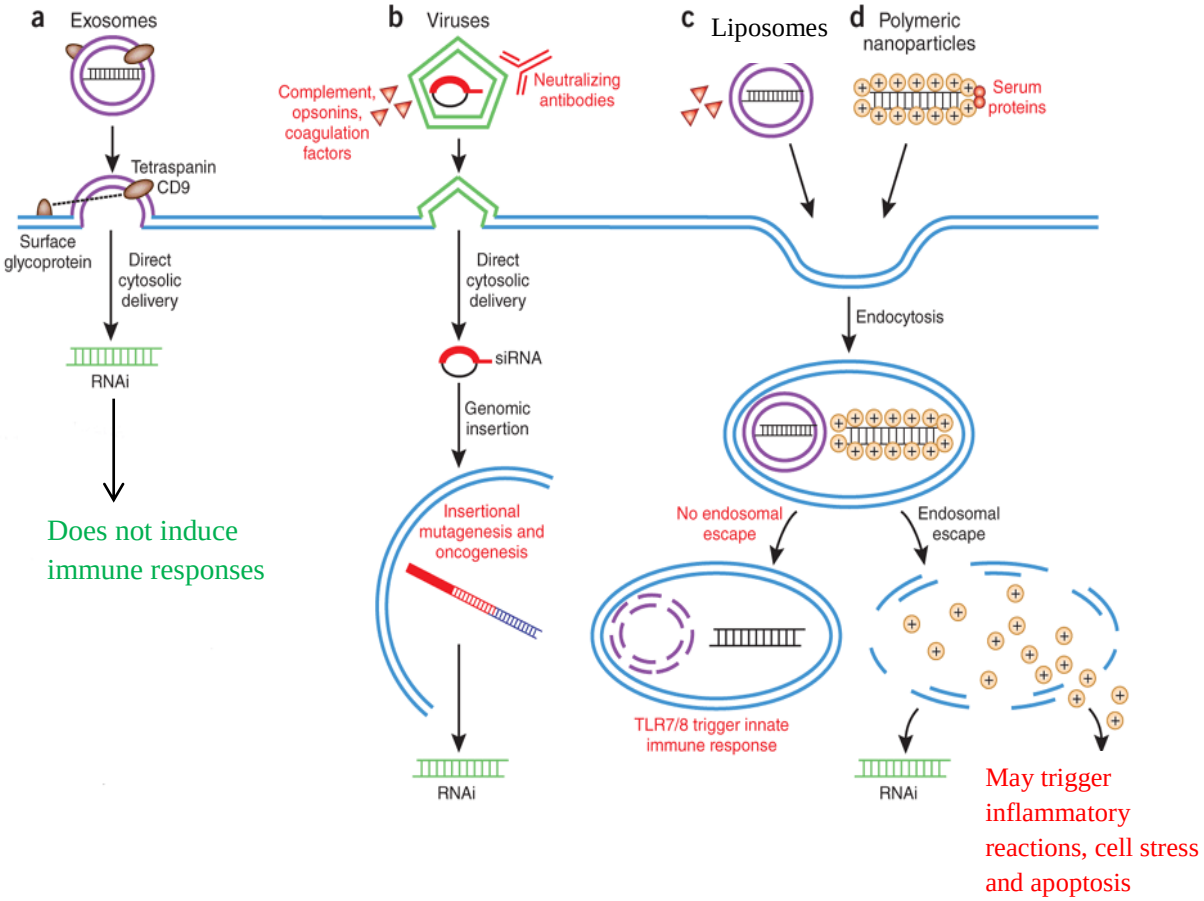

Figure 1.4: Advantages and disadvantages of siRNA delivery by different classes of vehicles. Major advantages are indicated in green and disadvantages are indicated in red. Figure adapted from Van den Boorn et al. (van den Boorn et al., 2011).

Delivery with virus poses unique problems. Viruses are very prone to clearance by complement, opsonins and coagulation factors. Insertional mutagenesis could also lead to gene dysregulation and oncogene activation (van den Boorn et al., 2011). Thus, important safety considerations for viral vectors including inflammatory reactions, immunogenicity, and oncogenic transformation need to be addressed.

Delivery with lipid nanoparticles also has limitations. They absorb opsonins that activate complement and coagulations factors and could be cleared by phagocytosis. Also if they do not escape from the endosome, they could lead to activation of TLR7/8, which play a fundamental role in the activation of innate immunity.

PEI nanoparticles may interact with serum protein, resulting in clearance. Release of the siRNA into cytosol depends on the rupture of the endosomal membrane and this could lead to inflammatory reactions, cell stress and apoptosis.

Another system has also been proposed by Guo et, al. They have utilised the packaging RNA of the DNA-packaging motor of bacteriophage phi29 and manipulated it by RNA nanotechnology to make chimeric RNAs that form dimers via interlocking right- and left-hand loops. Incubation of cells with dimer, one subunit of which carried siRNA and the other a RNA aptamer to CD4, resulted in successful binding, entry, and silencing of apoptotic genes (Guo et al., 2005).

The ability of exosomes to transfer nucleic acid to cells makes it possible to engineer specific DNA or RNA to be delivered to cells, making exosomes a potentially ideal candidate as vectors for gene therapy (Valadi et al., 2007). Sun et al was the first group that applied these naturally occurring exosomes for drug delivery (Sun et al., 2010). They have reported that exosomes can deliver anti-inflammatory agents, such as curcumin, to immune cells. A year later, the same group reported that exosomes encapsulating curcumin or the Stat3 inhibitor JSI124 have been delivered noninvasively

to microglia cells via an intranasal route in mice, and had significantly delayed brain tumour growth in their tumour model (Zhuang et al., 2011a, b).

The first proof-of-concept demonstration that exosomes are potential delivery vehicles for macromolecular drugs came from Alvarez-Erviti et al (Alvarez-Erviti et al., 2011). They have engineered exosomes derived from immature dendritic cells to express Lamp2, fused with a peptide derived from the rabies virus glycoprotein (RVG), which specifically binds to the nicotinic acetylcholine receptor (AchR) present on neurons and the vascular endothelium of the blood brain barrier. Modified exosomes have carried siRNA into brain tissue in mice, resulting in specific knock down of the gene BACE1, a therapeutic target in Alzheimer's disease.

A very recent study has used plasma exosomes as gene delivery vehicles to deliver siRNA to human mononuclear blood cells including monocytes and lymphocytes, leading to gene silencing of MAPK1 (Wahlgren et al., 2012).

These studies demonstrate the potential of exosomes in novel therapeutic treatments. Exosomes have distinct advantages over other existing siRNA delivery vehicles. They do not induce immune responses because they can be derived from a patient's own cells, and consequently avoid clearance by antibodies because of their self-derived nature. Exosomes could also avoid clearance by opsonins, coagulation factors and complement. The exosomes used in their study express the tetraspanin CD9 on their surface, which facilitate direct membrane fusion and release of the exosomal content directly to the target cell's cytosol. This entry method avoids the endosome-lysosome pathway, where

TLR7 and TLR8 could recognise the nucleic acids and activate innate immunity. The small size of exosomes is also an advantage, allowing the exosomes to escape from phagocytosis by the mononuclear phagocyte system that clears particles bigger than 100 nm in size (van den Boorn et al., 2011).

The role of exosomes *in vivo* and in disease

The role of exosomes secreted *in vivo* is still in debate and needs to be fully determined. Study of exosomes secreted from serum has been reported. A study by Taylor et al indicated that exosomes with T-cell inhibiting activity are increased in pregnant women who deliver at full term compare to women who deliver pre-term (Taylor et al., 2006).

Ultracentrifugation is the most used method to purify exosomes. It is likely that ultracentrifugation does not allow 100% recovery of the vesicles secreted at a given point of time because some of the vesicles are re-captured by cells rather than release in the culture medium or body fluid. It is difficult to predict whether the amount of vesicles used *in vitro* corresponds to amounts of vesicles secreted *in vivo* (Thery, 2011). It has been reported that functional differences exist when comparing exosomes secreted from tumour cells re-isolated from syngeneic mice to exosomes from tumour cells that have undergone numerous *in vitro* passages (Xiang et al., 2010), thus exosomes secreted *in vivo* may have different properties.

There are also studies that describe exosomes from biological fluids including sperm (Ronquist and Brody, 1985), urine (Pisitkun et al., 2004), milk (Admyre et al., 2006). All these studies suggest that exosomes should be secreted *in vivo*.

HIV particles utilize multivesicular compartments that are enriched in MHC II and CD63 as the major site for accumulation in human macrophages. Furthermore the released virus has proteins commonly found on exosomes. These findings formed the background for the "Trojan virus hypothesis", which suggested that viruses such as HIV could hijack and hide in exosomes secreted from an infected cell, and because the retroviruses are released in the form of exosomes, they could then escape the host defence (Figure 1.1). It has been demonstrated that the cellular prion protein (PrPc) and the transformed infectious PrPscrapie (PrPsc) are found in exosomes secreted into the culture medium and exosomes that express PrPsc were infectious, indicating the role of exosomes in the spread of prions (Fevrier et al., 2005)

Exosomes have also been shown to play a role in allergy. B-cell derived exosomes can present allergen-derived peptides and stimulate allergen-specific T-cells to proliferate and to produce cytokines, indicating that exosomes could be an immuno-stimulatory factor in an allergic immune response (Admyre et al., 2008). Another study has shown intranasal administration of tolerogenic exosomes in mice one week before sensitization/exposure to olive pollen allergen inhibited the development of IgE response, Th2 cytokine production, and airway inflammation and maintained long-term specific protection *in vivo* (Prado et al., 2008). Another group reported that exosomes derived from bronchoalveolar lavage fluid (BALF) from asthmatic and healthy people

have significantly different phenotypes and functions. BALF exosomes from people with allergic asthma may be involved in subclinical inflammation by promoting LTC_4 and IL-8 secretion in airway epithelium (Torregrosa Paredes et al., 2012).

Isolation of exosomes

Despite the increasing number of groups that are investigating the properties of exosomes and the sparked interest in this field, there is still not a standardised purification protocol for isolating exosomes. The most widely used technique to isolate exosomes is sequential centrifugation at 300 x g and 10,000 x g to get rid of cells, debris and large vesicles, and a final 100,000 x g ultracentrifugation for 2 hours to pellet exosomes. However, some vesicles bud from the plasma membrane and can be anywhere between 50 to 1,000 nm in diameter. As a result, the 100,000 x g pellet may be a mixture of exosomes and other vesicles. To further purify the exosomes, ultracentrifugation on a sucrose gradient can be used or filtration of the exosomes using a 0.2 μm filter.

Recently, a new product with unknown composition called 'Exoquick' was released on the market. This product claims to precipitate exosomes by a single step from a small volume of body fluid or cell culture supernatant. It is not possible to comment on the efficiency of this product until full characterisation of these particles in terms of size, floatation on sucrose gradient and protein composition has been performed. Thus it is not possible to conclude on the types of these particles at this stage, i.e. exosomes or other types of vesicles. A very recent study by Thery's group has found that CD9 could also be present on microvesicles larger than 100 nm and particles smaller than 50 nm

and thus concluded that CD9 was not a specific marker for exosomes. Since the particles recovered by using 'Exoquick' bear large amount of CD9 and low amounts of CD63, it was suggested that this procedure was not specific for exosomes derived from the endosomes (Bobrie et al., 2012a).

These techniques do not separate exosomes from viruses or other nano-sized vesicles that could exist in cell culture supernatants and have a similar density to the exosomes. To solve this problem, a modified protocol used 'Optiprep' (a density gradient medium). The exosomes were collected around 10% and HIV virions were collected around 15%. Unfortunately, the vesicles purified this way were not fully characterised as exosomes (Cantin et al., 2008).

Exosomes can also be purified by using immnoaffinity techniques, which use beads or other solid substrates coated with an antibody that recognise a marker on exosomes. CD63 could supposedly be used for exosomes from all cell types. Immunoaffinity techniques are very useful to isolate exosomes for further analysis of their composition, but cannot produce clinical grade exosomes or be applied for functional studies, because there may be possible alternations of the surface of the exosomes during the acid elution of exosomes from the beads and antibody. Thus, there is a need to develop better purification techniques to produce clinical grade exosomes. One good procedure has been reported. They used ultrafiltration of the medium through a 500-kDa NMWCO hollow fibre cartridge and ultracentrifugation into a 30% sucrose/ deuterium oxide (D2O) (98%) cushion (density 1.210 g/cm3), whereby exosomes from monocyte-derived dendritic cells were purified based on their unique size and density (Lamparski et al., 2002).

Flotation of vesicles on sucrose gradients can allow some separation but this separation is not absolute. Thus, completely satisfactory means for distinguishing different types of vesicles secreted by the same cell are still lacking. It should be taken into consideration that other possible contaminating vesicles should be minimised when culturing for the collection of exosomes. It was suggested that 3 things should be noted; first, cells should be cultured in either serum-free medium or medium with serum which has been depleted of small vesicles by ultracentrifugation at 100,000 x g. Second, apoptotic vesicles and other membrane vesicles of non-endocytic origin will contaminate the exosomes if there are more than 5% dead cells. Third, if large membrane vesicles have not been depleted from the cell supernatant or biological fluid before freezing, the large membrane vesicles will break into small exosomes-sized vesicles and will contaminate the pellet as well (Chaput and Thery, 2011).

Clinical implications

Use of exosomes as a potential immunotherapy vaccine and diagnostic biomarker.

Tumour cell-derived exosomes containing tumour antigens plus MHC class I molecules can transfer tumour antigens to DCs to induce a $CD8^+$ T cell dependent anti-tumour immune response. Exosomes released from DCs pulsed with tumour antigens were also shown to elicit strong anti-tumour responses. One study compared exosomes derived from tumour cells and exosomes derived from dendritic cells in aspects of the stimulatory efficiency of the antitumor immune responses induced by these two commonly used exosome vaccine (Hao et al., 2006).

As I have mentioned before, exosomes can induce tolerance and help protect against sensitization to allergen in mice. Thus, it is possible exosome-based vaccine could be developed and could be used as an alternative therapy to conventional therapies for diseases associated with allergies (Prado et al., 2008).

Clinical Trials

Two phase I clinical trials have been carried out on patients with advanced stage melanomas or non-small cell lung carcinomas expressing melanoma-associated antigen (MAGE). These trials required the establishment of good manufacturing procedures to obtain clinical-grade exosomes from patients' DC loaded with tumour antigen derived peptides. These studies proved that it is feasible and safe to give exosomes to human subjects and that the exosomes are efficient in inducing antigen-specific T-cell responses. The only side effects were mild localized reactions at the site of injection and mild fever in a few patients. The clinical outcomes were encouraging, showing transient stabilization of the disease in half of the patients in the melanoma trial and a third of the patients in the lung carcinoma trial (Escudier et al., 2005; Morse et al., 2005).

Another report that studied the use of ascites-derived exosomes (Aex) in combination with the granulocyte-macrophages colony-stimulating factor (GM-CSF) in the immunotherapy of colorectal cancer was also published. 40 patients with advanced colorectal cancer were involved in this study and they were randomly allocated to treatments with Aex alone or Aex with GM-CSF. Both treatments were safe and the

Aex plus GM-CSF can induce tumour-specific anti-tumour cytotoxic T lymphocyte (CTL) response (Dai et al., 2008)

The first clinical trials used exosomes released from immature dendritic cells. These exosomes could preferentially induce tolerance. The maturation stages of dendritic cells could also affect the immune properties of exosomes (Chaput and Thery, 2011). Based on these results, a phase II clinical trial is on-going in France in patients with non-small cell lung cancer that have been stabilized by chemotherapy. This study will use the second generation exosomes from IFNγ-treated DCs. IFNγ is a cytokine that induces the expression of CD40, CD80, CD86, and CD54 on dendritic cell-derived exosomes. These molecules are important for T cell priming and/or the DC/T cell interactions. The new generation of exosomes have enhanced immunostimulatory properties and could directly activate a Mart-1 specific CD8+ T cell clone and of NK cells *in vitro*, and the priming of CD8+ T cells *in vivo* (Viaud et al., 2011). The major goal of this clinical trial is to improve progression-free survival 4 months after chemotherapy. Other objectives include the clinical efficacy of these exosomes (overall survival, objective response rates and safety of these exosomes, etc (Chaput and Thery, 2011).

Depletion of tumour exosomes from blood as a possible treatment for cancer?

There are contradictory views on tumour exosomes. They carry antigens from the tumours and can present them to dendritic cells. They could also be immunosuppressive and inhibit the functions of T lymphocytes or natural killer cells The actual results of the effects of tumour exosomes *in vivo* are still not very clear, nevertheless, it was still

suggested that depletion of membrane vesicles from the blood circulation of patients is a possible anticancer treatment (Ichim et al., 2008). There were even products already developed called Hemopurifier and Her2osome produced by Aethlon medical. Both products belonged to the Aethlon ADAPT™ (adaptive dialysis-like affinity platform technology) system, an innovative device strategy involving extracorporeal hemofiltration and capture of target exosomes from the entire circulatory system of the patient using an affinity plasmapheresis platform (Marleau et al., 2012). It was claimed that both products can reduce circulating tumour secreted exosomes and Her2osome can also reduce circulating Her2 protein in patients with $Her2^{+}$ breast cancer.

Hemopurifier was claimed to have broad capabilities against viral pathogens such as Human Immunodeficiency Virus (HIV), Hepatitis C virus (HCV), etc. Studies demonstrated that Hemopurifier was safe for human and reduced more than 50% of viral load after 4-hour treatments in both HIV patients and HCV patients without the need of any antiviral drugs (Tullis et al., 2009). Hemopurifier is now being evaluated in a clinical study in India to test its efficiency to deplete viral load when it is combined with the use of HCV standard of care drug therapy. The company is also trying to initiate clinical studies in the United States. (www.aethlonmedical.com)

The other member of the Aethlon ADAPT™ system is HER2osome. Her2 stands for 'Human Epidermal Growth Factor Receptor 2' and is a protein giving higher aggressiveness in breast cancer. Approximately 25-30% of breast cancers have HER2 overexpression. The goal of HER2osome is to reduce circulatory HER2 protein and breast cancer exosomes, which has been identified as playing an important role in the

progression of breast cancer. The immobilization of a HER2 antibody and an exosome targeted affinity agent provides a mechanism to clear both targets from the circulatory system of $HER2^{+}$ breast cancer patients. It can be utilised on Dialysis machines already located in hospitals worldwide. (www.aethlonmedical.com)

An alternative explanation of tumour exosomes in the circulation of cancer patients suggested that they are not necessarily signs of tumour progression, but could simply be the result of tumour expansion (Thery, 2011). It is still unclear whether depletion of tumour-derived exosomes from cancer patients would be harmful or beneficial for the patient since the function of tumour-derived exosomes *in vivo* is still unclear. Thus, caution needs to be taken in using such approaches without proper understanding of what exosomes secreted by tumour cells do *in vivo*.

Breast cancer

The female breast is made up mainly of milk-producing glands called lobules, tiny tubes that carry the milk from the lobules to the nipple called ducts, and stroma that include fatty tissue, connective tissue surrounding the ducts and lobules, blood vessels, and lymphatic vessels. Most breast cancers begin in the cells that line the ducts (ductal cancers). Some begin in the cells that line the lobules (lobular cancers), while a small number start in other tissues (Figure 1.6). Breast cancer is the leading type of malignancy in women, with devastating properties such as invasiveness and abilities to metastasize. Prognosis and appropriate treatment depend on patient age, tumour size, hormone receptor status, and HER2 status, etc. Gene expression profiling has been used

to identify several major breast cancer subtypes including luminal A, luminal B, HER2-enriched, basal-like and normal like subtypes. Most breast cancers are luminal tumours. They are hormone receptor positive. Hormone receptor negative breast cancers include two major subtypes, HER2 and basal-like. Details of the gene expression, response to treatment, and prognosis are listed in Figure 1.6.

Breast cancer can also be categorized based on its histologic type. The two most common histologic types of invasive breast cancer include ductal and lobular carcinomas, which account for most cases of breast cancer. Less common invasive breast cancer includes inflammatory breast cancer and Paget's disease of the nipple. Other less common forms of invasive breast cancer are medullary, mucinous, papillary and tubular carcinoma, which together account for about 10% of all cases (Li et al., 2005).

Non-invasive breast cancer is an abnormal growth of cells still within the areas of cells where it started. They have not invaded and this is referred to as stage 0. Non-invasive breast cancer includes ductal carcinoma in situ and lobular carcinoma *in situ*.

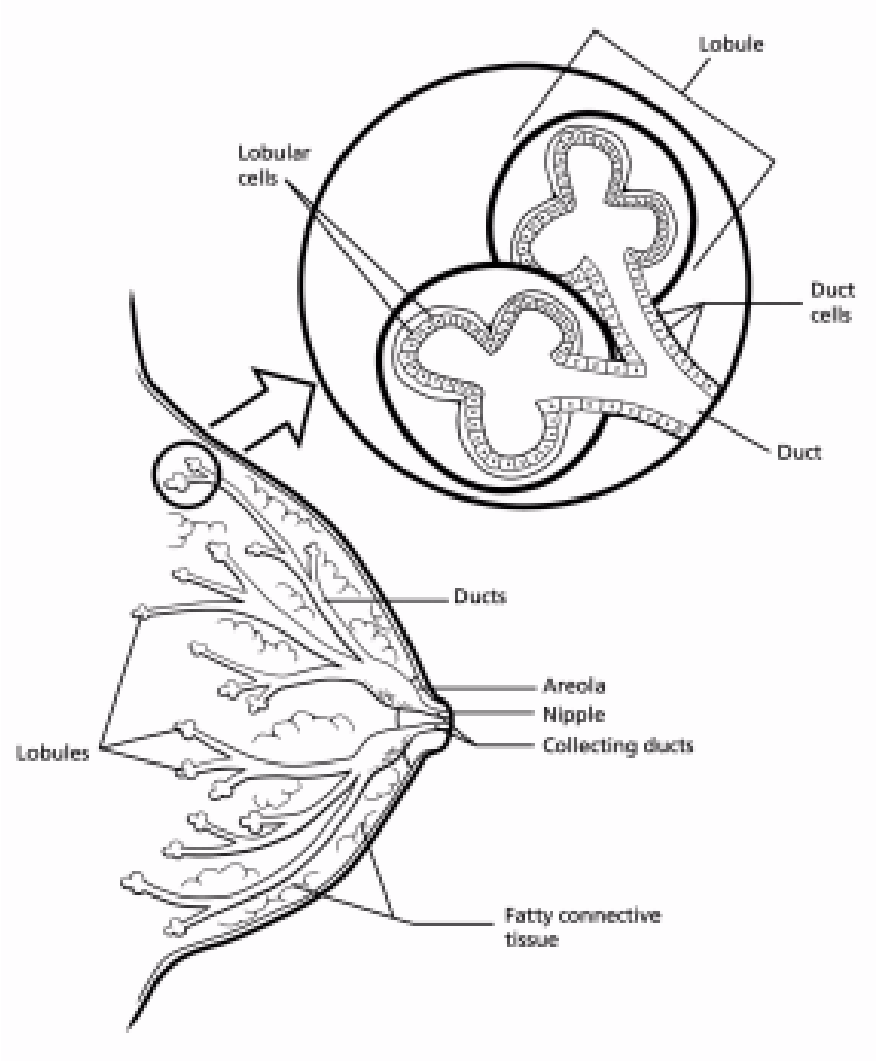

Figure 1.5: Structure of the normal breast. The female breast is made up mainly of lobules, ducts and stoma. Most breast cancer starts in cells that line the ducts. Some breast cancer starts in cells that line the lobules. A small number of breast cancers start in other tissues. Image was adapted from www.cancer.org/

MCF7 (Luminal A phenotype) → ← MDA-MB_231 (Basal phenotype)

	Molecular subtype		
	Luminal	*HER2*	*Basal*
Gene expression pattern	High expression of hormone receptors and associated genes (luminal A > luminal B)	High expression of HER2 and other genes in amplicon Low expression of ER and associated genes	High expression of basal epithelial genes, basal cytokeratins Low expression of ER and associated genes Low expression of HER2
Clinical features	~70% of invasive breast cancers ER/PR positive Luminal B tend to be higher histological grade than luminal A Some overexpress HER2 (luminal B)	~15% of invasive breast cancers ER/PR negative More likely to be high grade and node positive	~15% of invasive breast cancers Most ER/PR/HER2 negative ('triple negative') *BRCA1* dysfunction (germline, sporadic) Particularly common in African-American women
Treatment response and outcome	Respond to endocrine therapy (but response to tamoxifen and aromatase inhibitors may be different for luminal A and luminal B) Response to chemotherapy variable (greater in luminal B than in luminal A) Prognosis better for luminal A than luminal B	Respond to trastuzumab (Herceptin) Respond to anthracycline-based chemotherapy Generally poor prognosis	No response to endocrine therapy or trastuzumab (Herceptin) Appear to be sensitive to platinum-based chemotherapy and PARP inhibitors Generally poor prognosis (but not uniformly poor)

Figure 1.6: Major molecular subtypes of breast cancer determined by gene expression profiling. Adapted from Schnitt, et al, 2010 (Schnitt, 2010).

Causes of breast cancer

The causes of breast cancer are unknown. Certain risk factors can affect a person's chances of getting breast cancer. There are several risk factors. First, it is rare in women under the age of 35, and most breast cancers occur in women over 50. Second, previous cancers and other breast conditions could also increase the risk. These include previous breast cancer, ductal and lobular carcinoma in situ, over-production of slightly abnormal cells, and dense breast tissue. Third is hormonal factors including delayed age at first full term birth, use of combined hormone replacement therapy (HRT), not breastfeeding or breastfeeding for less than a year, early onset of period (before 12) or a late menopause (after 55) and taking the contraceptive pill. These factors could allow

exposure to the hormones oestrogen and progesterone for continuous long periods and thus increase the risk. The fourth one is lifestyle factors including smoking tobacco, excess body weight, lack of exercise and alcohol consumption. The final factor is genetic factor (family history). Breast cancer risk is higher in women who have close family relatives with this disease. A small percent of breast cancers are linked to inherited mutations in certain genes. The most commonly mutated genes are *BRCA1* and *BRCA2* genes, women with mutations in those genes have about 80% chance of developing breast cancer throughout their lives.

Prevention of breast cancer

Cancers are caused by multiple factors acting simultaneously and hence could be prevented by intervening on single or multiple risk factors. A healthy, balanced diet and regular exercise reduce lifetime weight gain and avoid or limit alcohol intake may help reduce the risk of breast cancer. For women at an increased risk, genetic testing for BRCA genes, chemoprevention using drugs such as Tamoxifen that lower breast cancer risk may help reduce the risk. For women with very high breast cancer risk, prophylactic surgical removal of the breasts or ovaries may be an option.

Treatment of breast cancer

The main treatments for breast cancer are surgery, radiotherapy, chemotherapy, hormone therapy and biological therapy (targeted therapy).

Rab27a

The RAB27A gene is a member of the RAS oncogene family. The protein encoded by Rab27a is a member of the GTPase Rab family and may be involved in protein transport. It was shown that overexpression of Rab27a could be related to the invasive and metastatic potential of cancer cells, and Rab27a expression increased in human breast cancer as invasive and metastatic potential increased (Wang et al., 2008). They have also shown that Rab27a overexpression could redistribute the cell cycle and the percentage of cells in S phase which were dramatically increased and cells in G_0 and G_1 phase were decreased, demonstrating that Rab27a overexpression in breast cancer cells could cause the tumour cells to divide faster. Consistent with these results, another very recent study has shown that inhibiting the expression of RAB27A decreased exosome production and the release of proangiogenic factors from tumour cells, and also inhibited tumour growth and metastasis. These data suggest that RAB27A should be considered as a potential therapeutic target in cancer (Peinado et al., 2012).

It was shown that Rab27a silencing can inhibit MVE docking with the plasma membrane and inhibit exosome release (Ostrowski et al., 2010). It has also been shown that knocking down Rab27a in Hela cells increases the size of MVE multivesicular bodies. It was reported that either Rab27a is required for docking and when it is absent, the vesicles fuse with each other instead of fusing with the plasma membrane; or Rab27a prevents the fusion of CD-63 positive compartments with each other and its absence causes the CD-63 positive compartments to fuse together, and the enlarged MVEs fails to fuse with the plasma membrane because of the size (Ostrowski et al.,

2010). Because of its identification in the secretion of exosomes, we have also used Rab27a as a target for disruption of the exosome pathway in this study.

Aims of the project

As there are contradictory views of tumour-derived exosomes, further characterising tumour-derived exosomes will contribute significantly to this emerging field, and contribute towards the possible future use of exosomes as biomarkers, vaccines, or gene delivery vehicles. The main aim of this project is to characterise exosomes and microvesicles secreted from breast cancer cells. Another major aim of the study is to investigate whether the Rab27a associated exosomes pathway can be monitored by Nanoparticle analysis (NTA), which will be introduced in a later chapter.

Chapter II Materials and Methods

Cell culture of human breast cancer cell lines.

MDA-MB-231 cells were cultured in RPMI 1640 (Lonza, UK) with 10% FCS (Globepharm, Cork, Ireland) and 10,000 units/ml penicillin, 10 mg/ml streptomycin and 2mM glutamine (PSG) (Sigma Aldrich, Poole, UK). MCF 7 cells were cultured in DMEM with 10% FCS, PSG and 10 μg/ml insulin Confluent cultures were routinely passaged by removing the culture medium and washing with approximately 1 ml of 0.5 % trypsin EDTA (ethylenediamine tetraacetic acid), and then a further 1 ml of trypsin was added to the cells and the flasks were incubated for approximately 2 minutes in the incubator. Trypsin was then neutralised with approximately 10 ml of complete culture medium. All tissue culture procedures were performed in a class 2 containment cabinet. Cells were grown in T75 cm^2 or T175 cm^2 tissue culture flasks (Thermo Fischer Scientific, Surrey, UK) in an incubator at 37 °C in a humidified atmosphere of 5 % CO_2 in air. The cells were tested for mycoplasma contamination and were negative.

In vitro cell culture of Jurkat T cells

Jurkat cells were grown in RPMI 1640 with 10% FCS and PSG and were routinely passaged by 1:1 dilution with fresh RPMI medium. Cells were inspected daily using an inverted phase microscope to ensure that they were healthy.

In vitro cell culture of HeLa cells

HeLa cells were grown in RPMI 1640 with 10% FCS and PSG and were routinely passaged with fresh RPMI medium using the trypsin technique described above.

Cell counting

Cell counting was facilitated by using a Z1 Coulter® Particle Counter (Coulter Particle Characterization, Hialeah, USA). Isoton was used as a blank count and the average was deducted from the reading when counting cells. Approximately 200 µl of cell suspension in medium was added to 20 ml of Isoton in a beaker. At least 3 readings were recorded on the coulter.

Freezing and thawing of cells

Cells were trypsinised and centrifuged at 300 x g for 10 minutes. The supernatant was then discarded and the cell pellet was re-suspended in freezing medium (90% FCS and 10% DMSO (dimethyl sulfoxide)). Approximately 1 ml of cells was added to each 1.5 ml cryo vials (Corning Incorporated, New York, USA). The vials were then transferred into an isopropanol-filled freezing container and were left at -80 °C for approximately 24 hours before being transferred to the liquid nitrogen storage tanks.

Before cells were taken out from the liquid nitrogen, appropriate medium was warmed in a 37 °C water bath. Cells were then taken out of liquid nitrogen and warmed in the

water bath. Cells were then pipetted into the flask and the warm culture medium was added slowly. Cells were returned to the incubator and the medium was changed after 24 hours.

Flow Cytometry

A Beckton Dickinson FACScan (Becton-Dickinson BioSciences, Oxford, UK) was used for all the flow cytometry studies. Data acquisition was performed using CellQuest software (San Jose, CA, USA), and analysis was performed by using Summit software (Dakocytomation, Glostrup, Denmark).

Annexin V staining

Approximately 500,000 Jurkat cells were seeded into each of the 4 wells of a 6 well plate. MDA-MB-231 and MCF 7-derived exosomes were added into 2 of the wells and PBS was added to another well as a control. Final concentration of the exosomes was 60 ug/ml. After 24 hours, Jurkat cells (250 µl) were harvested and pelleted on a desktop microfuge, Pellets were resuspended in 500 µl of binding buffer, Annexin V-FITC (5 µl) (Sigma-Aldrich, Poole, UK) was added and incubated for 5 minutes. Samples were then analysed by using flow cytometry

PI staining to study Jurkat cell apoptosis caused by MDA-MB-231/MCF7 conditioned medium or exosomes

Apoptosis induced by conditioned medium

Approximately 10 ml of RPMI, MDA supernatant, DMEM and MCF 7 supernatant was spun at 300 x g for 10 minutes and then 10,000 xg for 30 minutes. The pellet was then discarded and supernatant was added to Jurkat cells in a 6 well plate. After 48 hours, cells were centrifuged again on a desktop microfuge (VWR International, Leicestershire, UK), washed twice with ice-cold PBS, fixed with 70% ethanol in the cold room for at least 30 minutes, washed twice with ice-cold PBS and then stained with PI in the dark for 30 minutes. Data acquisition was achieved by using CellQuest software. FLH-1 channel was chosen for green fluorescence. Analysis was performed by using Summit software.

Apoptosis induced by exosomes

Approximately 300, 000 Jurkat T cells (250 µl) were seeded into each well of a 24 well plate. Approximately 250 µl of MDA exosomes (52 µg) was added to 250 µl of Jurkat cells (final exosome concentration 104 µg/ml). Jurkat cells with 250 µl PBS added was used as control. MCF7-derived exosomes was added to one well of Jurkat cells (final exosomes concentration 400 µg/ml). After 24 hours, cells were pelleted and washed twice with ice-cold PBS, fixed with 70% ethanol in the cold room for at least 30 minutes, washed twice again with ice-cold PBS and then stained with PI in the dark for

30 minutes. Data acquisition was achieved by using CellQuest software. FLH-1 channel was chosen for green fluorescence. Analysis was performed by using Summit software.

E. coli Transformation

Competent JM109 cells were thawed on ice, and 20 µl of cells and 0.5 µl of each DNA plasmid were added into each eppendorf, which was then incubated on ice for 20 minutes. Cells were heat shocked for 50 seconds at 42 °C and were then immediately put on ice for approximately 2 minutes. Luria Broth (LB) medium (100 µl) was added to each eppendorf. And all eppendorfs were incubated at 37 °C in a shaking incubator for 1 hour. Approximately 100 µl of each sample was taken and pipetted onto a LB agar plate containing Ampicillin (100 µg/ml). All plates were incubated overnight at 37 °C. One single colony from clone 1-4 and all 4 clones mixed together was taken and put into 5 ml LB medium with ampicillin (100 µg/ml) in a 50 ml tube. After approximately 8 hours, they were put into a shaking incubator overnight. Approximately 200 µl was then taken out from each tube and was added to 100 ml LB containing ampicillin, which was then subject to plasmid purification by using plasmid midi prep kit from Qiagen according to manufacturer's instructions, or aliquoted and stored at -80 °C to create stocks.

ScaI Digestion and Agarose Gel Electropheresis

All 5 Plasmid DNA's (Negative scrambled, shRNA 1, shRNA 2, shRNA 3 and shRNA 4) were checked by restriction digestion with the restriction enzyme *ScaI* (Roche Applied Science, Roche Diagnostics Ltd, West Sussex, UK).

Reaction solutions (10 µl) were made as follow: DNA (2 µl), 10x Buffer (1 µl), ScaI enzyme (0.5 µl), dH_2O (6.5 µl). Samples were analysed on either 1% or 2% agarose gels. To make the gel, 0.5 g (for 1%) or 1 g of Iberose (Webscientific, Crewe, UK) was added to 50 ml of 1x TAE buffer in a culture flask. The 1x TAE buffer was diluted from a 50x TAE buffer stock (242 g Tris, 18.6 g EDTA, 57.1 ml Glacial acetic acid, pH 8). It was covered with cling film, which was pierced a few times and heated in a microwave. It was mixed at regular intervals by swirling the flask. Approximately 2 µl of ethidium bromide (Sigma) was added after the mixture had cooled down. It was then allowed to set for about 20 minutes. Samples and Lambda *HindIII* marker (Promega Corporation, Southampton, UK) were mixed with loading dye (Bioline, London, UK) and loaded onto the gel. It was run at 100V for approximately one hour. DNA was visualised on a Molecular Imager ChemiDoc^{TM} XRS Imaging system. (Bio-Rad Laboratories Ltd, Hertfordshire, UK.)

Cell Transfection

Cells were grown in a six-well plate prior to transfection. The cells were transfected by either using a shRNA plasmid from Santa Cruz (Santa Cruz Biotechnology Inc,

Heidleberg, Germany) or using the SureSilencing shRNA plasmids for human Rab27a from Qiagen (Qiagen, Crawley, UK). Briefly, approximately 1 μg of each shRNA was added to 50 μl of serum free RPMI. Lipofectamine 2000 (2 μl) (Invitrogen, Paisley, UK) was added to another 50 μl of serum free RPMI and was incubated at room temperature for 5 minutes. The contents of the two tubes were then mixed together gently and incubated at room temperature for 20 minutes. The total 100 μl of the mixture was added to 1 ml of MDA cells and incubated overnight in a tissue culture incubator. The next morning, medium was replaced with RPMI containing 3 μg/ml puromycin to select for stable transfectants.

Soft agar assay

Agar (5%) was melted and diluted 1 in 10 in RPMI with additives to give 0.5 % agar. Approximately 2 ml of the mixture was added to each well of all the 6-well plates. Plates were allowed to set for approximately 1 hour. Stock of cells (10,000 cells/ml) were prepared for each cell line used. For the top layer, 1 ml 3% agar was added to 8 ml RPMI and was mixed gently. Approximately 1 ml of cells was added to the mixture and mixed gently. Approximately 2 ml of the mixture (2,000 cells) was added to each of the 3 wells. (Experiment was performed in triplicates). For soft agar assay with the addition of exosomes, exosomes (15 μg) was added into each well. Colonies was counted after 21 days.

Immunostaining of MDA-MB-231 cells.

Approximately 1 million MDA-MB-231 cells were collected and centrifugation at 300 x g was performed. Approximately 300 µl PFN buffer (PBS containing 2% FCS and 0.1 % sodium azide) was added to the cell pellet and 100 µl of the sample was added to each of 3 wells of a 96-well plate. Supernatant was discarded after centrifugation at 300 x g. For the negative control, PFN buffer (50 µl) was added to the well, 45 µl PFN buffer with either 5 µl anti-CD9 antibody or 45 µl PFN buffer with 5 µl anti-CD63 antibody was added accordingly. The plate was then left rotating for 30 minutes at 4 °C. The cells were then pelleted by centrifugation at 300 x g at 4 °C. The supernatant was discarded and the cell pellets washed in 200 µl PFN buffer again. Approximately 50 µl FITC-anti-mouse antibody (Sigma) was added into each well and the plate was left at 4 °C for 30 minutes with agitation. Cell were then pelleted again at 300 x g and washed in 200 µl PFN buffer. Each cell pellet was re-suspended in 100 µl PBS. Samples were transferred into flow cytometry tubes and 300 µl PBS was added to each sample. The samples were then analysed by flow cytometry.

CFSE and PE/RPE double staining

RPE-conjugated mouse anti-human CD9 antibody (AbD Serotec, Oxford UK) and PE-conjugated mouse anti-human CD63 antibody (Invitrogen) were pre-cleared by ultracentrifugation at 10,000 xg for 10 minutes. The same number of MDA-MB-231 cells was seeded into two 6-well plates and allowed to attach. A 2 mM stock was made by adding 11 mg CFSE powder to 10 ml PBS, 50 µl of which was added to 10 ml PBS

to further dilute it to 10 μM. Supernatant from cells were discarded and 2 ml of the 10 μM CFSE was added to each well. The plates were then incubated in dark in the incubator at 37 °C for 15 minutes. CFSE was then discarded and the wells were washed 3 times with serum-containing RPMI. Serum free RPMI (2 ml) was then added to each well. The plates were returned to the incubator for 48 hours. Supernatant was then collected and ultracentrifuged at 300 x g for 10 minutes and 10,000 x g for 30 minutes. The pellet was discarded and 5 μl either CD9 or CD63 antibody was added to 0.5 ml supernatant and left rotating for 3 hours at 4 ℃. Supernatant was then analysed by flow cytometry.

Scratch assay

Cells were trypsinised and 250,000 cells were plated onto each well of a 24 well plate. The plate was then incubated at 37 °C in an incubator of 5 % CO_2 for approximately 24 hours to allow cells to adhere and become confluent. The cell monolayer was scraped in a straight line to create a scratch with a P200 pipette tip. Cells were washed once with 1 ml of growth medium to get rid of cell debris and then 1 ml of fresh growth medium was added. A reference point was made at the bottom of each well with an ultrafine tip marker to allow the same field to be captured every time. The scratch made was immediately to the right of the reference point. The plate was then placed under a microscope and the first image of the scratch was taken. The plate was returned to the tissue culture incubator and incubated for further 12 hours, and then the second set of images was taken. Images were then taken every hour until all the gaps were closed.

Images were then imported to Image J and the results of scratch assays were plotted as percentage of wound closure relative to hour 0.

Bradford assay

Protein concentrations of samples were determined by using the Bradford assay. Bradford reagent was purchased from Sigma. Normally, for measuring exosomal protein concentration, 6 controls of known concentrations of BSA (Bovine serum albumin) were prepared using a stock concentration of 10 μg /ml: 0 μg/ml, 0.2 μg/ml, 0.4 μg/ml, 0.6 μg/ml, 0.8 μg/ml and 1 μg/ml. For measuring the protein concentration of cell lysates, 6 control samples of known concentration were prepared: 0 μg/ml, 2 μg/ml, 4 μg/ml, 6 μg/ml, 8 μg/ml and 10 μg/ml. A standard curve was then prepared using Microsoft excel. All samples' measurements were taken at wavelength 595 nm on a spectrophotometer. The concentrations of the samples were then calculated using the measurements and the equation from the standard curve.

Invasion assay

Inserts (Becton Dickinson UK, Biocoat^{TM} Gowth Factor Reduced Matrigel^{TM} Invasion Chamber 24 well plate 8.0 micron, Catalogue number 354483) were taken out from the freezer and were allowed to come to room temperature. Inserts were rehydrated by adding 0.5 ml of warm RPMI to the interior of each of the inserts. The plate was left for 2 hours in the incubator 37 °C 5% CO_2. After 2 hours this medium was carefully

removed and discarded. The same numbers of control inserts were prepared by using sterile forceps to transfer them onto another companion plate.

MDA-MB-231 and Rab27a-inhibited MDA-MB-231 cells were trypsinised and resuspended in RPMI with 10% FCS and centrifuged at 1,000 rpm for 10 minutes at room temperature. The supernatant was removed and the cells were resuspended in serum-free RPMI with 0.1 % Bovine serum albumin (BSA). Cell suspensions (5×10^4 cells/ml) in serum-free RPMI containing 0.1 % BSA were prepared.

RPMI medium containing the additives (10% FCS and PSG) was used as a chemoattractant. The RPMI medium (0.75 ml) was added to the bottom wells of both of the companion plates. Sterile forceps were used to transfer the chambers and control inserts to the wells containing the chemoattractant. Air bubbles were avoided by slightly tipping the inserts or chambers at a slight angle when putting in. Approximately 0.5 ml of cells (2.5×10^4 cells) was then added to each of the chambers and the inserts and the plates were incubated for 22 hours in the incubator.

After 22 hours the non-invading cells were removed from the upper surface of the membrane by scrubbing the membrane surface gently with a cotton swab. The scrubbing was repeated with a second cotton swab moistened with RPMI medium subsequently.

The cells on the lower surface of the membrane were stained with RAPI-DIFF II stain pack (Raymond A. Lamb, London, UK). This kit contains 3 different solutions. Solution A is the fixing solution which contains methanol. Solution B is an acid dye that contains

Eosin Y. Solution C is a basic dye which contains Methylene Blue. Each solution was added to three rows of two 24-well plate. Two beakers of distilled water were also prepared. The chambers and inserts were transferred sequentially through each solution and the two beakers of water for rinses. Inserts were immersed into each solution for approximately 30 seconds. The inserts were then taken out using forceps and were placed on a piece of paper towel to air dry for 60 minutes. The cells that had migrated through the control insert and invasion insert were counted using an inverted microscope under the 40X objective. Cell counting was facilitated by photographing the membrane through the microscope. Three fields of each insert were taken. For 'true' representation of the cell number throughout the membrane, fields were chosen in the centre as well as the peripheral of the membrane. Cells were then counted and average calculated.

Data was expressed as the percent invasion through the Matrigel matrix and membrane relative to the migration through the control inserts. Percent invasion was determined as follows:

$$\% \text{ invasion} = \frac{\text{Mean \# of cells invading through Matrigel insert membrane}}{\text{Mean \# of cells migrating through control insert membrane}} \times 100$$

SDS-PAGE and Western Blot

The glass plates were assembled and the resolving gel was made as follows.

A

	8% Resolving gel	12% Resolving gel	15% Resolving gel
H_2O	4.6 ml	3.3 ml	2.3 ml
Acrylamide	2.7 ml	4.0 ml	5.0 Ml
1.5 M Tris pH 8.8	2.5 ml	2.5 ml	2.5 ml
10 % SDS	100 µl	100 µl	100 µl
10% APS	100 µl	100 µl	100 µl
TEMED	6 µl	4 µl	4 µl

B

	Stacking gel
H_2O	5 ml
Acrylamide	1 ml
0.5 M Tris pH 6.8	2.5 ml
10 % SDS	100 µl
10% APS	100 µl
TEMED	10 µl

Table 2.1: Contents of resolving gels (A) and the stacking gel (B). Samples were resuspended in SDS sample buffer with or without the reducing agent Dithiothreitol) and denatured by heating at 70 °C for 1 minute. Electrophoresis was carried out in a Biorad mini-Protean II electrophoresis equipment in SDS-PAGE running buffer for approximately 1 hour at 150 V or until the dye reached the bottom of the gel.

Electrophoresis was carried out in SDS-PAGE running buffer for approximately 1 hour at 150 V. Protein samples were then transferred onto a nitrocellulose membrane (in blotting buffer (25 mM Tris, 192 mM Glycine) at 100 V for approximately 30 minutes). Ponceau S was used to check the protein transfer. The nitrocellulose membrane was washed in water and then with PBS containing 0.1% Tween 20. Blocking buffer (PBS containing 0.1% Tween and 5% Skimmed milk powder) was then added and the membrane was left on a shaker for approximately 15 minutes. Primary antibodies were diluted into PBS containing 0.1% Tween and incubated with the membrane and were left on a shaker in a cold room overnight unless specified. Membranes were washed 3 times with PBS containing 0.1% Tween at 10 minutes intervals. Appropriate secondary antibody was diluted in PBS containing 0.1% Tween and incubated with the membrane for approximately 20 minutes. Membranes were then washed 3 times with PBS containing 0.1% Tween at 10 minutes intervals. Approximately 1ml of PBS, 300 µl of Peroxide and 300 µl of enhancer (Super signal West Femto) (Pierce, Perbio Science UK Ltd, Northumberland, UK) was mixed together and incubated with the membrane for approximately 1 minute. Excess fluid was then absorbed with tissue. Antibody binding was then visualised with Fujifilm Intelligent Dark Box LAS-3000 (Fujifilm UK Ltd, Bedford, UK).

Cell Lysis

Cells were trypsinised and centrifuged at 1,000 rpm for 5 minutes and then washed in 100 µl of PBS. Cells were centrifuged again at 1,000 rpm for 5 minutes and then lysed in 100 µl of lysis buffer (10 mM Tris pH 7.6, 130 mM NaCl, 1 % Nonidet P-40 (NP40),

10 mM N-ethylmaleimide (NEM) and 1 mM phenylmethylsulfonyl fluoride (PMSF)) and incubated on ice for 10 minutes. Debris was then removed by centrifugation at 20,000 x g for 5 minutes at 4 °C. The pellet was then discarded and the supernatant contained all the nuclear material. Protein concentration was measured using the Bradford method as described before.

Isolation of exosomes

After cell culture reached 90% confluency, culture medium was discarded and then replaced with serum free culture medium. After 24-48 hours, cell culture supernatant was collected. Exosomes were isolated using centrifugation at 300 x g for 10 minutes to get rid of dead cells and debris, at 10,000 x g for 30 minutes to get rid of large particles, followed by ultracentrifugation at 100,000 x g for 2 hours to pellet the exosomes using either the SW55Ti rotor or the SW32Ti rotor in a Beckman Optima L-100 ultracentrifuge (Beckman Coulter, London, UK). The supernatent was then discarded and exosome pellets were resuspended in various volumes of PBS or lysis buffer. Concentrations were measured using Bradford method.

Electron Microscopy

Electron microscopy was performed in collaboration with Dr John Lucocq, School of Medicine. Briefly, 100,000 x g pellet resuspended in PBS was adsorbed to pioloform/carbon coated 150 mesh EM grids and embedded in uranyl acetate methyl cellulose films. Micrographs were taken in a systematic uniform random method (SUR;

Lucocq, 2012, in press) and in the horizontal direction on the micrograph, caliper diameters of all structures displaying clear membrane profiles over at least half of the particle profile were measured using photoshop CS5 (Adobe). Qualitative micrographs were selected to reflect the mean caliper diameter as determined by in the SUR sample.

Nanoparticle tracking analysis (NTA)

Approximately 300 µl of tissue culture samples were taken by a 1 ml syringe and introduced into the sample chamber through the luer fittings on the top plate of the Nanosight LM10 unit (Nanosight Ltd, Amesbury, UK) fitted with a 635 nm laser. The unit was held vertically and very gentle pressure was applied on the syringe to push the sample in. Sample was left to equilibrate to unit temperature for a moment and then was connected to the microscope and visualised by using the Nanosight's Nanoparticle Tracking Analysis (NTA) 2.2 Analytical software. Three videos of 30-60 seconds were recorded for each sample, with a shutter speed of 30 milliseconds and camera gain of 680. Other software settings vary for different experiments. If the sample concentration was too high and exceeds the analysis limit, a dilution was then made so the software gave a more accurate reading. Backward calculation was then used to get the concentration of the neat sample. In between samples, the chamber was cleaned thoroughly. First of all the sample was extracted via the Luer port, then the sealing nuts securing the top plate was screwed off and the inside of the window was cleaned with lens tissue dampened with 70% ethanol.

Estimation of the size of control beads

Polystyrene latex beads of known sizes were supplied by NanoSight. Approximately 10 µl of 100 nm or 200 nm beads, and 20 µl of 400 nm beads were diluted in 1 ml of PBS. The samples were loaded onto the NanoSight LM10 system and three 30 seconds videos for each sample were captured with camera level 12. The videos were then analysed using the NTA 2.2 software. Software settings for analysis were: Detection threshold: 6. blur: auto, minimum expected particle size: 50 nm.

Estimation of concentration of control beads

The 100 nm control beads (10 µl) were added to 1 ml of PBS in an Eppendorf. Approximately 0.5 ml of the solution was mixed with 0.5 ml PBS to generate a 1 in 2 dilution. 0.5 ml of the newly made solution was mixed with another 0.5 ml PBS to make a 1 in 4 dilution. This was performed once again to make the 1 in 8 dilution. The samples were then loaded onto the NanoSight system and three videos for each sample were captured with camera level 12. The videos were analysed using the NTA 2.2 software with the settings: detection threshold: 6, blur: auto and minimum expected Particle Size: 50nm.

Detection of Taxol and Curcumin induced apoptosis by NTA

The same number of MDA-MB-231 cells was seeded in each well of two 6-well plates. After cells attached to the surface, medium was replaced with serum free medium and 5

μM or 10 μM Curcumin (Sigma) was added accordingly. Two hours after addition of Curcumin, 5 μM or 10 μM paclitaxel/Taxol (Sigma) was added. After 24 and 48 hours, supernatant was collected and centrifuged at 300 x g. The pellets were discarded and supernatant was analysed on Nanosight to detect apoptotic vesicles. The extended dynamic range mode (EDR) was chosen as this mode allows the recording of a set of two videos at the same time with different shutter and gain settings, enabling the simultaneous analysis of large and small particles when highly polydisperse sample are expected. Three videos of 30 seconds were recorded for each sample. Software settings for analysis were: detection threshold: 6 and 10, camera level 12 and 16, blur: auto, minimum expected particle size: 50 nm.

Immunodepletion using Anti-CD9 and anti-CD63 coupled-beads

Approximately 25 μl Dynabeads (sheap anti-mouse IgG from Invitrogen) were washed with 1 ml PBS containing 1% BSA. Eppendorfs were placed in magnetic separator for 1 minute and supernatant was discarded. This was repeated twice and 25 μl of PBS containing 1% BSA was added to resuspend beads. Antibody (15 μl) was added to beads and left at 4 ℃ rotating for 1 hour. Eppendorfs were then taken out and placed on magnetic separator for 1 minute. Antibody-coupled beads were washed with 1 ml PBS containing 1% BSA twice as described before, and then resuspended in 25 μl of PBS containing 1% BSA. MDA-MB-231 cells were grown in tissue culture flasks to 90% confluency and the medium was replaced with serum free RPMI. Supernatant was collected after 48 hours and ultracentrifuged at 300 x g for 10 minutes and then 10,000 x g for 30 minutes. Different amounts of antibody-coupled beads (0 μl, 0.5 μl, 1 μl, 2 μl,

5 µl and 10 µl) were added to each 400 µl of supernatant accordingly. They were incubated together for 3 hours at 4 °*C*. Eppendorfs were then taken out and placed on magnetic separator for 1 minute. The beads were discarded and the supernatant was analysed on Nanosight. Three 30 seconds videos were recorded for each sample using camera level 15. The videos were analysed using the NTA 2.2 software with the settings: detection threshold: 6, blur: auto, and minimum expected particle size: 50nm.

Exosome pull down by antibody-coupled magnetic beads

Dynabeads were prepared as described before. MDA cells were grown to 90% confluency and the supernatant was collected and was spun at 300 x g for 10 minutes, 10,000 x g for 30 minutes and 100, 000 x g for 2 hours. The pellet was then resuspended in 1 ml serum free RPMI and was split into 2 eppendorfs. Either CD9 or CD63-coupled beads (25 µl) was added into each eppendorf. Samples were left on a rotator at 4 °C overnight. Samples were then placed on magnetic separator for 5 minutes, supernatant was then discarded and 200 µl of 0.2 M glycine, pH 2.8 was added into each sample. The samples were then incubated at 37 °*C* for 5 minutes. Samples were taken out and the process was neutralised by adding 5 µl of 2 M Tris, pH 8. Samples were then placed on magnetic separator for approximately 2 minutes. Supernatant was then collected and the beads were discarded. Debris or beads were cleared from the samples by ultracentrifugation at 10,000 x g. The top supernatant from each sample was collected and 500 µl serum free RPMI was added to each sample. Both samples were then analysed on Nanosight. Three 30 seconds videos were recorded for each sample using

camera level 16. The videos were analysed using the NTA 2.2 software with the settings: detection threshold: 6, blur: auto, and minimum expected particle size: 50 nm.

Multiple freezing-thawing of exosomes

CEM cells were grown to 90% confluency and the cell culture medium was replaced with serum free RPMI. Supernatant was collected after 48 hours and was analysed on Nanosight. Multiple freeze-thawing of the exosomes was accomplished by freezing of the sample contacting exosomes in dry ice for approximately 1 minute. Thawing was done by gentle shaking at room temperature for 3 minutes. Approximately 500 µl was taken out after each thawing step before the sample was returned to dry ice. Samples were analysed by NTA. Three 30 seconds videos were recorded for each sample using camera level 16. The videos were analysed using the NTA 2.2 software with the settings: detection threshold: 6, blur: auto, and minimum expected particle size: 50 nm.

Immunofluorescence Microscopy

A few drops of MDA-MB-231 cells, negative scrambled shRNA targeted MDA cells and Rab27a-targetted MDA cells (shRNA 2 and shRNA 3) were seeded on tissue culture dish with cover glass bottom called 'FluroDish^{TM}'. (World Precision Instruments, Hitchin, UK). This was done in duplicates so a total of 8 dishes were prepared. After approximately 20 hours, cells were fixed with 1.5 ml of 4% paraformaldehyde for 15 minutes at room temperature. Cells were then washed 3 times at 5 minutes intervals with PBS containing 0.1 M Glycine. Cells were then

permeabilized with PBS conatining 0.2% BSA and 0.05% Saponin for 5 minutes at room temperature. Cells were then rinsed with PBS. Primary anti-CD63 mouse monoclonal antibody (1 μg/ml) (Santa Cruz) was added and incubated for 1 hour at room temperature. Cells were then washed 3 times with PBS at 5 minutes intervals. Secondary Donkey-Anti-Mouse FITC antibody was added and incubated for approximately 1 hour. Cells were then washed with PBS for 3 times at 5 minutes intervals. PBS was then removed and 1 drop of Vectashield with DAPI (Vector Laboratories, Peterborough, UK) was added to each dish. Then immediately a siliconized circle coverslide (Hampton Research, Aliso Viejo, USA) was put onto the dish and edges were sealed with nail vanish. Slides were viewed under 100 x magnification under a fluorescence microscope.

RNA Purification and quantification

RNA was purified using RNeasy® Mini kit (Qiagen) following manufacturer's instructions and the concentration was measured on Nanovue (Nanovue 4282 V1.7.3, GE Healthcare, Little Chalfont, UK). Briefly, cells were pelleted and 350 μl of RLT buffer was added to each cell pellet. Cells were then homogenised to reduce lysate viscosity by shearing high molecular weight genomic DNA and cellular components with a 21-gauge needle for 10 times. Approximately 350 μl of 70% ethanol was then added. All 700 μl of each sample was transferred to a silica column in a 2 ml collecting tube and spun for about 3000 x g for 15-30 seconds on a desktop centrifuge to allow the RNA to bind to the columns. Liquid was then discarded and the column was washed with 700 μl RW1 buffer. Samples were centrifuged again the columns were washed

again in RW1 buffer. They were then spun and washed twice with 500 µl RPE buffer. After the last wash, the columns were spun for 2 minutes instead of 30 seconds. The column was then transferred to new 1.5 ml tubes with the lids cut off. Sterile water (30 µl) was added to each column and after centrifugation for 1 minute, the RNA was eluted. Samples were then stored at -80 °C straight away.

cDNA conversion

Total RNA (0.5 µg) was used to reverse-transcribe into cDNA. Each sample was made up to a final volume of 8 µl with DNAse-free water. Approximately 1.5 µl of buffer and 5 µl of DNase 1 enzyme were added (All from Roche). Samples were left in the PCR machine for 30 minutes. After 30 minutes, samples were taken out and 1 µl of RQ1 DNAse stop solution (Promega) was added. Samples were then heated at 65°C in the PCR machine for 10 minutes. Approximately 4 µl of RNA was taken out and mixed with 20 µl distilled water and 2 µl Hexanucleotide Mix (Roche). Samples were heated on the PCR machine for 10 minutes at 65°C. Samples were taken out and put on ice. Approximately 1 µl RNase inhibitor, 8 µl 5x RT buffer, 4 µl deoxynucleoside triphosphates (DNTPs) and 1 µl reverse transcriptase enzyme (all from Roche) was added to all samples, which were then heated at 25 °C for 10 minutes, 55 °C for 30 minutes and 95 °C for 2 minutes on the PCR machine.

RT-PCR

PCR was performed using ReadyMix^{TM} Taq PCR Reaction Mix (Sigma). The table below show the amount of reagent added.

	Samples	Negative control
Master mix	12.5 µl	12.5 µl
dH_2O	9.5 µl	10.5 µl
Primer (forward)	1 µl of 10 µM stock	1 µl of 10 µM stock
Primer (Reverse)	1 µl of 10 µM stock	1 µl of 10 µM stock
cDNA	1 µl	/

Table 2.2: Components of the reaction mix used for RT-PCR.

The Rab27a and β-actin primers used were as follows: Rab27A forward primer: 5'-GCCACTGGCAGAGGCCAG-3'; Rab27A Reverse primer: 5'-GAGTGCTATGGCTTCCTCCT-3'; β-actin forward primer: 5'-AATATGGCACCACACCTTCTACA-3'; β-actin reverse primer: 5'-CGACGTAGCACAGCTTCTCCTTA-3'.

Primer sequences were based on Herrero-Turrión, et al (Herrero-Turrion et al., 2008). PCR amplification was as follows: 1 cycle as initial denaturation at 95 °C for 3 minutes, denaturation at 95 °C for 30 seconds, annealing at 62 °C for 30 seconds, extension at 72 °C for 1 minute (35 cycles of denaturation, annealing and extension in total), and final extension at 72 °C for 10 minutes. For PCR using Rab27b primers (Santa Cruz), annealing was performed at 59 °C for 30 seconds and all other steps were the same as

Rab27a. 5 µl loading buffer (Bioline) was added to each of the 25 µl PCR products and 10 µl of which was loaded onto a 2% agarose gel in 1X TAE buffer and visualised by ethidium bromide staining on an ultraviolet (UV) transilluminator.

Loading of Fluorescent siRNA onto exosomes

Exosomes (7 µg) derived from MDA-MB-231 cells and 500 nM 'AllStars Negative Control siRNA, Alexa Fluor 488' (Qiagen) were mixed with various volume of electroporation buffer to make final volume of 200 µl. The composition of the electroporation buffer is listed below: 1.15 mM potassium phosphate pH 7.2 (To make up 10 ml of a stock of 1 M potassium phosphate buffer with pH 7.2, mix 7.17 ml 1 M K_2HPO_4 and 2.83 ml 1 M KH_2PO_4), 25 mM potassium chloride (KCL) (Sigma), and 21% Optiprep (Sigma). For all experiments, the samples were electroporated in a 4 mm cuvette at 125 µF, 400 Volts or 500 µF, 400 volts. For loading of the 'AllStars Negative control siRNA' onto exosomes, a sample of exosomes with siRNA added but was not electroporated was also prepared as a negative control. And each sample was then separated into two parts, 300 µl filtered PBS was added to one part of each sample and was analysed by flow cytometry. Filtered PBS (4 ml) was added to the other part of each sample and ultracentrifugation at 100, 000 x g was performed. The resulting pellet from each sample was then resuspended in 400 µl filtered PBS and was analysed using flow cytometry.

Loading of Rab27a or Erap1 siRNA onto exosomes

Exosomes (7 µg) from MDA-MB-231 cells or Jurkat T cells was added to electroporation buffer to make up final volume of 200 µl in 4 mm cuvettes. Different volume of Rab27a siRNA (Santa Cruz), or Erap1 (Santa Cruz) siRNA, or 'AllStars negative control' siRNA was also added. Samples were then electroporated at 500 µF, 400 volts. Samples were then washed in 4 ml filtered PBS. Ultracentrifugation at 100,000 x g was then performed for 2 hours to pellet the exosomes with encapsulated siRNA. The supernatant was discarded and the pellet was re-suspended in 30 µl filtered PBS. All samples were then added to either MDA-MB-231 cells or HeLa cells in a 6-well plate (90% confluency). Cells were also transfected with different volume of Lipofectamine 2000 as a positive control. Supernatant was removed after 24 hours and the cells were lysed directly in lysis buffer by using the wide end of a yellow tip to gently scrape the cells off. Samples were incubated for 20 minutes on ice. ultracentrifugation at 20,000 x g was then performed for 5 minutes to get rid of debris. Supernatant was kept and the pellet was discarded. The concentration of samples was measured by using the Bradford method. Protein (20 µg) was loaded either onto a 12% gel (for checking Rab27a knock down) or an 8% gel (for checking erap1 knock down), the gel was ran at 150 V for approximately 1 hour and transferred to a nitrocellulose membrane at 100V for 30 minutes. Blocking buffer was added to the membrane and incubated for 20 minutes on a shaker. Rab27a mouse monoclonal antibody (Sigma) or 6H9 anti-Erap1 mouse monoclonal antibody (R&D Systems, Abingdon, UK) was added to the membrane and left shaking overnight at 4 °C. The membrane was then washed with PBS-tween for 1 hour at 20 minutes intervals. Secondary antibody was added and

incubated at room temperature for 20 minutes. The membrane was then washed again for 1 hour at 20 minutes intervals. Antibody binding was then visualised with Fujifilm Intelligent Dark Box LAS-3000.

Treatment of cells with 5-(*N*,*N*-Dimethyl) amiloride hydrochloride (DMA)

Approximately 50,000 MDA-MB-231 cells were seeded into each well of a six-well plate. After the cells were approximately 50 % confluent, the medium was replaced with serum free medium and different concentrations of DMA (Sigma, UK) was added to cells. Cells with no DMA added were used as a control. After 24 hours, the supernatant was collected and centrifugation was performed at 300 x g for 10 minutes then 10, 000 x g for 30 minutes. The resulting supernatant was then analysed by using NTA.

Lipidomics analysis of exosomes derived from MDA-MB-231 cells and the parental cells

Lipidomics was performed by Dr Terrence Smith in the Biomedical Sciences Research Complex (BSRC), University of St. Andrews. Briefly, MDA-MB-231 cells were detached by incubating with 5mM EDTA for approximately 4 minutes. Cells were then pelleted after centrifugation at 300 xg. Cells were washed in PBS and re-suspended in 100 µl PBS. Exosomes were collected by using sequential centrifugation and ultracentrifugation described earlier. The 100, 000 x g pellets were re-suspended in 100 µl PBS. Lipids from cells and exosomes were extracted by the Bligh-Dyer method**,** i.e.

with chloroform/methanol (1:2), and the lipids were analysed using an Absceix 4000 QTrap, a triple quadrupole mass spectrometer equipped with a nanoelectrospray source.

Chapter III: Studying Exosomes and Microvesicles using Flow Cytometry, Western Blot and Lipidomics.

Introduction

The two tumour cells lines used in this chapter were MDA-MB-231 and MCF7. The MDA-MB-231 breast cancer cell line was obtained from the pleural effusions of a Caucasian breast cancer patient in 1973 at the M. D. Anderson Cancer Centre. The MDA-MB-231 cell line is estrogen receptor (ER), progesterone receptor (PR) and Human Epidermal Growth Factor Receptor 2 (HER2/ERBB2) triple negative. The tumour type is a metastatic adenocarcinoma and it is a basal B subtype. MCF7 is a breast cancer cell line isolated in 1970 from a 69-year-old Caucasian woman. The MCF7 cell line is ER and PR positive and has HER2 overexpression. The tumour type is a metastatic adenocarcinoma and it is luminal subtype (Kao et al., 2009).

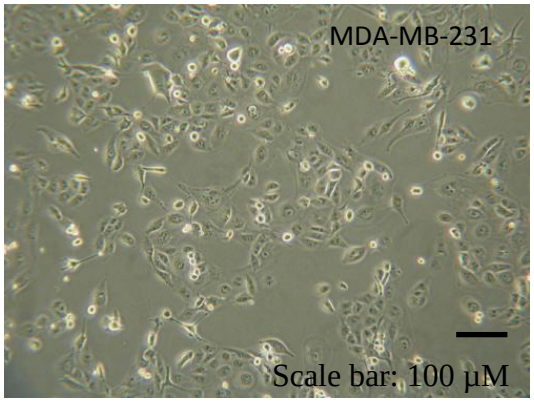

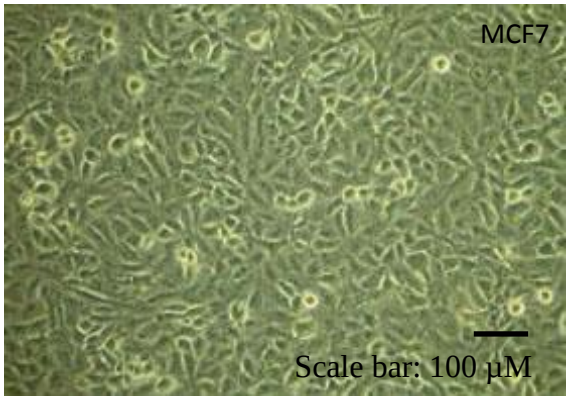

	MDA-MB-231	MCF7
Origin	Isolated from pleural effusions of a 51 year old Caucasian female	Isolated from pleural effusions of a 69 year old Caucasian female
Cell type	Epithelial (Adenocarcinoma)	Epithelial (Adenocarcinoma)
Hormone receptor status	ER, PR and HER2/ERBB2 triple negative	ER and PR positive with HER2 over-expression
Invasiveness	Highly invasive	Weakly invasive

Figure 3.1: Examples of images and summary of the two breast cancer cell lines used in this study.

Jurkat cell line is an immortalized line of T lymphocyte cells; it was isolated from the peripheral blood of a 14 year old boy with T cell leukemia in the late 1970s. The human lymphoid CEM T-cell line has also been used in this study.

The aim of this chapter was to confirm the presence of exosomes in our conditioned cell cultures preparations by western blotting, electron microscopy and flow cytometry.

It has been reported that tumour-secreted exosomes have immunosuppressive functions. Exosomes derived from tumour cell lines bear Fas ligand (FASL) that can induce T cell apoptosis leading to suppression of T-cell responses *in vitro* (Abusamra et al., 2005). Tumour derived exosomes have also been shown to express NKG2D ligands such as MICA and possibly MICB, which down regulates NKG2D and supresses the function of $CD8^+$ T cell or NK cell (Clayton et al., 2008).

To determine whether MDA-MB-231 and MCF7 secreted exosomes affect the growth of T cells and investigate whether they are consistent with Abusamra et al and Clayton et al's findings, exosomes derived from both tumour cell lines were added to Jurkat cells.

Results

Exosomes exist in our 100,000 x g preparation

Cell supernatants were collected and centrifuged at 300 x g for 10 minutes, 10,000 x g for 30 minutes and 100,000 x g for 2 hours. The pellet was then resuspended in PBS. To confirm the presence of exosomes in our preparation, the resuspended pellet was analysed by immunoblotting to check for the characteristic exosomal markers Alix and Tsg 101. MHC class I has also been detected in both cell lines, although the MCF 7 cell line express low levels of MHC class I, and even lower levels were detected on MCF 7 exosomes (Figure 3.2).

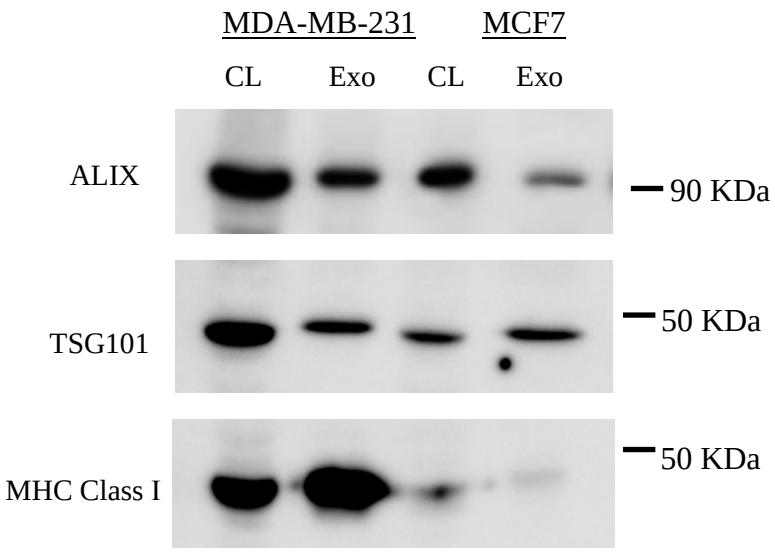

Figure 3.2: Western Blot of MDA and MCF7 Exosomes. Cells were lysed and protein concentration was measured using the Bradford method. Equal amount of protein of cell lysates (CL) and exosomes (Exo) were loaded onto a 12% gel. Membranes were probed with the indicated antibodies and then Fujifilm Intelligent Dark Box LAS-3000.

An analysis of a sample of the MDA exosome preparation with electron microscopy also revealed typical cup-shaped exosomes (Figure 3.3). This indicates that exosomes are present in our preparations.

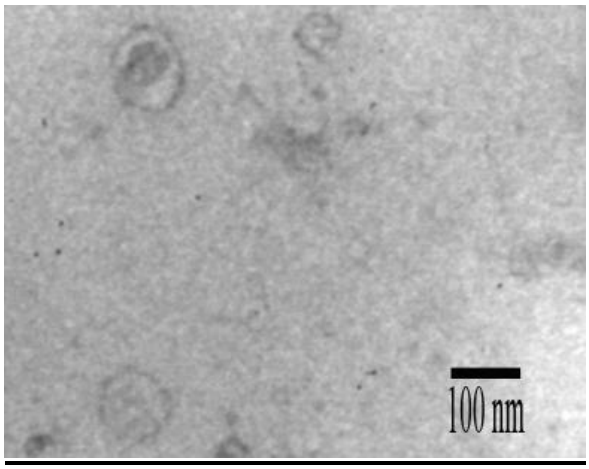

Figure 3.3: Electron Microscopy of MDA Exosomes. Typical cup-shaped exosomes are present in our preparation. Electron microscopy was performed by Dr John Lucocq.

To illustrate the inherent problems (limitivity to detect particles lower than 200 nm) associated with analysing exosomes and microvesicles by flow cytometry, MDA-MB-231 cells were grown to 90% confluence and the medium was replaced with serum free medium. After 48 hours, the supernatant was collected and centrifuged at 300 x g for 10 minutes, 10,000 x g for 30 minutes and 100,000 x g for 2 hours. The supernatant after each centrifugation was kept and analysed on a FACScan flow cytometer. PBS, 48 nm, 100 nm, 410 nm beads and serum free medium were used as controls.

A

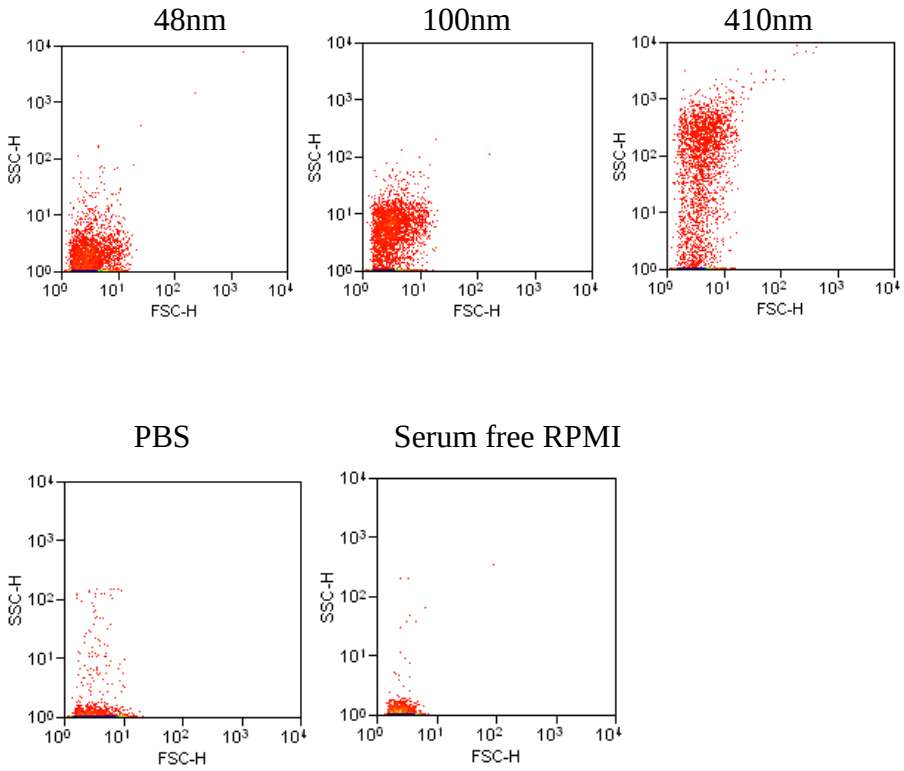

B

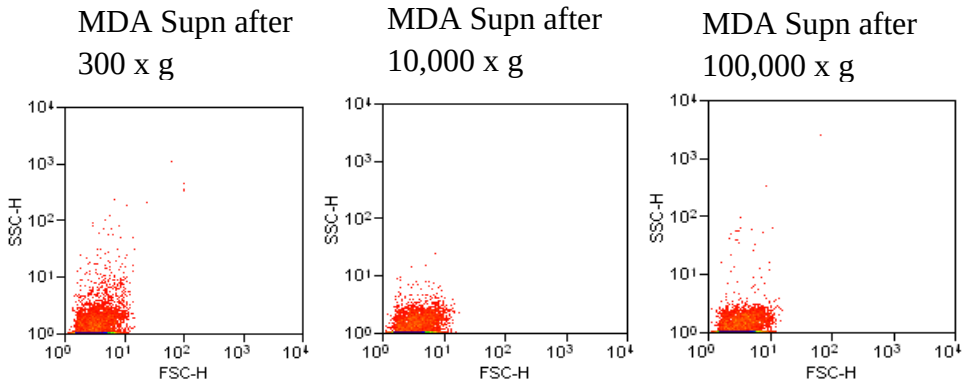

Figure 3.4: Flow Cytometry Analysis of beads, controls and MDA supernatant. (A). 48 nm, 100 nm and 410 nm beads were measured using flow cytometry. PBS and serum free RPMI was used as background control. **(B).** Medium was replaced with serum free medium when MDA cells reached 90% confluence, supernatant was collected after 48 hours and centrifuged at 300 x g, 10,000 x g and 100,000 x g. Supernatant was collected after each centrifugation and analysed by flow cytometry.

48 nm and, to a lesser extent, 100 nm beads display signals that overlap with the control PBS sample and the control serum free medium sample (Figure 3.4A). There was a reduction in the signal after 10,000 x g and 100,000 x g ultracentrifugation of cell supernantants. Comparing the supernatant after 10,000 x g and the supernatant after 100,000 x g, we can see some material was depleted after the 100,000 x g ultracentrifugation and the material was within the correct size range of exosomes when compared with the control beads (Figure 3.4B). Although all the samples do overlap with the background noise, the data did reveal that exosome-sized particles existed in the tissue culture supernatant preparations.

Adding antibiotics to MDA-MB-231 cells.

We wanted to study antibiotic-induced exosome/microvesicle release. Antibiotics including G418 and Hygromycin were used in this experiment.

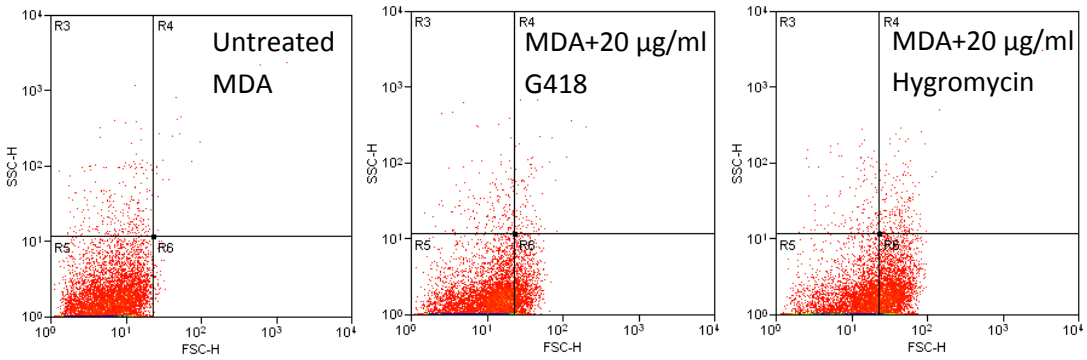

Figure 3.5: Adding antibiotics to MDA-MB-231 cells. 60 µl of G418 and 60 µl of Hygromycin were added to 3 mls of MDA cells in a 6 well plate. Supernatant was then collected after 72 hours and centrifuged at 300 x g and then analysed on the Facs machine to study antibiotics induced microvesicle release.

The increase in side scatter observed in Figure 3.4A when using synthetic polystyrene beads does not always reflect the data seen in real exosome and microvesicle samples. Primarily this is because the synthetic beads do not allow laser light to pass through them, so disperse light mostly in side scatter. An example of the more complex signals seen in both forward and side scatter profiles in 'real' vesicles can be detected when antibiotics are added to cell cultures. For example, we added antibiotics to MDA cells, and observed the population of microvesicles shifted to the right (FSC) (Figire 3.5). Interestingly, if the side scatter is a better indicator of size when analysing small nanoparticles, then it is tempting to assume that G418 and Hygromycin does not necessarily affect the size of the microvesicles released, but has increased the complexity of the microvesicles.

Exosomes derived from MDA-MB-231 and MCF 7 cells induce apoptosis of Leukaemic Jurkat T cell line as identified by Annexin V staining.

The induction of apoptosis of immune cells by tumour-derived exosomes has been previously reported. To investigate whether our tumour-cell derived exosomes can affect the growth of T lymphocytes, exosomes derived from MDA-MB-231 cells and MCF 7 cells were added to the Jurkat T cell line. Annexin V staining shows an increase in apoptosis in Jurkat cells following treatment with exosomes derived from MDA-MB-231 and MCF 7 cells, with MDA-derived exosomes being more potent than MCF7 exosomes.

A

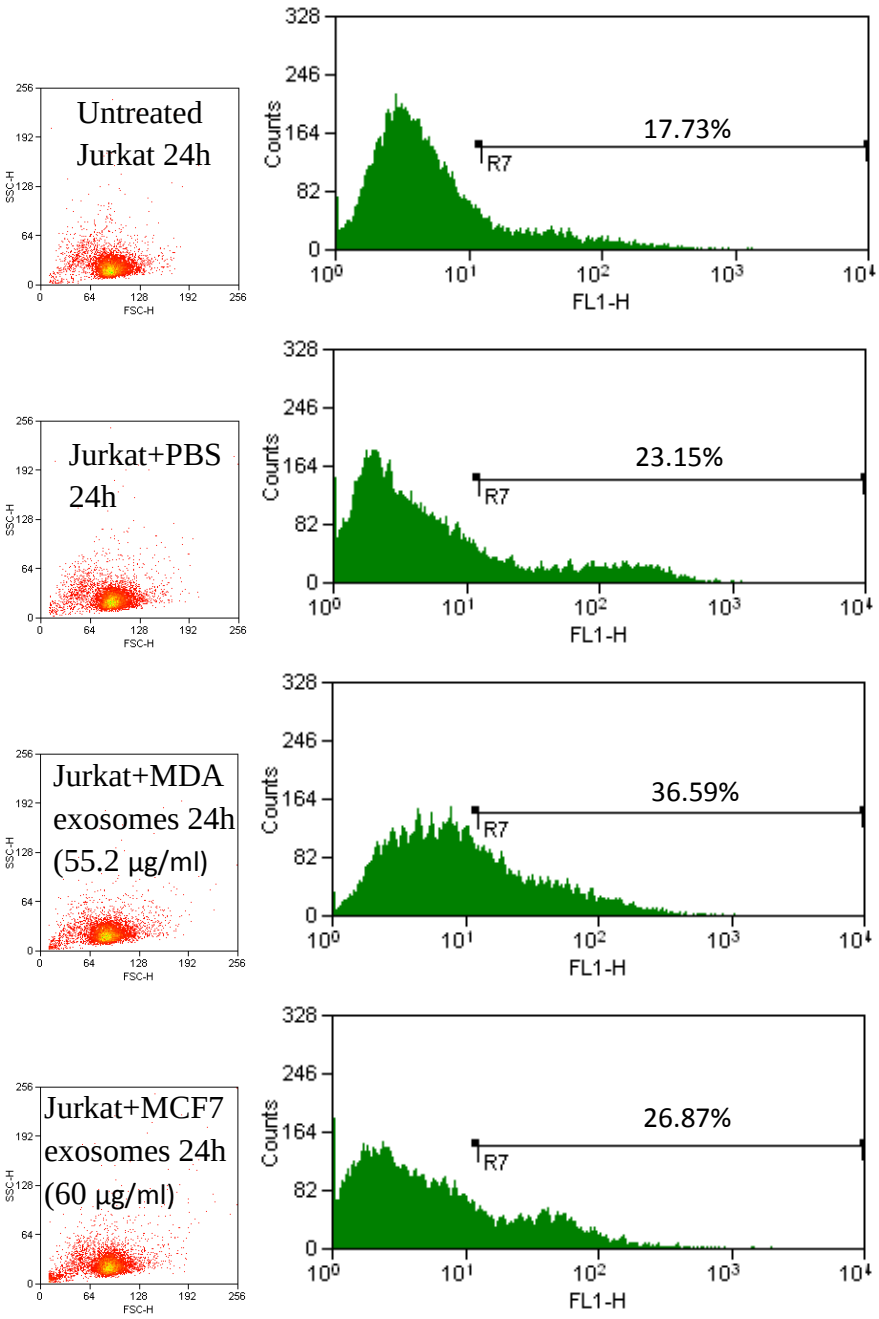
Untreated Jurkat 24h
17.73%
Jurkat+PBS 24h
23.15%
Jurkat+MDA exosomes 24h (55.2 µg/ml)
36.59%
Jurkat+MCF7 exosomes 24h (60 µg/ml)
26.87%
R7
Counts
FL1-H
SSC-H
FSC-H

B

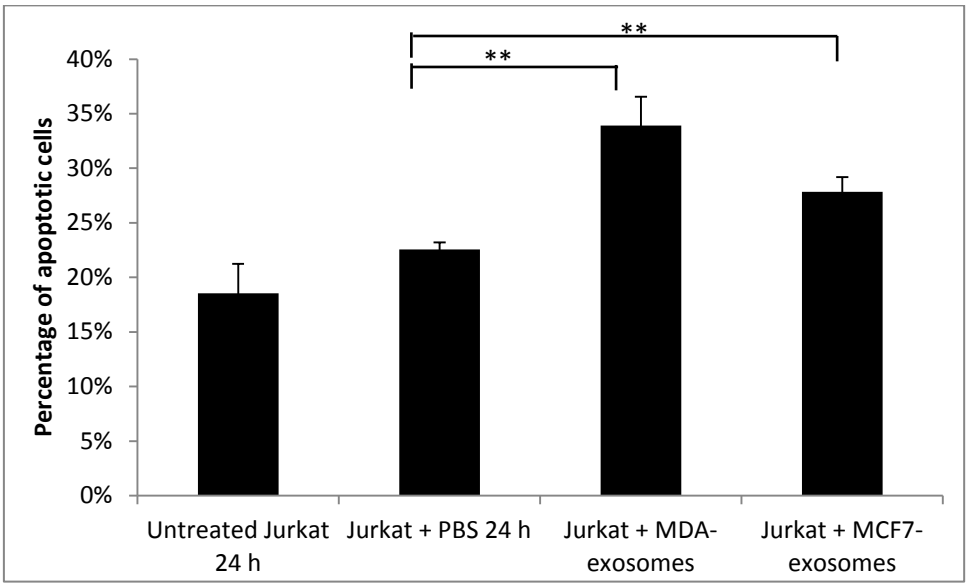

Figure 3.6: Annexin-v staining of untreated Jurkat cells and Jurkat cells treated with MDA and MCF7 exosomes. Approximately 500,000 Jurkat cells were seeded into each of the 4 wells of a 6 well plate. MDA and MCF 7 exosomes were added into 2 of the wells and PBS added to another. After 24 hours, 250 µl of Jurkat cells were harvested and spun down on desktop microfuge, Pellets were resuspended in 500 µl of binding buffer, 5 µl of Annexin V-FITC were added and incubated for 5 minutes. Samples were then analysed by using flow cytometry. Experiment was performed three times. **(A).** One representative experiment result was shown. **(B)**. Bar chart of comparison of percentage of apoptotic cells between samples from three experiments. Error bars indicate standard deviation. ** $P<0.01$

After 24 hours, 36.59 % of the Jurkat cells were apoptotic after addition of exosomes derived from MDA-MB-231 and 26.87 % of the Jurkat cells were apoptotic after the addition of exosomes derived from MCF 7, whereas the apoptotic cells were 17.73 % and 23.15 % accordingly in the control untreated Jurkat cell and Jurkat cells with PBS added (Figure 3.6A). The differences are statistically significant (Figure 3.6B). Thus our purified preparations of exosomes display previously reported characteristic behaviour, further confirming their identity.

MDA-MB-231 and MCF 7 cells-conditioned medium (supernatant) induces apoptosis of Jutkat T cells

To further investigate the effect of tumour cell-derived exosomes on cell cycle and apoptosis, cell conditioned medium, rather then purified exosomes, from MDA-MB-231 and MCF7 cells were added to Jurkat cells, which were then subsequently stained with propidium iodide. Apoptosis in Jurkat cells was detected as a sub-G0 population in flow cytometric analysis and the percentage of apoptotic cells were gated and calculated by using Summit software.

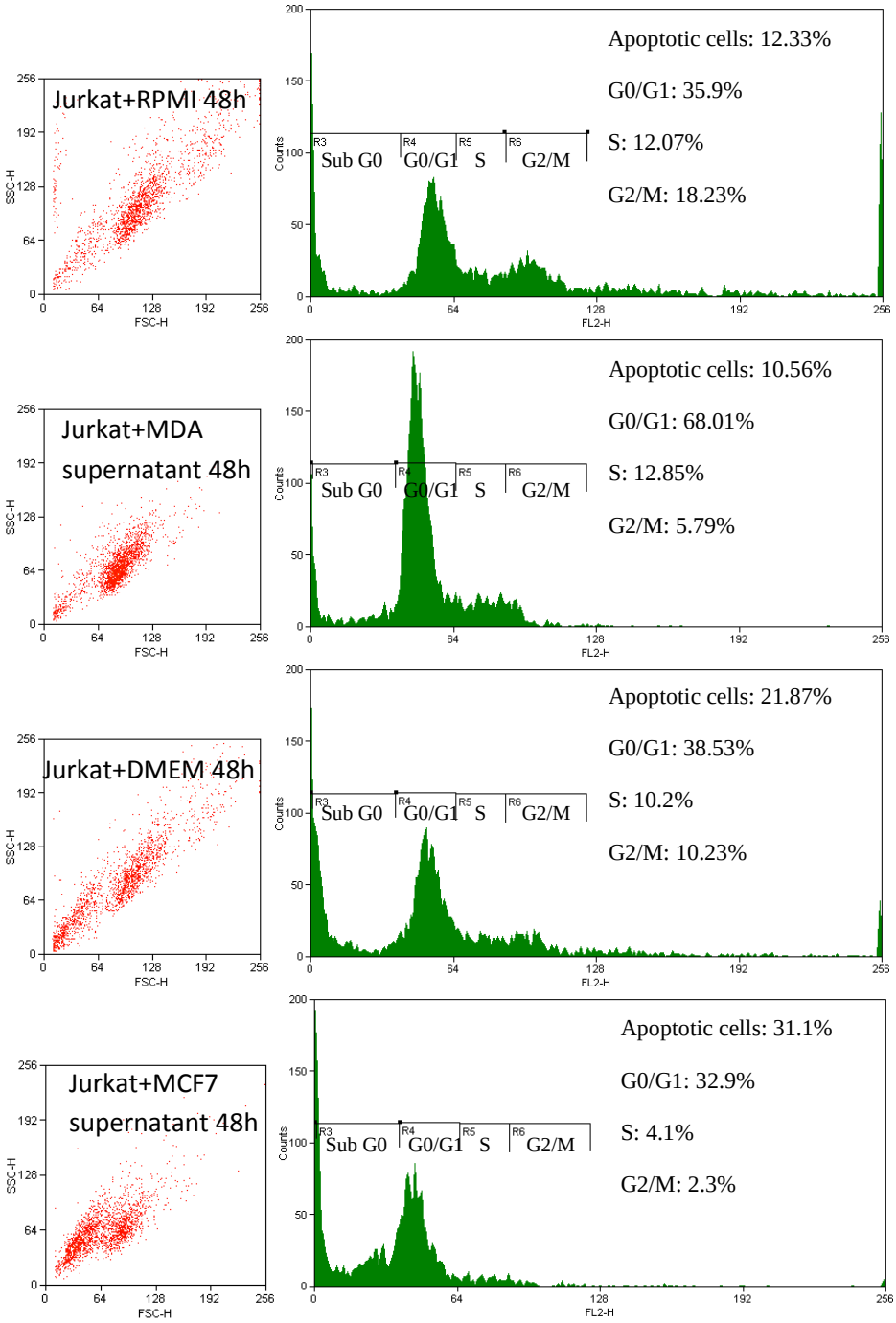

Figure 3.7: Comparison of adding unconditioned MDA/MCF7 medium and conditioned MDA-MB-231/MCF7 medium to Jurkat cells. Approximately 10 mls of medium and supernatant was spun at 300 x g for 10 minutes, then 10,000 xg for 30 minutes. The supernatant was then added to Jurkat cells. After 48 hours, cells were washed withice-cold PBS, fixed with 70% ethanol, washed twice with ice-cold PBS and then stained with PI for 30 minutes. Data are representative of two experiments.

Adding 48 hour MDA-MB-231 supernatant/conditioned medium to Jurkat cells did not induce more apoptosis (10.56%) compare to the Jurkat cells with unconditioned serum free RPMI medium added (12.33%), whereas adding 48 hour MCF 7 supernatant to Jurkat cells has increased the number of apoptotic cells to 31.1% from 21.87% with the unconditioned serum free DMEM medium added (Figure 3.7). The G0/G1 peak was dramatically increased after addition of MDA-MB-231 cells-conditioned medium to 68.01% compared to 35.9% after addition of RPMI medium (Figure 3.7, first and second panel), whereas adding MCF7-conditioned medium did not increase the G0/G1 peak compared to the addition of DMEM medium (Figure 3.7, third and fourth panel). G2/M phase fraction was 18.23% and 10.23% in the control groups (with addition of RPMI and DMEM), respectively, but decreased significantly to 5.79% and 2.3% after the addition of conditioned medium derived from MDA-MB-231 cells and MCF7 cells.

MDA-MB-231 and MCF 7 cells-derived exosomes induces apoptosis of Jurkat T cells identified by PI staining.

To confirm the exosomes-induced Jurkat cell apoptosis, MDA-MB-231 and MCF 7-derived exosomes were added to Jurkat cells. Because our exosomes were resuspended in PBS, PBS was added to Jurkat cells as a control. Apoptosis in Jurkat cells was detected by PI staining and appeared as a sub-G0 population in flow cytometric analysis and the percentage of apoptotic cells were gated and calculated by using Summit software.

A

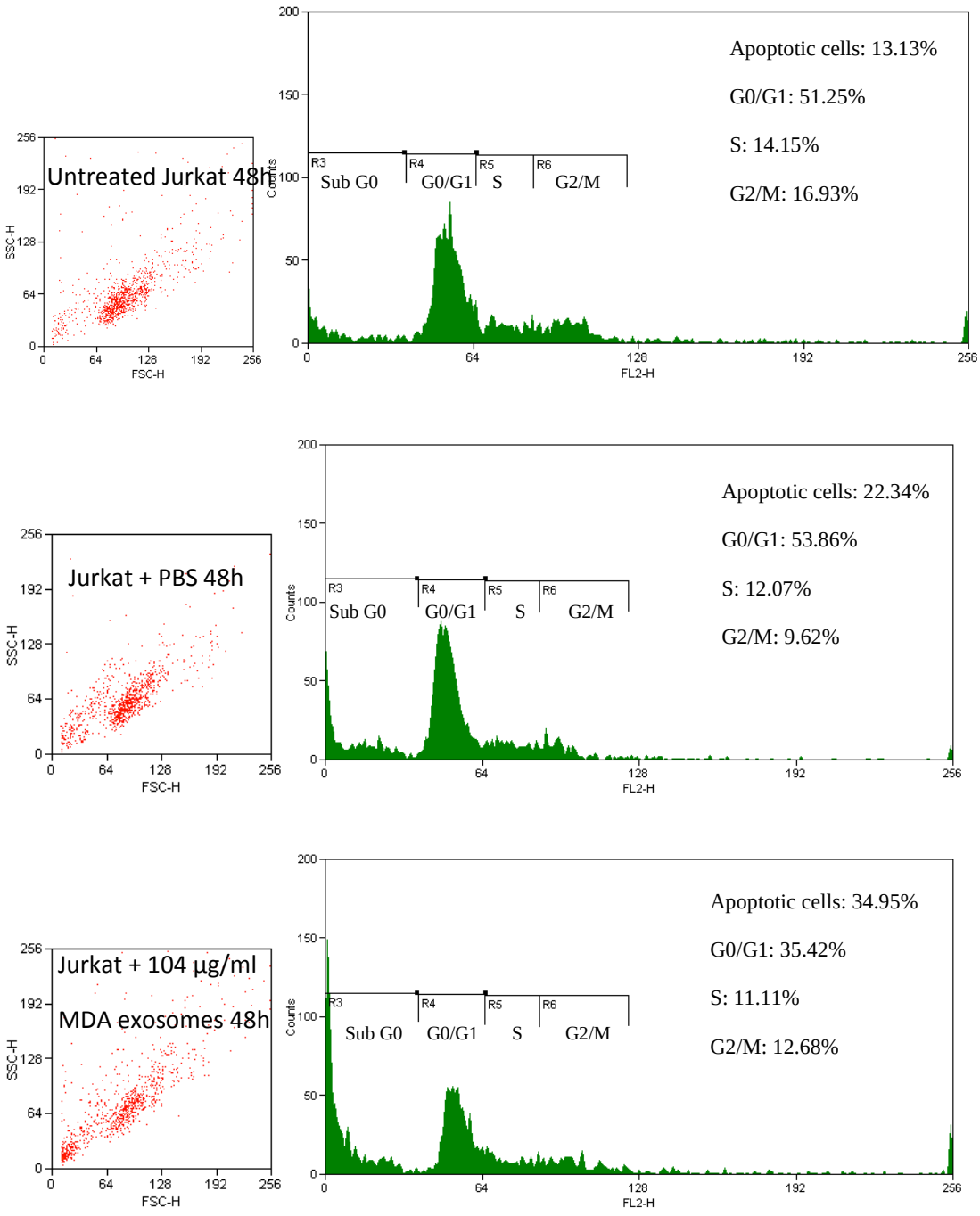
Untreated Jurkat 48h
Apoptotic cells: 13.13%
G0/G1: 51.25%
S: 14.15%
G2/M: 16.93%
Jurkat + PBS 48h
Apoptotic cells: 22.34%
G0/G1: 53.86%
S: 12.07%
G2/M: 9.62%
Jurkat + 104 µg/ml
MDA exosomes 48h
Apoptotic cells: 34.95%
G0/G1: 35.42%
S: 11.11%
G2/M: 12.68%
R3 Sub G0
R4 G0/G1
R5 S
R6 G2/M
SSC-H
FSC-H
Counts
FL2-H

B

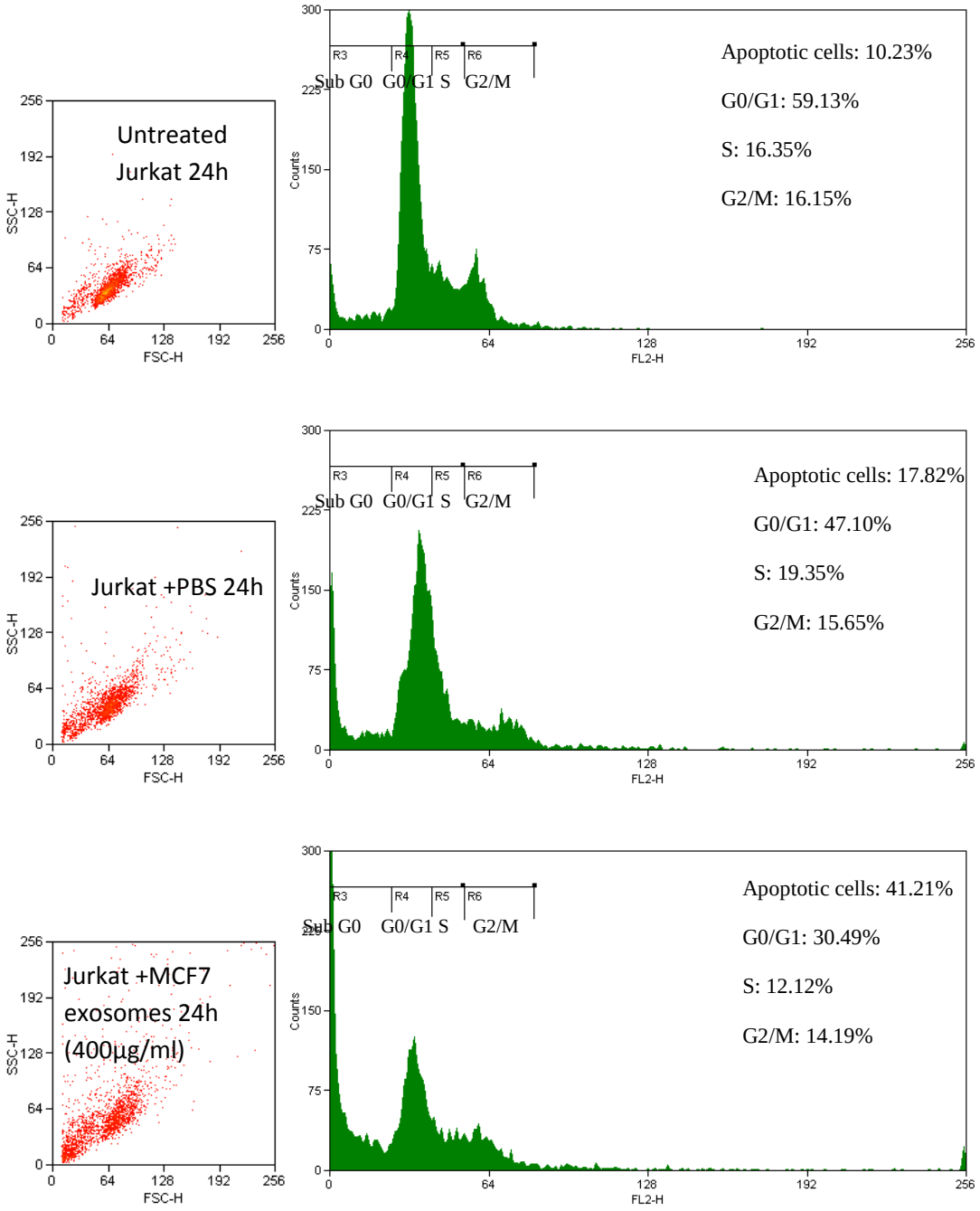
Untreated
Jurkat 24h
SSC-H
FSC-H
Counts
FL2-H
R3
R4
R5
R6
Sub G0
G0/G1
S
G2/M
Apoptotic cells: 10.23%
G0/G1: 59.13%
S: 16.35%
G2/M: 16.15%
Jurkat +PBS 24h
Apoptotic cells: 17.82%
G0/G1: 47.10%
S: 19.35%
G2/M: 15.65%
Jurkat +MCF7
exosomes 24h
(400µg/ml)
Apoptotic cells: 41.21%
G0/G1: 30.49%
S: 12.12%
G2/M: 14.19%

C

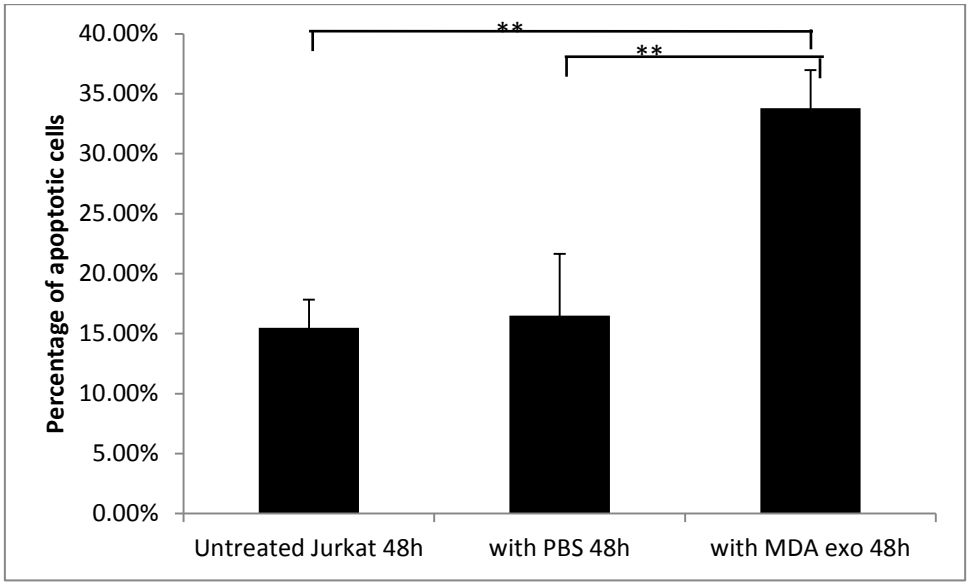
**
**
40.00%
35.00%
30.00%
25.00%
20.00%
15.00%
10.00%
5.00%
0.00%
Percentage of apoptotic cells
Untreated Jurkat 48h
with PBS 48h
with MDA exo 48h

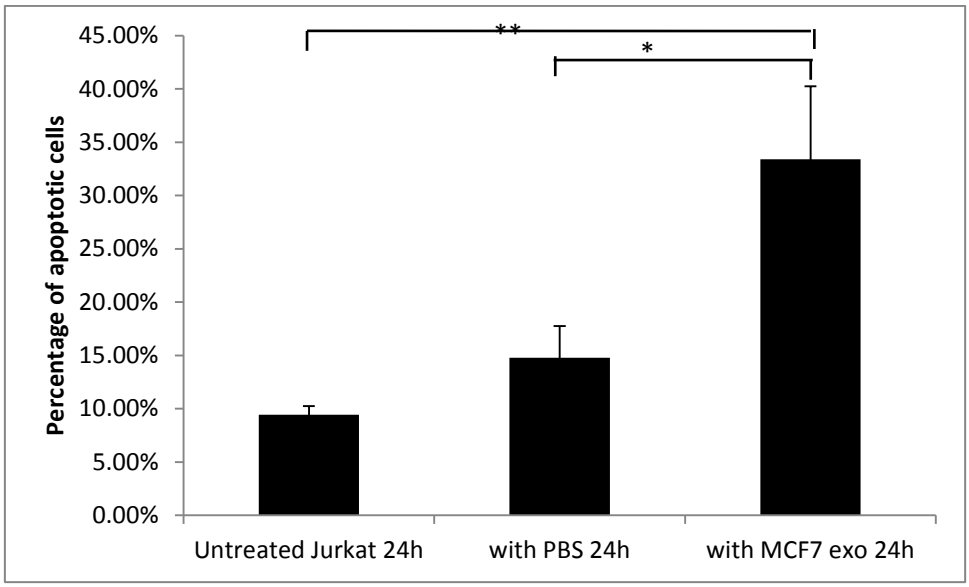
**
*
45.00%
40.00%
35.00%
30.00%
25.00%
20.00%
15.00%
10.00%
5.00%
0.00%
Percentage of apoptotic cells
Untreated Jurkat 24h
with PBS 24h
with MCF7 exo 24h

D

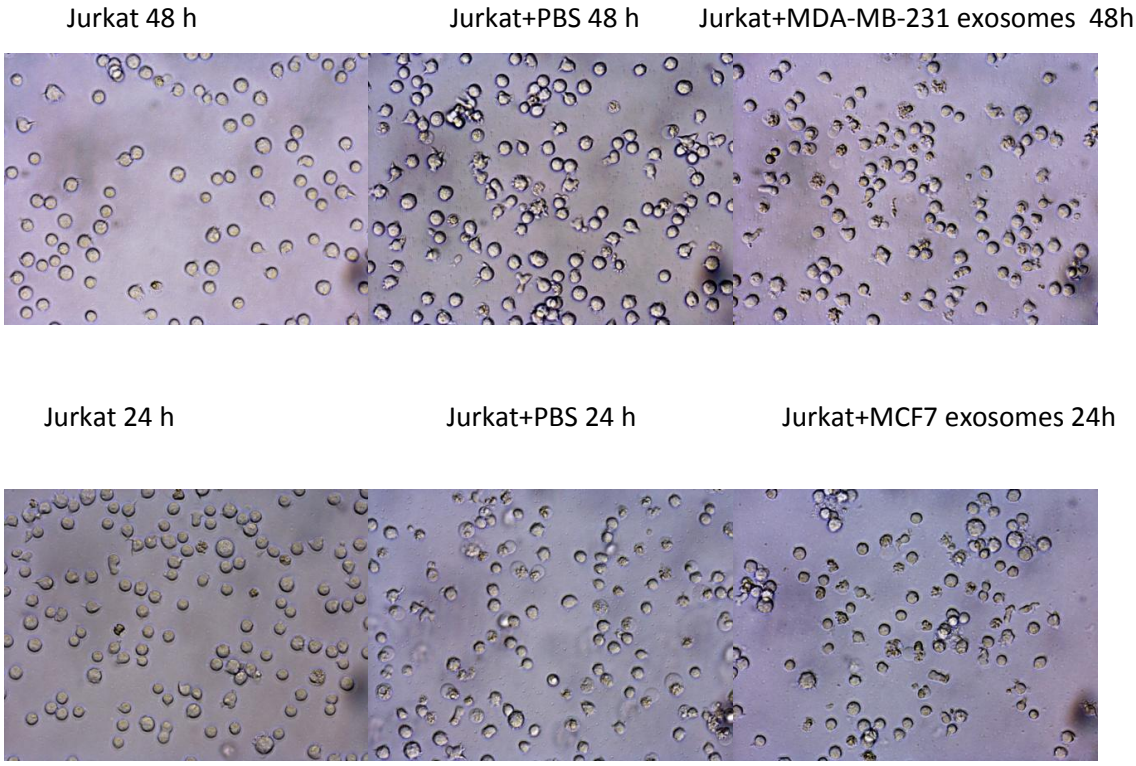

Figure 3.8: PI staining of MDA-MB-231 and MCF 7 derived exosomes induced Jurkat cell Apoptosis. (A) 250 µl of MDA exosomes (52 µg) was added to 250 µl of Jurkat cells. Jurkat cells with PBS added was used as control. After 48 hours, Jurkat cells were fixed then stained with PI. **(B)** MCF7-derived exosomes were added to Jurkat cells (final exosomes concentration 400 µg/ml. Jurkat cells were fixed and stained with PI after 24 hours. Data are representative of three independent experiments. **(C).** Percentage of apoptotic cells calculated from three experiments. Error bars indicate standard deviation. * $P<0.05$ ** $P<0.01$. **(D).** Images of untreated Jurkat cells and Jurkat cells treated with exosomes derived from MDA-MB-231 and MCF 7 cells.

After 48 hours, 13.13% of untreated Jurkat cells and 22.34% of Jurkat cells treated with PBS were apoptotic as measured by the sub-G0 phase fraction. Incubation of 104 µg/ml MDA-MB-231 exosomes with Jurkat cells for 48 hours has increased the number of

apoptotic cells to 34.95 % (Figure 3.8A). Microscopic images show changed morphology of apoptotic cells (Figure 3.8C, first panel). After 24 hours, 10.23% of untreated Jurkat cells and 17.82% of Jurkat cells treated with PBS were apoptotic. Incubation of 400 μg/ml MCF7 exosomes with Jurkat cells for 24 hours has dramatically increased the number of apoptotic cells to 41.21 % (Figure 3.8B). The percentage of apoptotic cells after tumour exosomes treatments were significantly different from that from untreated controls or cells treated with PBS. (Figure 3.8C) Images show increased number of apoptotic cells compare to untreated cells (Figure 3.8D, second panel).

Detection of CD9 and CD63 positive vesicles in our preparation by CFSE and PE double staining.

CD9 and CD63 are both members of the tetraspanin family. They are typically found on the surface of exosomes. We wanted to confirm the presence of CD63 and CD9 on MDA-MB-231 cells and find out the percentage of CD9 and CD63 positive particles. The cells were incubated with mouse monoclonal CD9 or CD63 antibodies and a fluorescent FITC-anti-mouse secondary antibody and then analysed by flow cytometry.

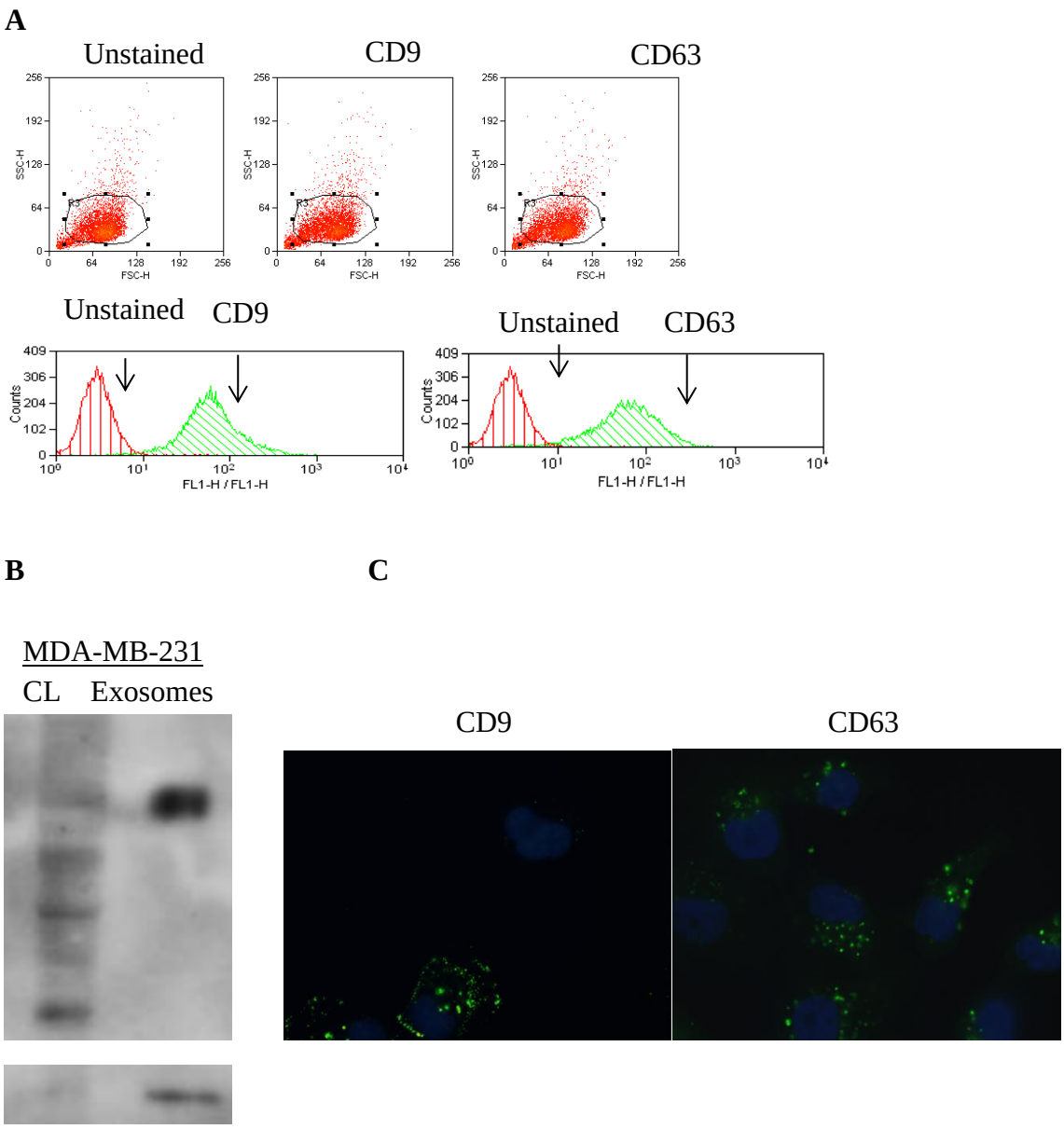

Figure 3.9: Confirmation that CD9 and CD63 are present on MDA-MB-231 cells and are more enriched in exosomes (A). Expression of CD9 and CD63 on MDA-MB-231 cells were analysed by flow cytometry. MDA-MB-231 cells were pelleted, stained and analysed by flow cytometry. **(B)**. Expression of CD9 and CD63 on MDA-MB-231 cells and on exosomes were analysed by western blot. **(C).** CD9 is mainly expressed at the cell surface and some intracellular compartments. **(D).** CD 63 accumulates at intracellular compartments only (multivesicular bodies).

The flow cytometry results indicate that MDA-MB-231 cells do express CD9 and CD63 as a very significant shift has been observed for both antibodies (Figure 3.9A). Nevertheless, when analysing 5 µg of cell lysate protein by western blotting, the bands for both CD9 and CD63 were very faint, or even invisible, whereas the signal for both protein in exosomes was very strong (Figure 3.9 B). These results indicate that CD9 and CD63 are present on MDA-MB-231 cells and are highly enriched on MDA-MB-231 cell-derived exosomes. Unexpectedly, the cellular distribution of CD9 and CD63 as determined by fluorescence microscopy was significantly different. CD9 was mainly expressed in patches on the plasma membrane and also in some intracellular compartments (possibly MVB) (Figure 3.9C left panel). CD63 accumulates at intracellular compartments only (MVBs) and is not found at the plasma membrane (Figure 3.9C right panel).

Our preparation is likely to be a mixed population of exosomes and other types of microvesicles or subtypes of exosomes. We wanted to compare the percentage of CD9 and CD63 containing vesicles in our preparation. In order to do this, MDA cells were stained with CFSE first and then stained with either RPE-conjugated mouse anti-human CD9 antibody (AbD Serotec) or PE-conjugated mouse anti-human CD63 antibody. Antibodies were also added to serum free RPMI to act as controls.

A

Serum fee RPMI+CD9 MDA-MB-231 + CFSE MDA-MB-231 + CFSE + CD9

R4: 9.97% R4: 26.26%

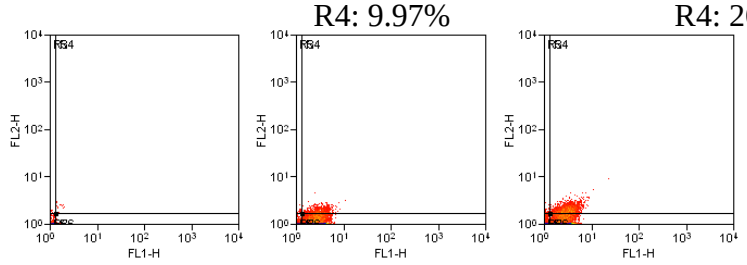

Serum fee RPMI+CD63 MDA-MB-231 + CFSE MDA-MB-231 + CFSE + CD63

R4: 0.02% R4:23.92%

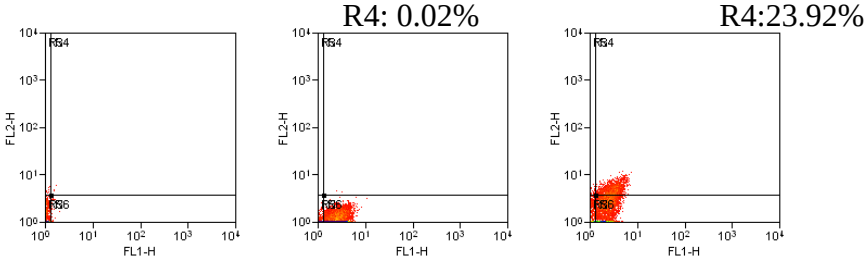

B

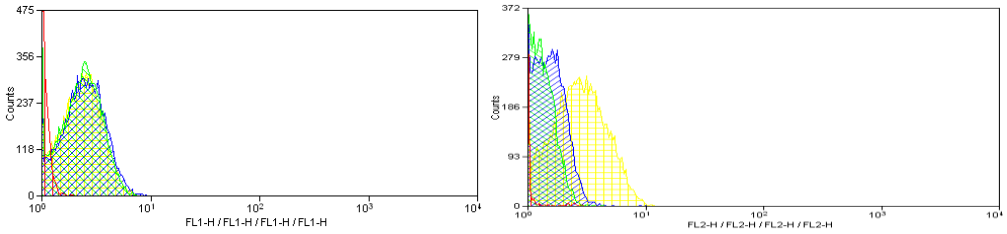

Figure 3.10: CFSE and PE double staining of MDA-MB-231 supernatant. (A) Data were plotted as FL2 channel versus FL1 channel. **(B)** Overlays of control MDA-MB-231 supernatant and stained supernatant were produced by using summit software. Red: MDA-MB-231, Green: MDA-MB-231+CFSE, Blue: MDA-MB-231+CD9, Yellow: MDA-MB-231+CD63. Results are representative of at least three experiments.

Serum free RPMI with CD9 antibody added was excluded by applying gates using the Summit software. We want particles that were stained positive for both CFSE (green) and PE (red), so Gate R4 is what we are interested in (Figure 3.10A). The data indicated that MDA-MB-231 supernatant treated with both CFSE and PE-conjugated CD9 showed that approximately 26.26% particles were stained both green and red (Figure 3.10A, first row, last image). However, MDA-MB-231 cells that were stained with CFSE alone had also shown 9.97% red fluorescence (Figure 3.10A, first row, second image), because CFSE green staining leaked into the red channel, so the proper percentage of CD9 containing particles secreted by the cells should be calculated as 26.26%-9.97%=16.29%. The same applied for anti-CD63 antibody, with 23.92%-0.02%=23.9% CD63 containing particles.

The overlay of the data showed that unstained MDA-MB-231 was negative for green fluorescence. MDA-MB-231 cells stained with CFSE alone or with either antibody showed the peak has shifted to the right in FL1 and the peaks overlapped nicely. In FL2 channel, unstained MDA-MB-231 cells were negative, cells that were stained with CFSE alone shifted to the right slightly (indicating the leak over into FL2 channel). Cells stained with CD9 antibody shifted further to the right and cells stained with CD63 antibody showed a more dramatic shift (Figure 3.10 B).

Insertion of foreign genetic material into exosomes and into cells by using exosomes as delivery vehicles

Exosomes are perfect candidates for drug or siRNA delivery because they could be self-derived and thus should not provoke any immune responses. Thus, we wanted to investigate whether we could load siRNA onto exosomes derived from MDA-MB-231 cells and jurkat cells and whether those exosomes could deliver the siRNA into targt cells.

First, we wanted to investigate whether we could load siRNA into exosomes by using electroporation. Exosomes from MDA-MB-231 cells were collected as described before. First, AllStars Negative Control siRNA, 'Alexa Fluor 488' (Qiagen) was used to test whether this technique works. This siRNA has green fluorescence so it is detectable by flow cytometry. The siRNA was added to 7 µg MDA-MB-231-derived exosomes and were either electroporated or un-electroporated as a control.

A

Exosomes + SiRNA un-electroporated and spin at 100, 000 x g

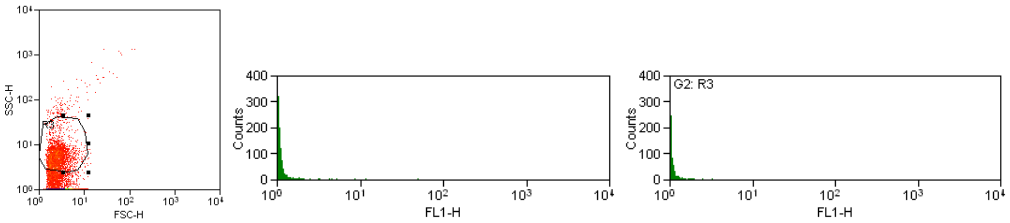

B

Exosomes + SiRNA electroporated (125 µF, 400 volts) and spin at 100, 000 x g

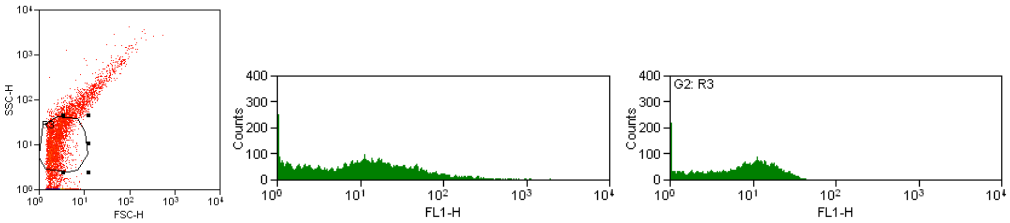

C

Exosomes + SiRNA electroporated (500 µF, 400 volts) and spin at 100, 000 x g

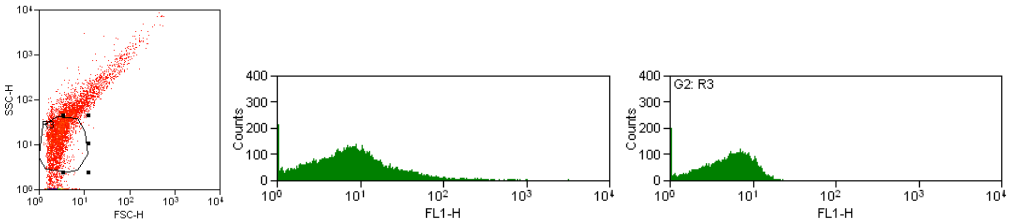

Figure 3.11: Loading of Alexa Fluor 488-tagged siRNA into exosomes. 7 µg MDA-MB-231 derived exosomes were mixed with 500 nM Alexa Fluor 488-tagged siRNA, and were subsequently exposed to an electric field pulse. A sample of exosomes with siRNA without electroporation was also prepared as a negative control. After electroporation, Exosomes were washed in PBS and ultracentrifugation at 100, 000 x g was used to pellet the exosomes. The pellets were then re-suspended in PBS and analysed by flow cytometry.

As expected, no fluorescence could be detected if the sample was not electroporated (Figure 3.11A). The sample that was electroporated with the settings of 125 µF and 400 volts showed fluorescence (Figure 3.11B), and the sample that was electroporated with the settings of 500 µF and 400 volts showed more significant fluorescence (Figure 3.11C). These data indicate that the siRNA was transferred, or associated with the exosomes by using electroporation.

Next, we investigated whether MDA-MB-231 derived exosomes were able to transfer the encapsulated siRNA to the parental cells and whether the siRNA can knock down the targeted gene. Rab27a siRNA was transfected into the exosomes using the described electroporation method. A non-targeting siRNA (Allstars negative control siRNA) was used as a negative control. The exosomes were co-cultured with MDA-MB-231 cells and the effect of the siRNA was examined by using western blot to check the Rab27a protein expression level. The cells were also transfected by using the siRNA in conjunction with lipofectamine 2000 as a positive control.

A

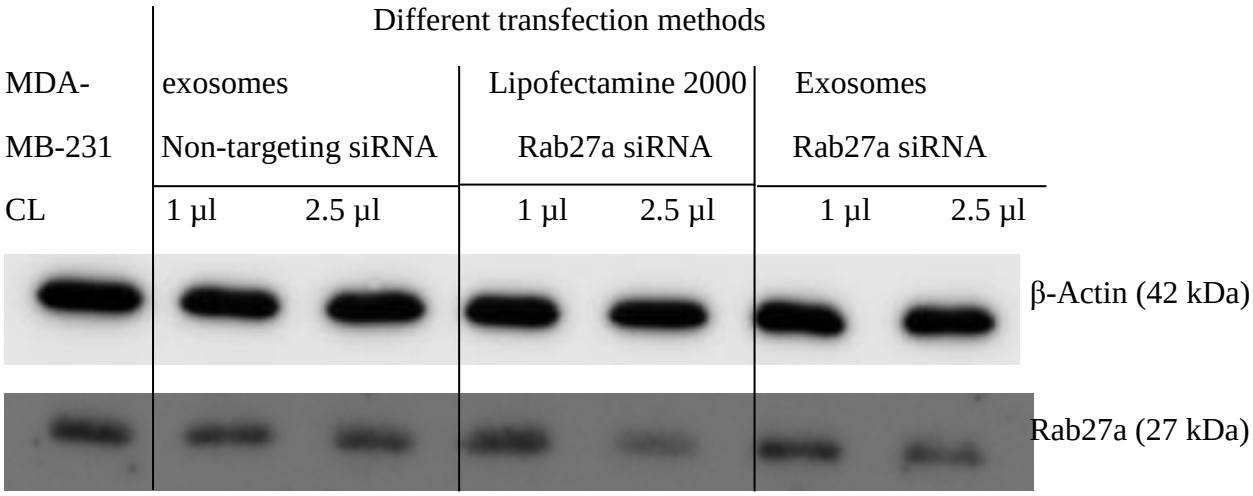

B

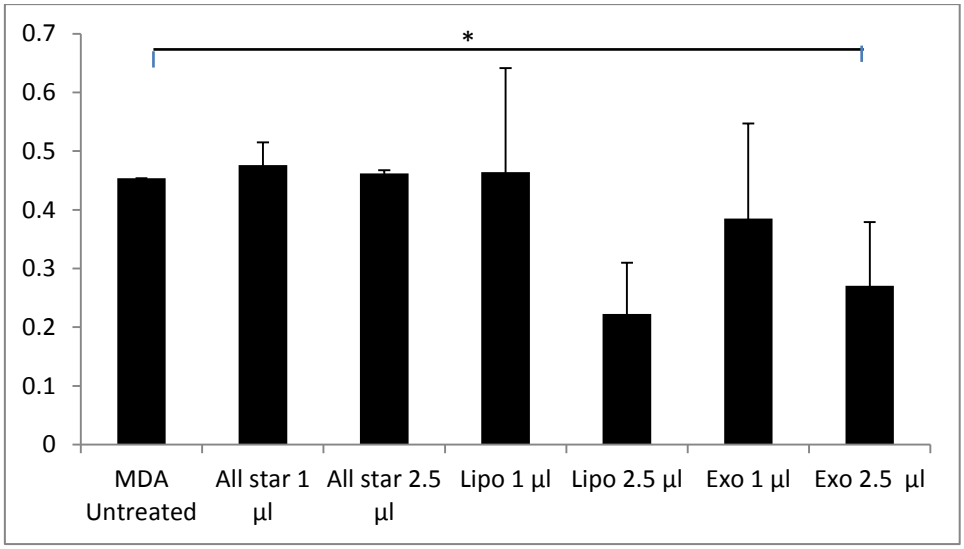

Figure 3.12: Transfecting MDA-MB-231 cells by various methods. A. Western blot analysis of MDA-MB-231 cells transfected with Rab27a and Allstars negative control siRNA using self-derived exosomes by electroporation to load siRNA into exosomes and incubating the exosomes with the cells. MDA-MB-231 cells were also transfected with Rab27a siRNA using the well-established reagent lipofectamine 2000 as a positive control. The western blot result was representative of three experiments. **B**. Analysis through densitometry of western blot data probed against Rab27a and normalised against β-actin levels. Data was obtained by using ImageJ to analyse results from three experiments. Error bars indicate standard deviation. * $P<0.05$

Transfecting the cells with different volume of the non-targeting 'Allstars negative control' siRNA did not affect Rab27a expression level when compared with the untreated control. Transfecting 1 µl Rab27a siRNA using either Lipofectamine 2000 or exosomes did not appear to influence Rab27a expression, whereas using 2.5 µl Rab27a siRNA knocked down Rab27a successfully, with Lipofectamine slightly more effective compared to exosomes (Figure 3.12 A and B). Thus, this preliminary experiment suggests that exosomes containing siRNA can be used to target specific proteins of interest.

To further confirm the ability of exosomes to transfer siRNA, we have decided to use Jurkat T cells to transfer siRNA in HeLa cells to knock down the Erap1 gene, which has recently been shown to be associated with the arthritic condition ankylosing spondylitis, an area of research our laboratory is interested in. Erap1 targeting siRNA was transfected into the exosomes using the above described electroporation method. As before, non-targeting siRNA (Allstars negative control siRNA) was used as a negative control. The exosomes were co-cultured with HeLa cells and the effect of the siRNA was examined by using western blot to check the Erap1 protein expression level.

A

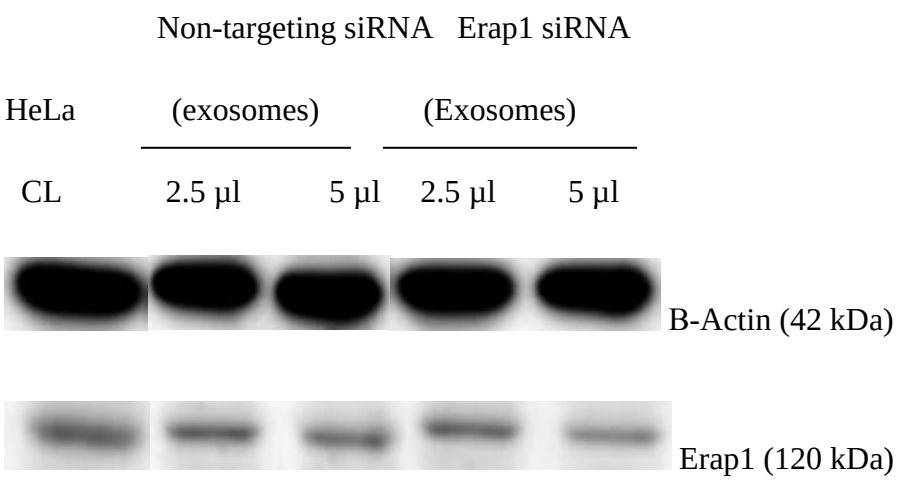

B

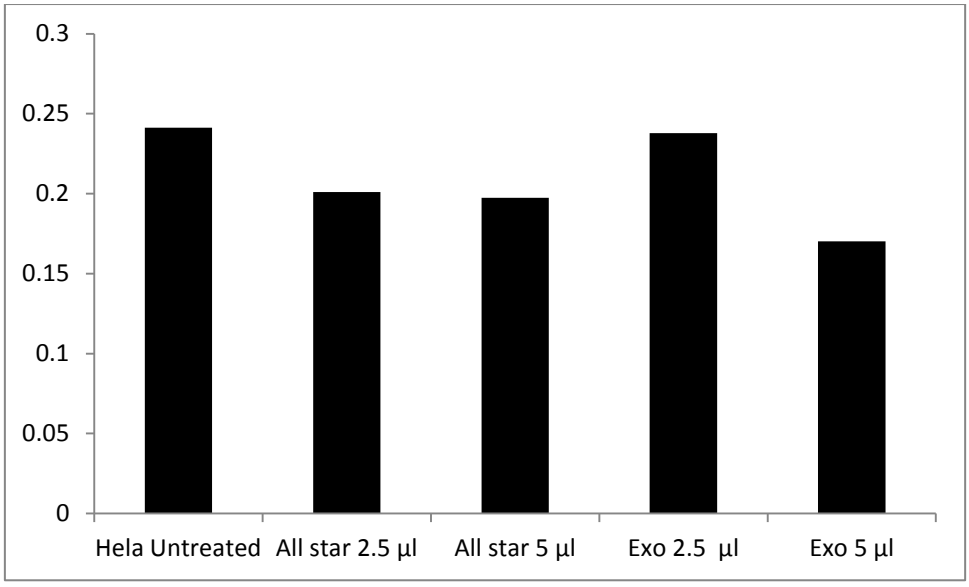

Figure 3.13: Transfecting HeLa cells with Erap1 siRNA. A. Western blot analysis of HeLa transfected with Erap1 and Allstars negative control siRNA using self-derived exosomes by electroporation to load siRNA into Jurkat T cells-derived exosomes and incubating the exosomes with the cells. **B**. Analysis through densitometry of western blot data probed against Erap1 and normalised against β-actin levels that represent protein loading. Data are representative of two experiments.

Transfecting the cells with different volume of the non-targeting 'Allstars negative control' siRNA appeared to inhibit Erap1 expression level slightly when compared with the untreated control, but was not different between the two concentrations. In contrast transfecting 2.5 µl Erap1 siRNA using exosomes did not knock down the gene, whereas using 5 µl Erap1 siRNA appeared to inhibit Erap1 successfully (Figure 3.13 A and B).

Lipidomics analysis of MDA-MB-231 cells and exosomes

The biogenesis of exosomes undoubtedly requires appropriate lipid mediators, such as LBPA and Ceramide. Lipidomics appeared as an emerging field in the early 2000s and lipid and protein composition of exosomes would be a starting point to characterise these fascinating particles. Lipid composition of exosomes have been analysed on exosomes derived from reticulocytes (Vidal et al., 1989), a B lymphocyte cell line (Wubbolts et al., 2003), a rat mast cell line and a human dendritic cell line (Laulagnier et al., 2004). The phospholipid composition of reticulocyte-derived exosomes were shown to be very similar to that of the plasma membrane (Vidal et al., 1989). Whereas the cholesterol/phospholipid ratio in B cell-derived exosomes was increased three times compared to the composition of the parental cells, and the class of sphingomyelin (SM) was also increased. (although only MHC- II enriched exosomes were considered in this experiment) (Wubbolts et al., 2003). Exosomes from a rat mast cell line or human dendritic cell line also showed specific phospholipid composition different from that of the parent cells, with no change in cholesterol/phospholipid ratio, but showed a 2-fold increase in the class of SM compared to the cell membrane (Laulagnier et al., 2004).

This increase in SM is consistent with the results from the B cell-derived exosomes. Therefore a high SM content could be a general feature of exosomes.

Thus, it will be intriguing to investigate whether MDA-MD-231 cells and the exosomes derived from these cells show any differences in lipid composition. Lipid analysis of both components was then performed.

A

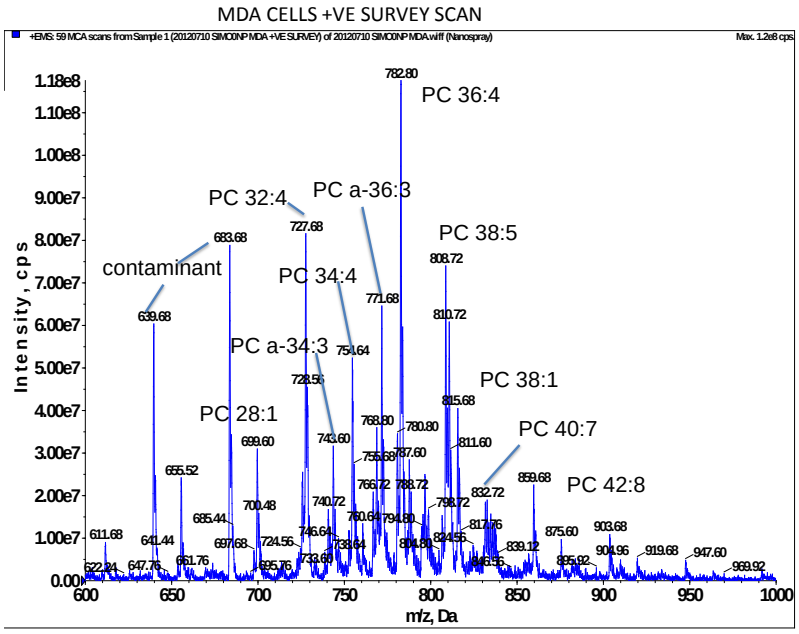
MDA CELLS +VE SURVEY SCAN
+EMS: 59 MCA scans from Sample 1 (20120710 SIMCONP MDA +VE SURVEY) of 20120710 SIMCONP MDA.wiff (Nanospray)
Max. 1.2e8 cps
Intensity, cps
m/z, Da
PC 36:4
PC 32:4
PC a-36:3
PC 38:5
contaminant
PC 34:4
PC a-34:3
PC 38:1
PC 28:1
PC 40:7
PC 42:8

B

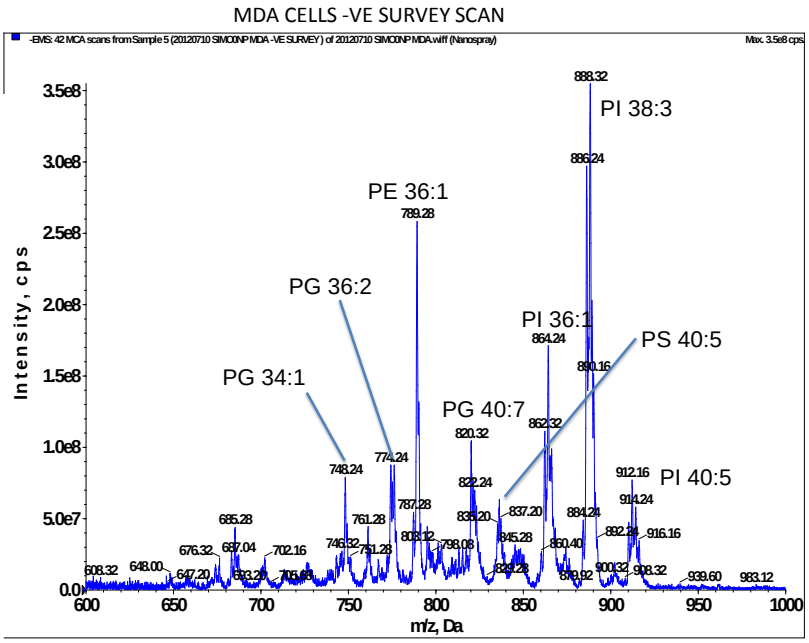
MDA CELLS -VE SURVEY SCAN
-EMS: 42 MCA scans from Sample 5 (20120710 SIMCONP MDA -VE SURVEY) of 20120710 SIMCONP MDA.wiff (Nanospray)
Max. 3.5e8 cps
Intensity, cps
m/z, Da
PI 38:3
PE 36:1
PG 36:2
PI 36:1
PS 40:5
PG 34:1
PG 40:7
PI 40:5

C

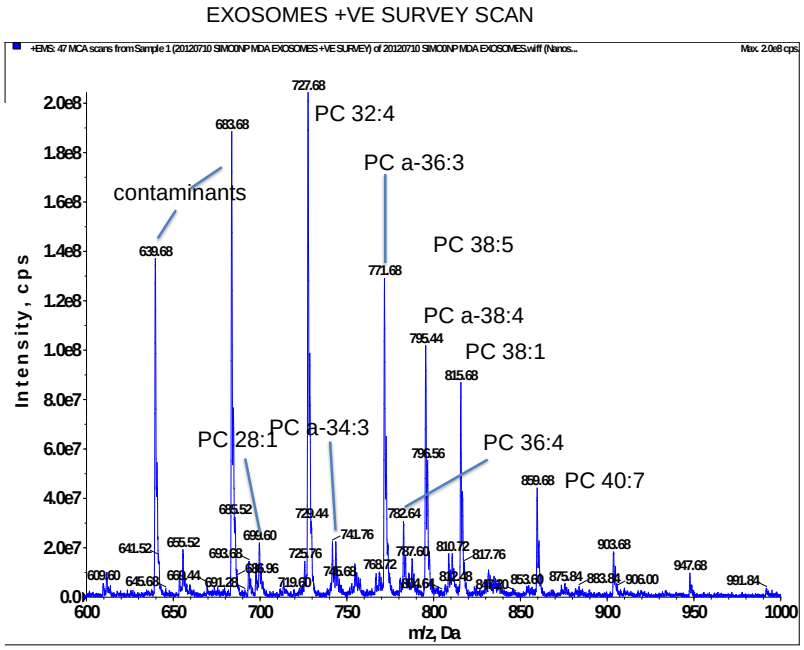
EXOSOMES +VE SURVEY SCAN
PC 32:4
PC a-36:3
contaminants
PC 38:5
PC a-38:4
PC 38:1
PC 28:1
PC a-34:3
PC 36:4
PC 40:7
Intensity, cps
m/z, Da

D

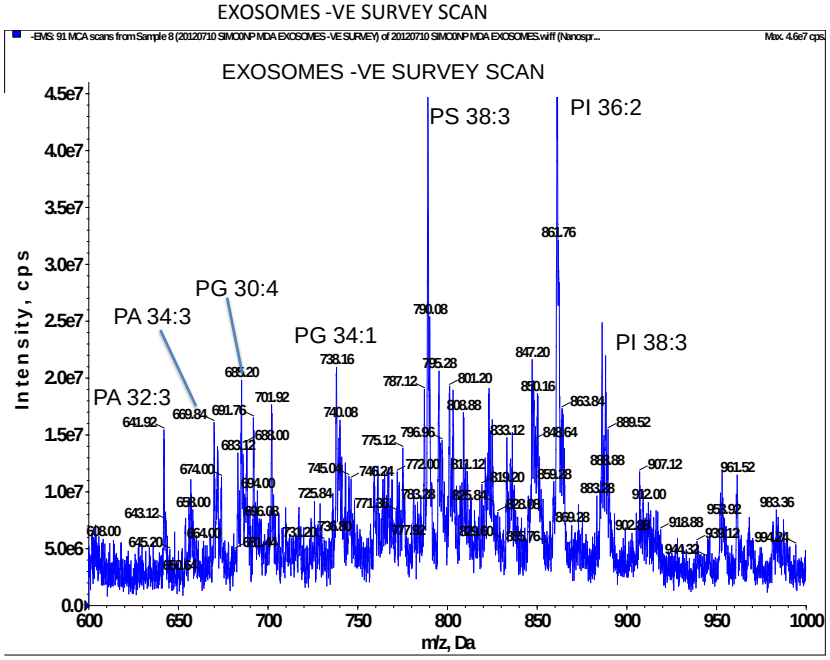
EXOSOMES -VE SURVEY SCAN
PS 38:3
PI 36:2
PG 30:4
PA 34:3
PG 34:1
PI 38:3
PA 32:3
Intensity, cps
m/z, Da

E

	Cells	Exosomes
Major PI	38:3	36:2
Identified lipids	PC, PI, PS, PE, PG, cardilipin, phosphorylated PIs	PA, PG, PS, PI, some evidence of PIPs

Figure 3.14: Lipid composition analysis. Lipid extracts from MDA-MB-231 cells were analysed by electrospray-mass spectrometry by positive survey scans (600-1000 m/z) **(A)**, and negative survey scans (600-1000 m/z) **(B).** Exosomes derived from MDA-MB-231 cells were analysed by positive scans **(C)** and negative scans **(D)** the same way. Lipid species identified are annotated as lipid class with total number of lipid carbons: number of double bonds, (C:DB). **(E).** Summary of the Lipidomics study.

The lipid analysis of MDA cells by electrospray mass spectrometry (Figure 3.14) revealed the expected classes of phospholipids such as phosphatidylcholine (PC), as observed in the positive ion mode survey scans (Figure 3.14A), while the negative ion mode survey scan (Figure 3.14B) showed phosphatidylinositol (PI), phosphatidylserine (PS), phosphatidylethanolamine (PE) and phosphatidylglycerol (PG). Other lipids that were observed include cardilipin and the signaling molecules phosphorylated PIs (data not shown).

The extracted exosomes show the same classes of phospholipid species (Figure 3.14C&D), but the distribution is significantly different. For example the major PI in the MDA-MB-231 cells is PI 38:3, however in the extracted exosomes, this is only a minor PI species and the PI 36:2 is the major PI species. The exosomes also showed some evidence of PIPs, however due to limiting amounts of material, their

characterisation was not possible. The classes of lipids identified from our prelimary study are shown in table 3.14E (Figure 3.14E).

Discussion

Determining the presence of exosomes secreted by breast cancer cell lines.

We have isolated exosomes from MDA-MB-231 cells and MCF7 cell cultures. Confirmation of the presence of exosomes in our preparation was confirmed by a combination of several different techniques, including western blotting (Figure 3.2), electron microscopy (Figure 3.3), and flow cytometry (Figure 3.4). Overall, the exosomes exhibited typical 'cup' shaped morphology, expressed typical protein markers, and were within the expected size range (50-150nm).

Tumour cell-conditioned medium and tumour cell-derived exosomes induced Jurkat T cell apoptosis

Immune escape by tumours is a critical factor in avoiding destruction by the host immune system. It has been reported that tumour-derived exosomes can have immunosuppressive functions. Exosomes derived from tumour cells can bear Fas ligand that can induce T cell apoptosis leading to suppression of T-cell responses *in vitro* (Abusamra et al., 2005; Andreola et al., 2002). Tumour derived exosomes may also bear NKG2D ligands such as MICA and MICB that can down-regulate MKG2D present on $CD8^+$ T cell or NK cell subsets (Clayton et al., 2008).

Our data show that MDA-MB-231 supernatant/conditioned medium did not induce more apoptosis (10.56%) compared to the Jurkat cells with unconditioned serum free

RPMI medium added (12.33%), but has dramatically increased the G0/G1 phase from 35.9% to 68.01% and decrease the G2/M phase significantly from 18.23% to 5.79%, whereas adding 48 hour MCF 7 supernatant to Jurkat cells has increased the number of apoptotic cells to 31.1% from 21.87%) and decreased the G2/M phase from 10.23% to 2.3%. In contrast with the MDA-MB-231 cell-conditioned medium, MCF7-conditioned medium did not increase the G0/G1 phase. These data suggest that MDA-MB-231 conditioned medium have induced cell arrest in the G0/G1 phase, delayed the progression of cell cycle, and inhibited cell proliferation, whereas MCF7-conditioned medium was more potent in inducing apotosis, but did not arrest the cells in the G0/G1 phase. These data also indicate that conditioned medium from different tumour lines have different behaviours.

Our data show that treatment of Jurkat cells with MDA-MB-231 or MCF7 derived exosomes induced apoptosis as determined by Annexin-V staining. Treatment of Jurkat cells with MDA-MB-231 cell and MCF7 cell-conditioned medium also induced apoptosis as determined by PI staining. PI staining also revealed that treatment of Jurkat cells with 104 µg/ml MDA-MB-231 derived exosomes or 400 µ/ml MCF 7 derived exosomes drove 35.21 % and 41.21 % cells toward apoptosis. One could argue that 400 µg/ml seems like a very high concentration and this is unlikely to be the case *in vivo*. However, such high concentrations are not uncommon in the literature. Furthermore exosomes are likely to be short-range messengers, meaning that the concentration of exosomes near the originating cells will be high and will decrease as the distance increases. Thus the physiological concentration of relevance in any system remains an open question, and is a significant problem in the field currently.

CFSE and PE double staining

Next, we confirmed the presence of CD9 and CD63 on MDA-MB-231 cells by immuno-staining and both CD9 and CD63 were present on the cells. The presence of CD9 and CD63 on the MDA-MB-231 cells and exosomes were confirmed by western blotting. CD9 and especially CD63 were more enriched in exosomes compared to parental cells. The enrichment of CD9 and CD63 in exosomes was a reason they were selected as exosome markers. However, a very recent study by Thery's group suggested that CD9 is not a specific marker for exosomes as it is also present in larger, possibly plasma membrane-derived, microvesicles pelleted at 10,000 x g and also particles smaller than 50 nm that co-pelleted with exosomes (Bobrie et al., 2012a). We investigated the intracellular distribution of CD9 and CD63 in MDA-MB-231 cells by using immunofluorescence methods and they do not localise in the same intracellular departments. CD9 was found mainly in patches on the plasma membrane and rarely in intracellular compartments but CD63 was only found in intracellular compartments (most likely MVBs). This is consistent with the recent study by Thery's group (Bobrie et al., 2012a). In most cells, CD63 is present in intracellular compartments of endosome/lysosome origin (Pols and Klumperman, 2009); this is also the case for MDA-MB-231 cells used in this study. In comparison, CD9 was observed mainly at the cell surface in MDA-MB-231 cells (Figure 3.7). CD9 has been described both at the cell surface and at intracellular multivesicular bodies/endosomes (Buschow et al., 2009; Cramer et al., 1994)

The percentage of CD9 and CD63 containing vesicles were analysed in this study by using CFSE and PE double staining. 23.9% of vesicles were stained positive for CD63 and 16.29% vesicles were stained positive for CD9. Overlay of the FL2 channels also showed that more vesicles stained positive for CD63 compare to the number of vesicles that stained positive for CD9. It is hard to conclude from these data the percentage of exosomes in our preparation. As CD9 is expressed in patches on the plasma membrane, it is possible that CD9 are only present in some multivesicular bodies and not all of them, and thus are not present on all exosomes. This will explain why CD63 antibody stained more vesicles compare to CD9 antibody. On the other hand, if CD9 was not only present on exosomes, but also present in larger microvesicles (over 100 nm) and smaller vesicles (smaller than 50 nm) (Bobrie et al., 2012a), with the latter co-pelleting with exosomes at 100, 000 x g, the CD9 antibody should have labelled more vesicles compare to CD63 antibody. It is possible that the antibodies did not work effectively and did not bind to all the CD9/CD63 positive vesicles. Nevertheless, CD63 is a more reliable exosomes marker compare to CD9.

Insertion of foreign genetic material into exosomes and into cells by using exosomes as delivery vehicles

Viruses, polyethylenimine (PEI)-based nanoparticles and liposomes are the three main classes of delivery vehicles that have been the centre of research on therapeutic RNAi. A study that successfully engineered exosomes to specifically target brain tissue and successfully transited the blood brain barrier to knock down a therapeutic target gene of Alzheimer's disease has sparked interest to use exosomes as new generation of delivery

vehicle (Alvarez-Erviti et al., 2011). A more recent study has successfully demonstrated that exosomes from peripheral blood delivered the administered siRNA into monocytes and lymphocytes, causing selective gene silencing (Wahlgren et al., 2012).

We have successfully introduced non-targeting fluorescent siRNA and Rab27a siRNA into MDA-MB-231 cells-derived exosomes using electroporation, and these exosomes effectively delivered the siRNA into the MDA-MB-231 cells causing knock down of Rab27a gene expression. Since exosomes can be produced by the recipients' own cells make them an ideal non-immunogenic vector to transfer heterologous nucleic acids such as therapeutic siRNAs. siRNAs were chosen as the genetic material because they were small in size (21-23 nt) and can lead to gene-silencing (Wahlgren et al., 2012). To use the exosomes as gene delivery vehicles, the siRNAs were required to be transferred into the exsomes. Electroporation was the chosen method. The settings were adopted from Alvarez-Erviti et al (Alvarez-Erviti et al., 2011). Next, two different methods were used to transfer the siRNA into cells. Lipofectamine 2000 was a well-known transfection reagent and was used to transfer Rab27a siRNA into cells. Exosomes encapsulating the siRNA were also tested for the ability to transfer the siRNA into cells. Although the effect of gene knock down was more visible when lipofectamine 2000 was used compared to exosomes (Figure 3.12), it is undeniable that the data does suggest that the exosomes transferred Rab27a siRNA into the cells successfully and caused Rab27a knock down.

We have also used Jurkat T cells-derived exosomes to transfer encapsulated siRNA into HeLa cells and knocked down the Erap1 gene, which is associated with ankylosing spondylitis. The knock down was not as efficient as using MDA-MB-231-derived exosomes to transfer siRNA into MDA-MB-231 cells. This could be due to various factors, such as exosomes may interact differently with parental cells compared to other cells, and exosomes derived from different cells will have different properties, or that an improved siRNA target sequence is required. Nevertheless, both experiments showed in principle that exosomes are capable of delivery siRNA into cells and knocking down a target gene.

Current vectors pose a unique problem and they have not been proven successful in clinical trials because they have issues such as toxicity, immunogenic concerns and targeting problems. It is very important to discover a safe gene delivery vector. Exosomes maybe a perfect candidate because they can be derived from the patients' bodies and should not provoke any immune responses. Our data complement the findings of the other two groups (Alvarez-Erviti et al., 2011; Wahlgren et al., 2012) and suggested that exosomes can be used as gene delivery vectors.

Lipidomics analysis of MDA-MB-231 cells and exosomes

The mechanisms for sorting lipids onto exosomes and the lipid composition of exosomes are still unclear. Thus any lipid composition study will significantly contribute towards the characterisation of exosomes. Our prelimary data showed that the lipid composition of exosomes derived from MDA-MB-231 cells were different from that of the parental cells.

It has been reported that the secretion of the PLP in association with exosomes was independent of the ESCRT machinery, but required the sphingolipid ceramide. (Trajkovic et al., 2008), suggesting that by using different intracellular machinery, subpopulations of MVBs can be formed which may also lead to different types of exosomes. Bobrie et al has suggested that sub-populations of exosomes exist in the 100,000 x g preparation and these particles could be derived from other organelles, or even formed out of the secretory pathway (Bobrie et al., 2012a) (Bobrie et al., 2012b). Thus it is possible that our preparation of exosomes contain these 'sub-types' of exosomes derived from a source other than endosomes, or the sorting of lipids into exosomes is uniquely regulated. The different results obtained from other studies may indicate that different cells use different mechanisms for lipid sorting into exosomes.

Chapter IV: Nanoparticle tracking analysis with Nanosight.

Introduction

Why Nanosight?

Due to the small sizes of exosomes and microvesicles, their analysis has been quite problematic. Commonly used techniques include isolation by centrifugation, immunoisolation by using antibodies, western blotting, coupling onto latex beads followed by flow cytometry, and electron microscopy. Flow cytometry analysis of exosomes/microvescles has also been reported (Abusamra et al, 2005), but most flow cytometers have a lower detection limit of 200-300 nm, and thus are not very accurate in detecting exosomes, and as indicated in the previous chapter, and it may be hard to distinguish exosomes from other microvesicles and the background.

The Technology

Nanoparticle tracking analysis (NTA) was developed in 2006 and allows direct and real-time visualisation and analysis of nanoparticles in liquids (Carr et al, 2009). Nanosight visualises and measures many types of nanoparticles with the size range of 30 nm to 1000 nm.

The Nanosight model we used in this study is the LM 10 (Figure 4.1 A). The unit is made of a metal housing containing a single mode laser diode which aims a focussed laser beam through the sample chamber. On top of the metal housing is an optical window mounted in a detachable stainless steel top plate. Samples (Approximately 300

μl) are introduced into the chamber by using a 1 ml disposable syringe through Luer fittings (Figure 4.1B). Particles move in the liquid sample under Brownian motion and are seen as small point scatterers of light when they pass through the laser beam (Figure 4.1C). This can then be visualised by looking down the microscope, with videos recorded and analysed, or saved and analysed at a later time.

A **B**

C

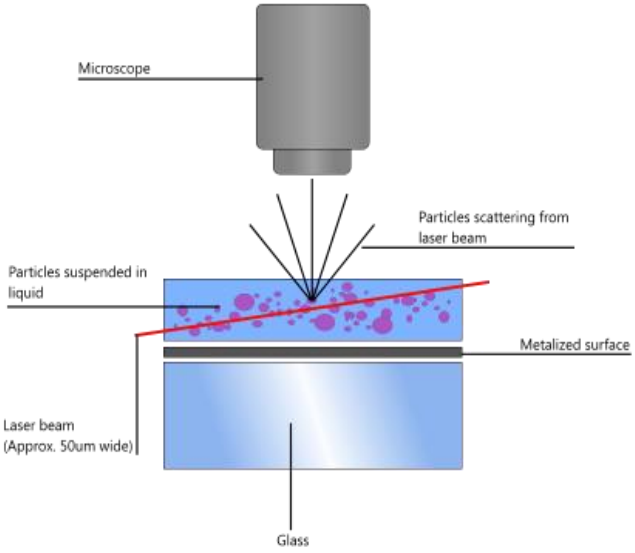

Figure 4.1: Nanosight and the technology. (A). Nanosight model LM-10. **(B)**. A 635 nm laser beam is fired through the sample chamber. **(C)**. Particles resuspended in liquid are seen as little point of light moving rapidly, which can be visualised by using the microscope or NTA on the computer screen. Diagram adapted from www.Nanosight.com

Nanoparticle Tracking Analysis software (NTA)

The video captured can be analysed by a dedicated single nanoparticle tracking programme (NTA). Videos are captured directly and analysed straight away or imported for analysis at a later time. The first frame of the video is normally used to adjust the settings of the software such as detection threshold, background subtraction, blurring, etc. Detection threshold should be set at a level where a small red cross is placed on the centre of each individual particle. It then tracks the movement of the particle per frame, all the particles are tracked simultaneously until at least two hundred tracks are completed (Figure 4.2). The NTA then analyses the distance each particle travelled and converts it to size, based on the Stokes-Einstein equation (Figure 4.2). The differential size distribution is shown on NTA in real time and a graph constructed at the end of the analysis. Cumulative undersize and cumulative oversize data can also be shown on the graph.

A

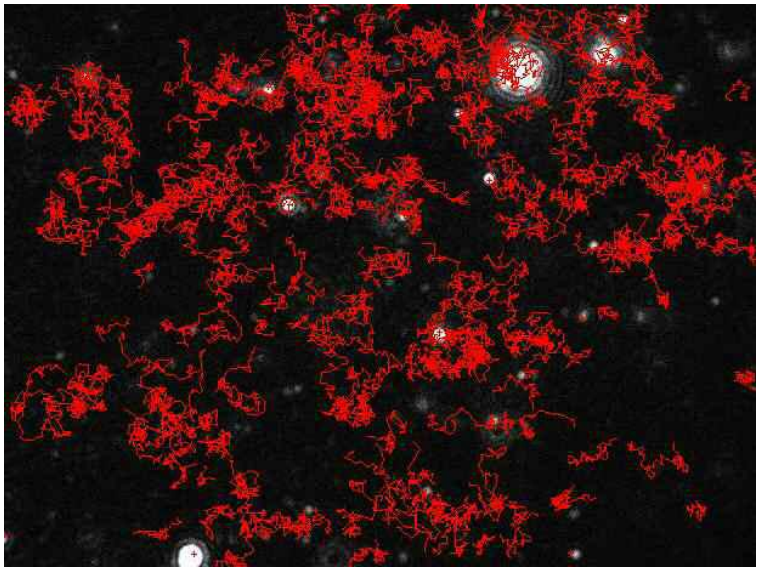

B

$$\frac{\overline{(x,y)}^2}{4} = Dt = \frac{TK_B}{3\pi\eta d}$$

where K_B is Boltzmann's constant.

Figure 4.2. NTA analysis of nanoparticles. (A) Red tracks are the distance that each particle travelled. (B). The Stokes-Einstein equation used by NTA. X and y are average distance each particle moved as tracked by the software, Dt is particle diffusion coefficient, T is temperature, η is solvent viscosity, d is the particle hydrodynamic diameter and KB is Boltzmann's constant. Diagram adapted www.Nanosight.com

Results

The accuracy of Nanosight in measuring size and concentration.

To be able to use the Nanosight for analysing samples, we need to first test its accuracy in measuring size and concentration. By analysing particles of a known size and comparing it with the detected size, we were able to evaluate the accuracy of Nanosight on measuring size.

A

Actual size	100 nm	200 nm	400 nm
Detected size	100 nm	199 nm	403 nm

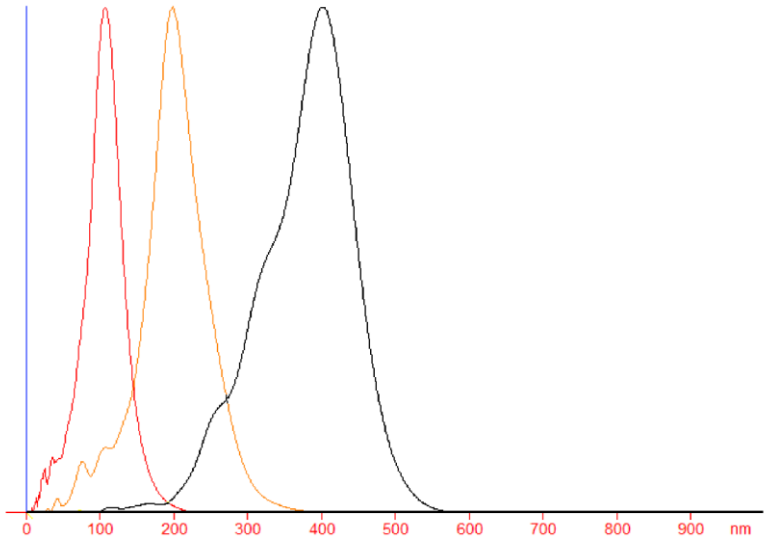

B

100 nm 200 nm 400 nm

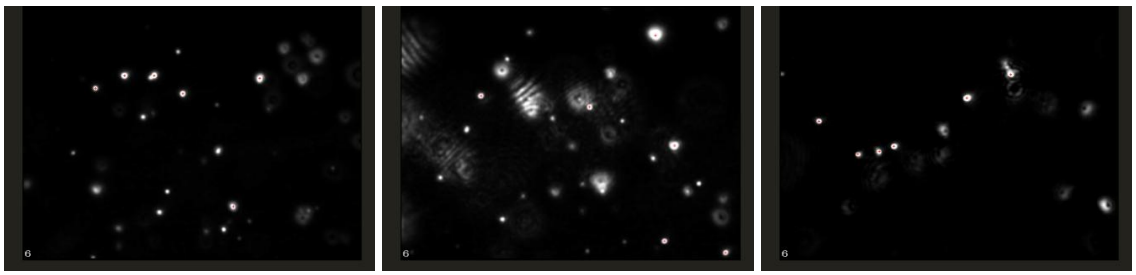

C

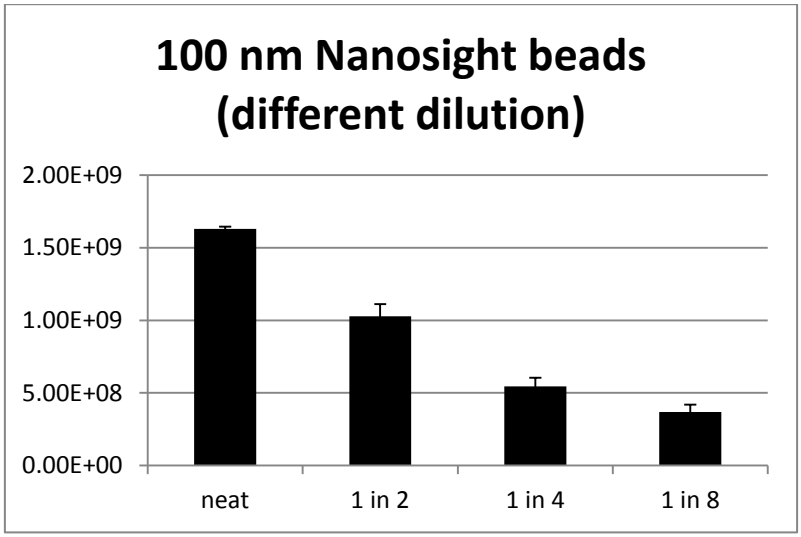

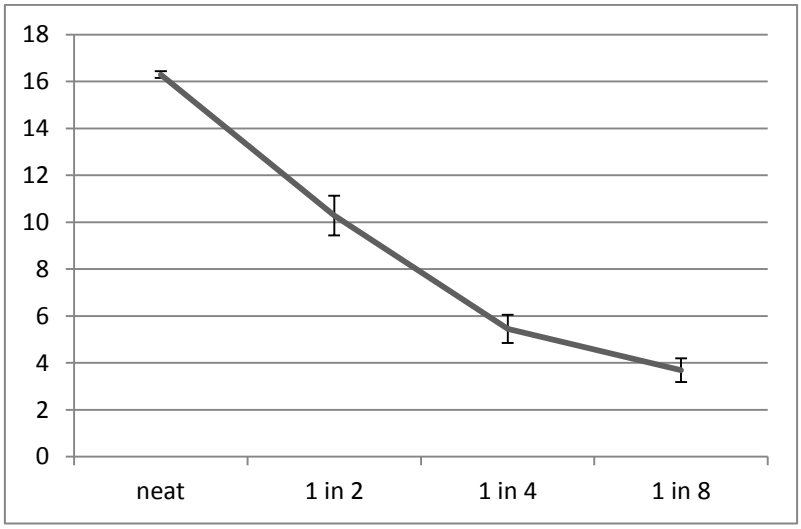

Figure 4.3: Measurement of size and concentration by using Nanosight. (A). The 100 nm, 200 nm and 400 nm beads supplied by Nanosight were diluted in PBS and analysed on the Nanosight. Black writing shows the actual size of the beads and red writing shows the sizes detected by Nanosight. (B).Screen shots of the 100 nm, 200 nm and 400 nm beads from NTA. (C). 5 µl of the 100 nm beads was diluted into 1 ml PBS. And a 1 in 2, 1 in 4 and 1 in 8 dilution was made. Samples were then analysed on the Nanosight and three 30 seconds videos were taken. Error bars indicate standard deviation. Data are representative of four experiments.

Approximately 5 µl 100 nm, 200 nm and 400 nm Nanosight beads were suspended in 1 ml PBS and 300 µl of each sample was taken and run on the Nanosight. The differential size distribution of 3 samples is shown in Figure 4.3 A. The detected peak size was 100 nm, 199 nm and 403 nm accordingly. This shows that the Nanosight is very accurate at determining particle size. Figure 4.3 B shows screen shots of the videos of the Nanosight beads that NTA has recorded.

We next determined the ability of NTA to determine concentration. Approximately 5 µl of 100 nm beads was diluted into 1 ml PBS and 500 µl of the mixture was added into 500 µl PBS to make a 1 in 2 dilution. The same was repeated to make 1 in 4 dilutions and then 1 in 8 dilutions. All 4 samples were then run on the nanosight. Results show an almost straight line, indicating that the Nanosight is acceptably accurate, although not perfect, in determining concentration differences (Figure 4.3 C).

Supernatant from MDA-MB-231 and MCF 7 after 300 x g and then 10, 000 x g

To investigate the sizes of the exosomes/microvesicles secreted from MDA-MB-231 cells and MCF 7 cells. Medium from both cell lines was replaced with serum free medium when cells were 90% confluent and supernatant was collected after 48 hours. Cell and supernatant were spun at 300 x g and then 10, 000 x g to remove debris. The resulting supernatant was then analysed on Nanosight. The peak size of MDA-MB-231 cell-derived exosomes was 129 nm and the peak size of MCF7 cell-derived exosomes was larger at 153 nm.

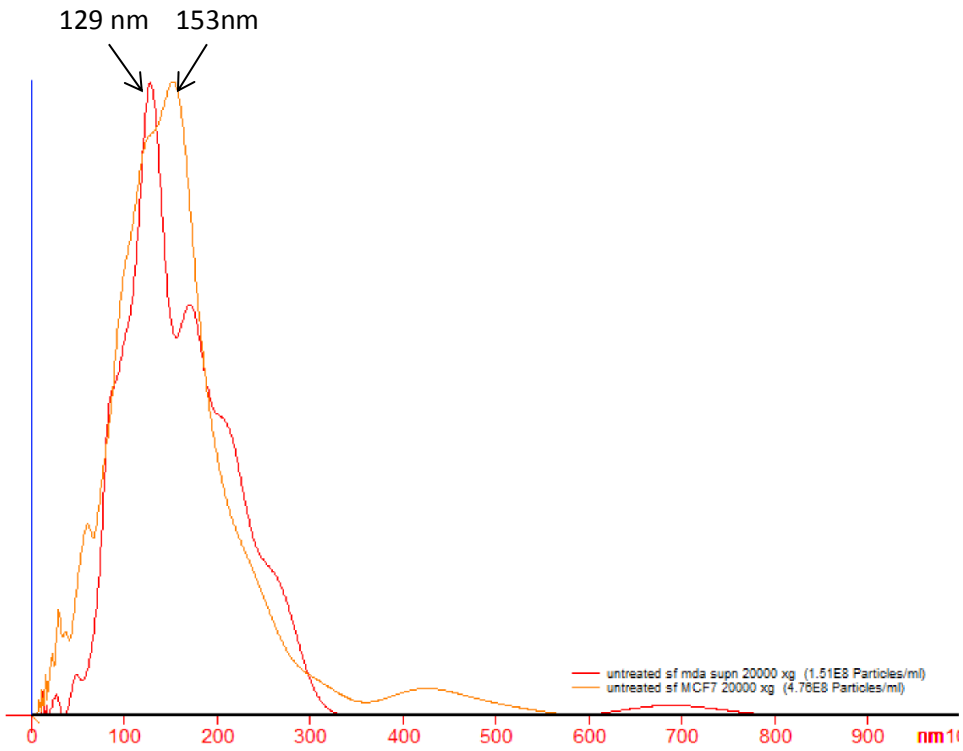

Figure 4.4: Comparison of the size of exosomes from MDA-MB-231 and MCF 7 as detected by the Nanosight. MDA-MB-231 cells and MCF 7 cells were grown to 90 % confluency and supernatant was collected. Cells and debris were depleted by centrifugation at 300 x g and large microvesicles were depleted by ultracentrifugation at 10,000 x g. The remaining supernatant was analysed on the Nanosight. Data are representative of at least three experiments.

Immunodepletion of exosomes/microvesicles using antibody-coupled magnetic beads.

As with many other published preparations of exosomes, ours is likely to contain a mixture of microvesicles including exosomes. I have described the labelling of CD9 or CD63 positive vesicles using CFSE and PE double staining method in the last chapter.

To further investigate the percentage of CD9 or CD63 positive vesicles, an immunodepletion experiment was performed.

The percentage of CD9 and CD63-containing microvesicles was analysed by coupling primary antibody to secondary antibody-coated dynabeads and then incubating the beads with cell supernatant after centrifugation at 300 x g and ultracentrifugation at 10, 000 x g. The technique is shown in schematic drawing in Figure 4.5.

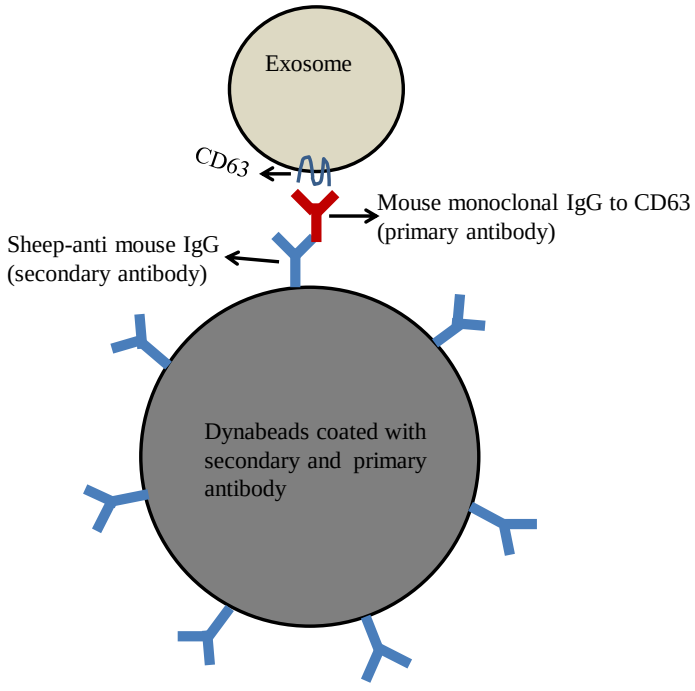

Figure 4.5: **Schematic drawing of the technical approach used to selectively capture exosomes present in cell culture supernatants by coupling of anti-CD63 mouse monoclonal antibody to sheep-anti-mouse antibody coated dynabeads.**

Supernatant was collected and spun at 300 x g for 10 minutes then 10,000 x g for 30 minutes. The resulting supernatant was pre-cleared with dynabeads without specific antibody to allow for non-specific binding of microvesicles to the beads. Different amounts of antibody-coupled dynabeads were then added and incubated with supernatant overnight. The beads were then separated out with a magnetic separator and the supernatant was analysed on NTA to check for depletion. Figure 4.6 shows the binding of antibody-coated dynabeads to CD63 on exosomes. Depletion using anti-CD9 antibody was performed the same way.

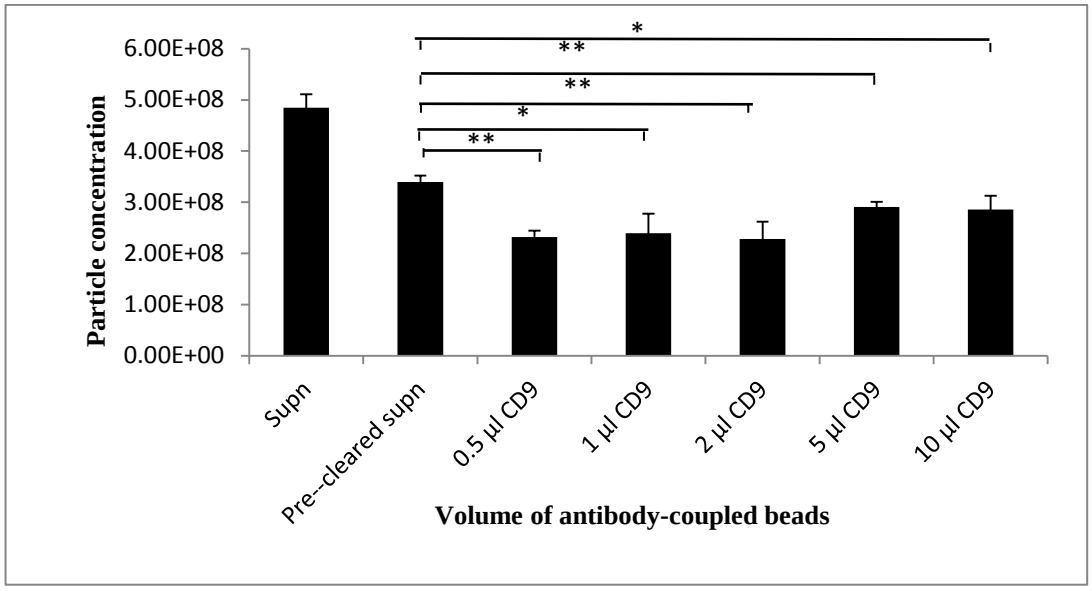

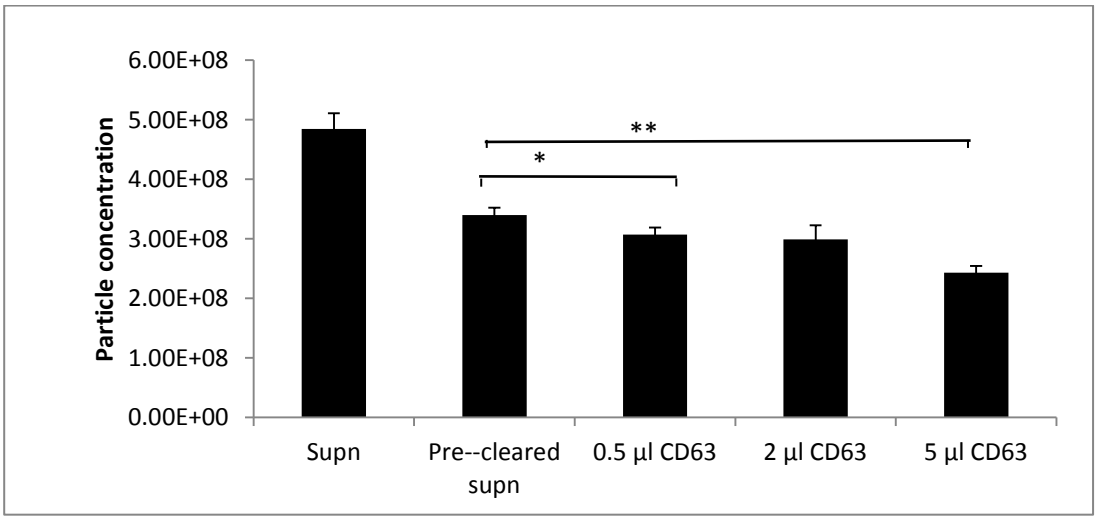

Figure 4.6: Immuno depletion of the supernatant post 10,000 x g spin using anti-CD9 and anti-CD63 antibody coupled magnetic dynabeads. 24 h culture supernatant was centrifuged at 300 x g and 10, 000 x g and the resulting supernatant was pre-cleared with beads for 30 minutes. Antibody-coupled beads werethen added to 400 µl pre-cleared supernatant. After 3 hours, the samples were placed on a magnetic separator. The beads were discarded and supernatant were analysed on the Nanosight. This experiment was performed three times. Error bars indicate standard deviation.

The data shows that pre-clearing the supernatant with magnetic beads leads to a decrease in microvesicles in the supernatant as analysed by NTA (Figure 4.6), and this applies for both antibodies. Adding a small amount of anti CD9 antibody (0.5 µl) seems to have achieved the optimum depletion efficacy, with 52.1% particles depleted when compare to supernatant and 31.7% when compare to pre-cleared supernatant. Increased antibody concentration did not seem to affect the depletion. Nevertheless, at higher concentrations of CD9, there was a decrease in the depletion of CD9-positive particles. It is possible that higher concentration of the CD9 antibody contaminated the result with debris. For CD63, 5 µl of the antibody achieved the best depletion result, with 49.9 % of particles depleted when compare to the supernatant and 28.5% depleted when compare with the per-cleared supernatant.

Nanosight analysis of exosomes pulled down by CD9 and CD63 coupled-magnetic beads

Sequential centrifugation and ultracentrifugation are the most common way used to isolate exosomes. It is unknown whether the size of our exosomes prepared by sequential centrifugation and ultracentrifugation would differ from the size of exosomes purified by bead-based purification. In order to find out about the size of such purified exosomes, an exosomes pull down assay was performed. The technique used was similar to the immune-depletion experiment illustrated in Figure 4.5.

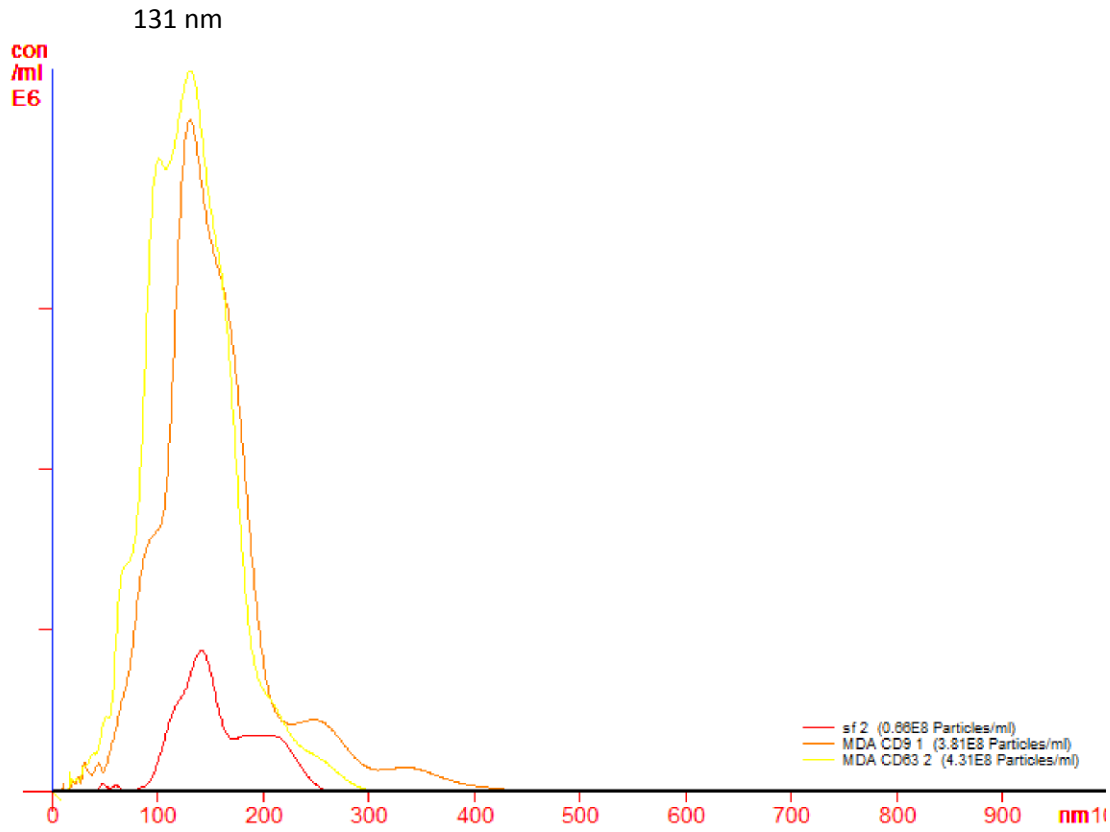

Figure 4.7: The size of exosomes purified by immunoaffinity capture method. CD9 or CD63 antibody was coupled onto the beads. 25 µl of antibody-coupled beads were added into 0.5 ml exosomes in serum free RPMI. Samples were left rotating at 4 °C overnight. Exosomes were eluted from the beads by adding 200 µl 0.2M Glycine, PH 2.8 at 37 °C for 5 minutes and then neutralised by adding 5 µl of 2M Tris PH 8. Supernatant was spun at 300 xg for 10 minutes and 10, 000 x g for 30 minutes, 0.5 nm serum free RPMI was added to each sample and then analysed on the Nanosight. Results are representative of three experiments.

Exosomes pulled down by both CD9 and CD63 showed a peak size of 131 nm. The orange line indicates exosomes pulled down by CD9-coupled magnetic dynabeads and yellow line shows exosomes pulled down by CD63-coupled dynabeads. The red line is the control with beads added to serum free RPMI (Figure 4.7).

Comparing the exosomes purified by immunoaffinity binding (Figure 4.7) and our 'usual' preparation of exosomes (Figure 4.4) together, our results show that the peak size of the 'usual' preparation of exosomes was 129 nm (Figure 4.4) and the peak size of the purified exosomes was 131 nm (Figure 4.7).

These data suggest that the size of the population of exosomes purified by immunoaffinity binding does not significantly differ from the exosomes prepared by ultracentrifugation.

NTA detection of apoptosis induced by Paclitaxel and Curcumin.

Paclitaxel was isolated from the bark of the Pacific yew tree, *Taxus brevifolia.* It is sold under the trade name Taxol. It is the best anti-cancer drug isolated from plants (Bava et al., 2005). It interferes mechanistically with the dynamic instability of microtubules, protecting them from disassembly and thereby arrests the cell cycle at the G2/M phase, finally leading to apoptotic cell death or reversion to the G0-phase of the cell cycle without cell division (Horwitz, 1994). The major disadvantage is the drug's dose limiting toxicity. It was reported that a combination of Taxol and Curcumin achieved better anticancer effects compare to Taxol alone (Bava et al., 2005). Therefore it would be intriguing to be able to detect apoptotic vesicles induced by adding Taxol and Curcumin to MDA-MB-231 cells, which could potentially be of use in a clinical setting to monitor chemotherapeutic efficacy. Apoptotic vesicles can have a size range between 50-500 nm (Thery et al., 2009), thus placing many of them above the normal size of exosomes observed here by NTA.

Briefly, MDA-MB-231 cells were grown to approximately 50% confluence. This was to avoid significant apoptotic vesicles in our controls. The growth medium was replaced with serum free RPMI and the appropriate concentration of Curcumin was added to sensitize the cells. After 2 hours, Taxol was added to appropriate wells. Samples were collected after 48 hours and spun at 300 x g to remove dead cells and debris, and were then analysed by NTA to investigate whether apoptotic vesicles can be detected by using the 'extended dynamic range' (EDR) function of NTA.

A

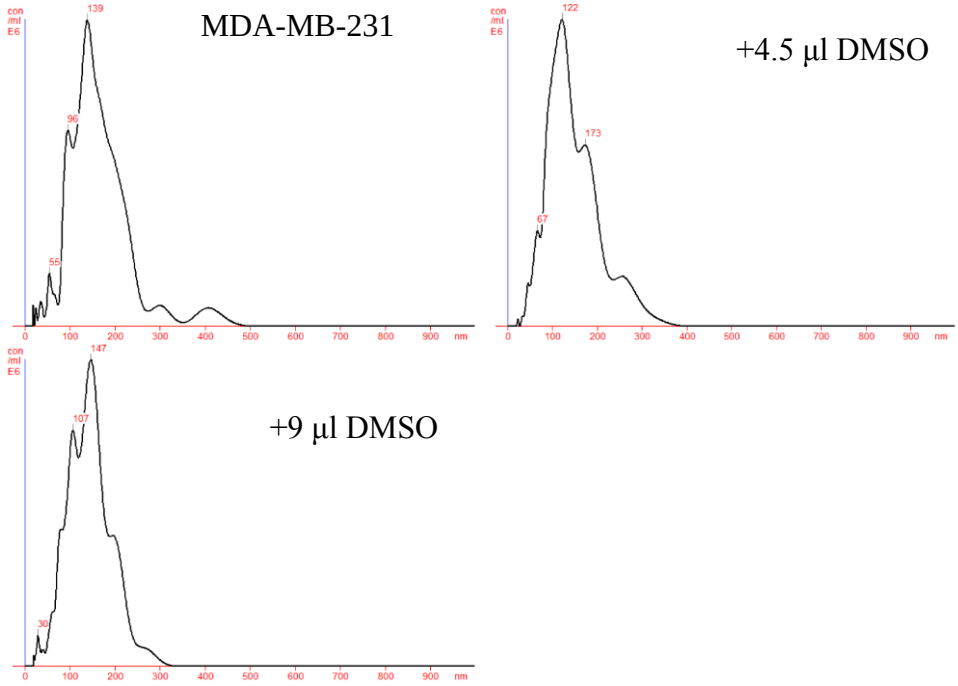
MDA-MB-231
+4.5 µl DMSO
+9 µl DMSO

B

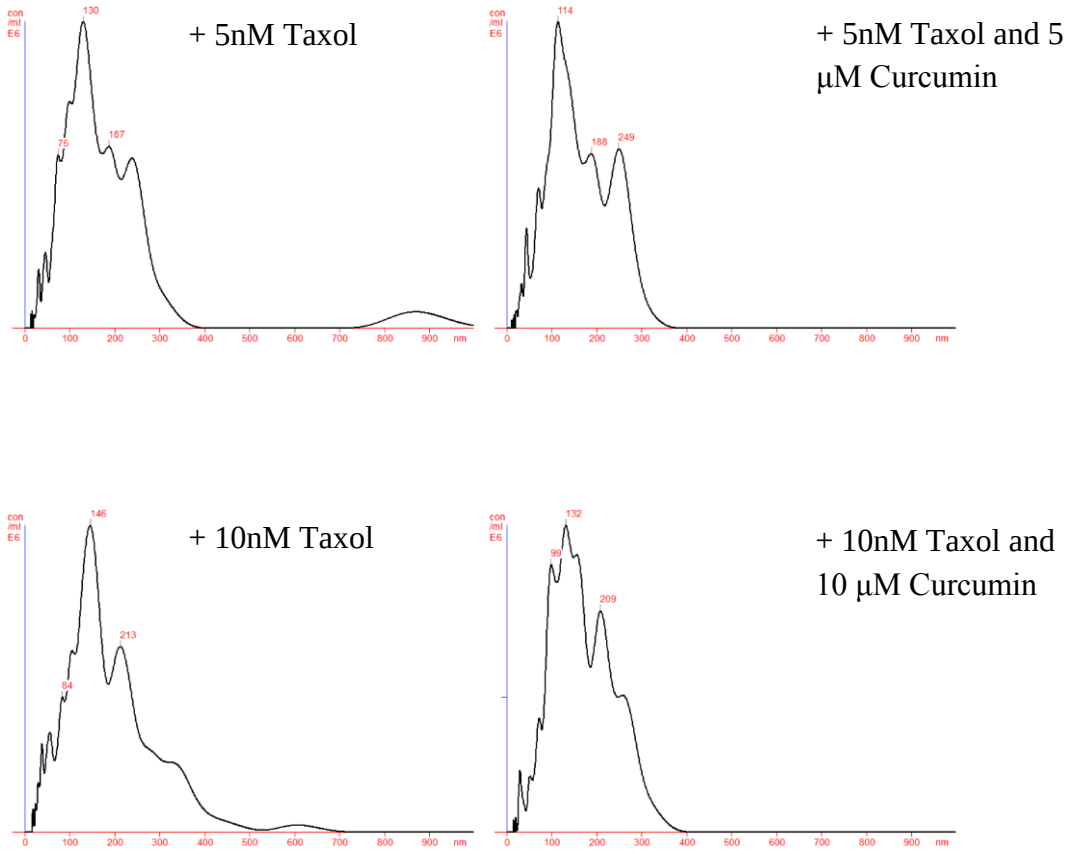
+ 5nM Taxol
+ 5nM Taxol and 5 µM Curcumin
+ 10nM Taxol
+ 10nM Taxol and 10 µM Curcumin

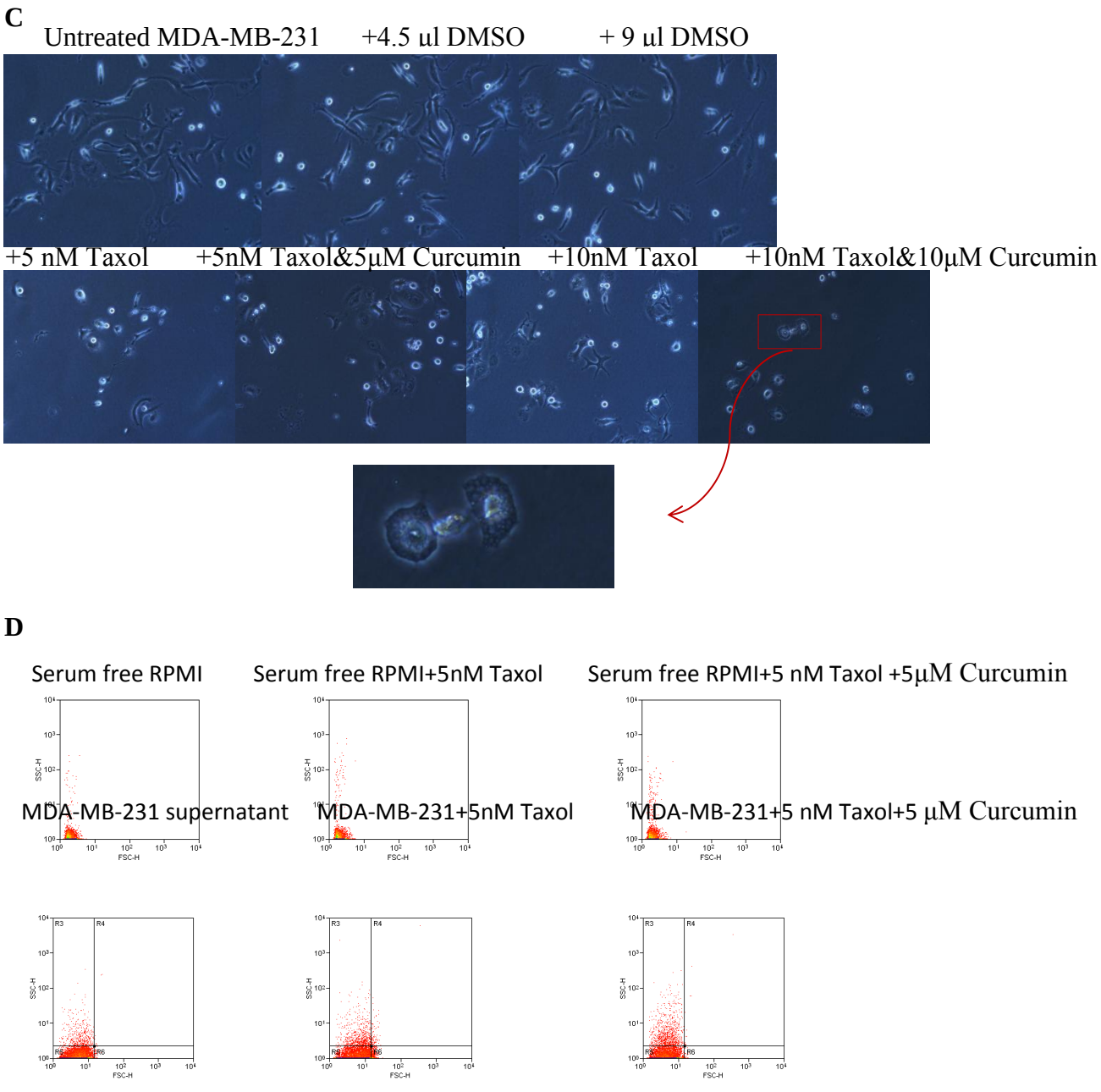

Figure 4.8: Detection of apoptotic vesicles induced by adding Taxol and Curcumin to MDA-MB-231 cells. (A). Untreated MDA-MB-231 control and MDA-MB-231 treated with DMSO. **(B).** MDA-MB-231 cells treated with Taxol alone or Taxol and Curcumin. **(C).** Images show the morphology of treated versus untreated cells. Cells treated with 10 nM Taxol&10 µM Curcumin show vesicle formation in cytoplasm. **(D).** Taxol and Curcumin treated MDA-MB-231 cell supernatant was centrifuged at 300 x g and analysed by flow cytometry after 48 hours. Serum free RPMI was used as a control. These data are representative of four experiments.

The results indicated that our controls (MDA-MB-231 alone and MDA-MB-231 with different volumes of DMSO) show a major peak of approximately 139nm, 122 nm and 147 nm (Figure 4.8 A) and very low amount of large/apoptotic vesicles, thus DMSO did not significantly influence the cell culture distribution of particles. In marked contrast, NTA detected a very identifiable second peak after drug treatment, and adding Curcumin had boosted the peak (Figure 4.8 B). This second peak was within the size range of 180-300 nm and is likely to be apoptotic vesicles induced by treatment with Taxol and Curcumin. It needs to be highlighted that previously sensitization of the cells with Curcumin prior to treatment with Taxol has boosted apoptosis, and increase the concentration of Taxol and Curcumin has induced more apoptosis. It should also be noted that 24 hours after adding 10 nM Taxol and 10 μM Curcumin, cells appeared to be enlarged and there was visible vesicle formation in the cytoplasm (Figure 4.8 C). There was no vesicle formation in the cytoplasm when cells were treated with a combination with both drugs at a lower concentration, or with Taxol alone at a higher concentration.

Samples were also analysed by flow cytometry (Figure 4.8 D), which detected extra material after addition of Taxol alone or Taxol with Curcumin. It seems to have shifted to the right and slightly upwards after adding 5 nM Taxol and shifted upwards more significantly after adding both drugs with no visible shift to the right. This further proved that treatment with drugs has induced particle release. As expected, it is hard to use the flow cytometry data alone to interpret the size and complexity of the extra particles secreted by adding drugs because of the insensitivity of flow cytometer with small nanoparticles.

Multiple freeze/thaw does not affect exosome size.

Since exosomes are being recognised more and more as mediators of intercellular communications and could be used within clinical settings, it is very important to know how stable exosomes are during storage. Thus, we have measured the size and integrity of exosomes after multiple freezing and thawing over 6 sequential cycles using dry ice.

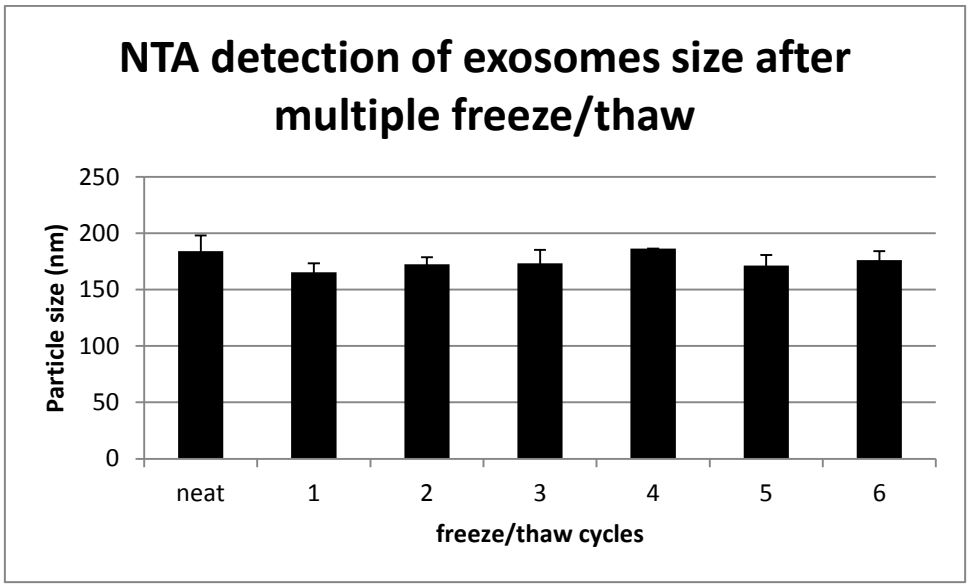

Figure 4.9: Multiple freezing/thawing of CEM supernatant. CEM cells were grown to 90% confluency. Medium was replace with serum free RPMI. Supernatant was collected after 48 hours. Freezing and thawing was accomplished by freezing the sample on dry ice, followed by thawing at room temperature for 3 minutes. Error bars indicate standard deviation.

The data show that multiple freezing and thawing does not cause changes in exosome size and no significant fragmentation was observed (Figure 4.9). These data suggest that this storage method is well-suited for storing exosomes.

Comparison of MDA-MB-231 supernatant after 300 x g and then 10, 000 x g and MDA-MB-231 exosomes purified by centrifugation and suspension in PBS.

Commonly used purification steps of exosomes include centrifugation and ultracentrifugation and suspension of exosomes in PBS. It is unknown whether pelleting exosomes and re-suspension in PBS would cause the formation of any exosome aggregates. Large aggregates could have different behaviour in many biological assay systems in comparison to disperse particle solutions. To investigate whether some exosomes could be clumped together after pelleting, a sample of MDA-MB-231 supernatant after 300 x g and then 10, 000 x g ultracentrifugation and a sample of exosomes purified after 100,000 x g and resuspended in PBS were compared on the Nanosight.

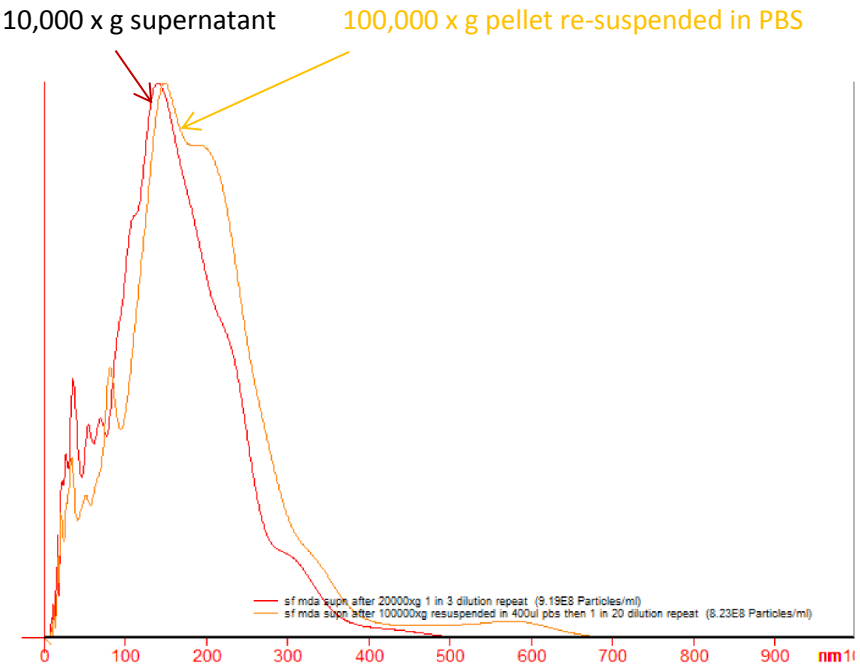

Figure 4.10: NTA comparison of supernatant after 10, 000 x g ultracentrifugation and pellet after 100,000 x g ultracentrifugation re-suspended in PBS. 48 hour MDA-MB-231 supernatant was collected and centrifuged at 300 x g then 10,000 x g. The resulting supernatant was split into 2 parts, one part was analysed directly on the Nanosight (Red line) and the other part was spun at 100, 000 x g and the pellet was re-suspended in PBS (yellow line). Data were representative of two experiments.

Analysis of both samples by the Nanosight shows no obvious difference between the two samples (Figure 4.10). Both samples have a peak size of approximately 130 nm. Although a small amount of large particles/aggregates with sizes between 400-700 nm were detected in the 100,000 x g pellet, no significant aggregates were detected by the Nanosight.

NTA can detect increases in microvesicle release

To test the ability of NTA to detect increases in microvesicle release, we treated the MDA-MB-231 cells with Tamoxifen and Thimerosal. Tamoxifen is an antagonist of the estrogen receptor. The binding of Tamoxifen to the estrogen receptor does not activate the receptor but this stops the hormone from binding to the receptor. It is widely used for the treatment of both early and advanced estrogen receptor positive breast cancers. Thimerosal is a drug known to induce apoptosis.

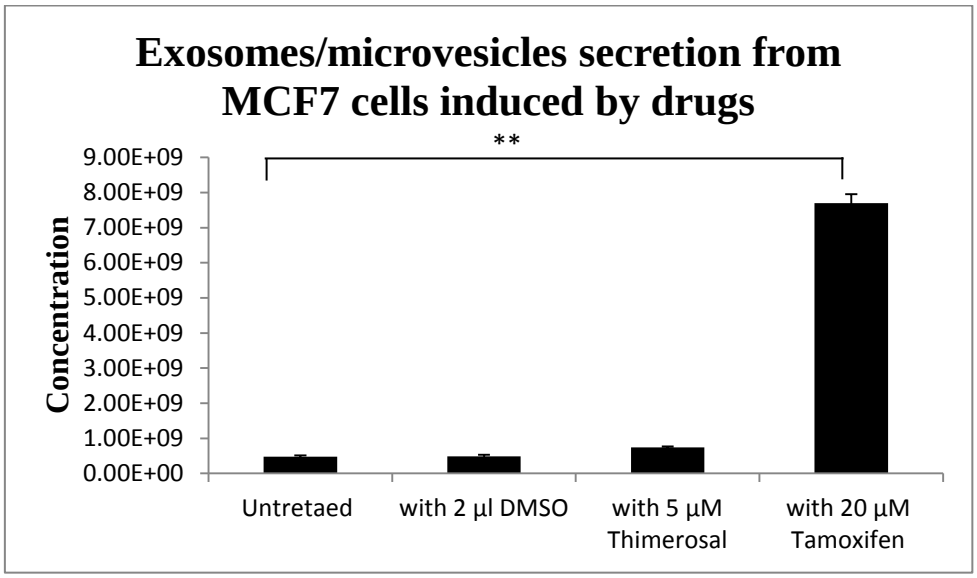

Figure 4.11: Microvesicles released from MCF7 cells were increased after addition of Thimerosal or Tamoxifen. 200,000 MCF7 cells were seeded into each well of a six-well plate. Medium were replaced with serum free medium and drugs were added after cells attached. After 48 hours, cell supernatant was collected and spun at 300 x g then 10,000 x g. The samples were then analysed by NTA and 3 videos were recorded. ** $P<0.01$. Error bars indicate standard deviation. These results were representative of three experiments.

Results show that cells treated with 5 µM Thimerosal and 20 µM Tamoxifen increased exosomes/microvesicles release compared to untreated cells and cells treated with DMSO. Increase in exosomes/microvesicles release was highly significant when cells were treated with 20 µM Tamoxifen.

Treatment with MDA-MB-231 with DMA

In order to investigate whether NTA is a suitable tool for rapid screening of drug inhibition of exosome secretion, we treated the MDA-MB-231 cells with 25 µg/ml 5-(*N*,*N*-dimethyl)-hydrochloride (DMA), inhibitor of the H^+/Na^+ and $Na^+/Ca2^+$ channels, which has previously been shown to reduce the secretion of exosomes (Chalmin et al., 2010; Sreekumar et al., 2010)

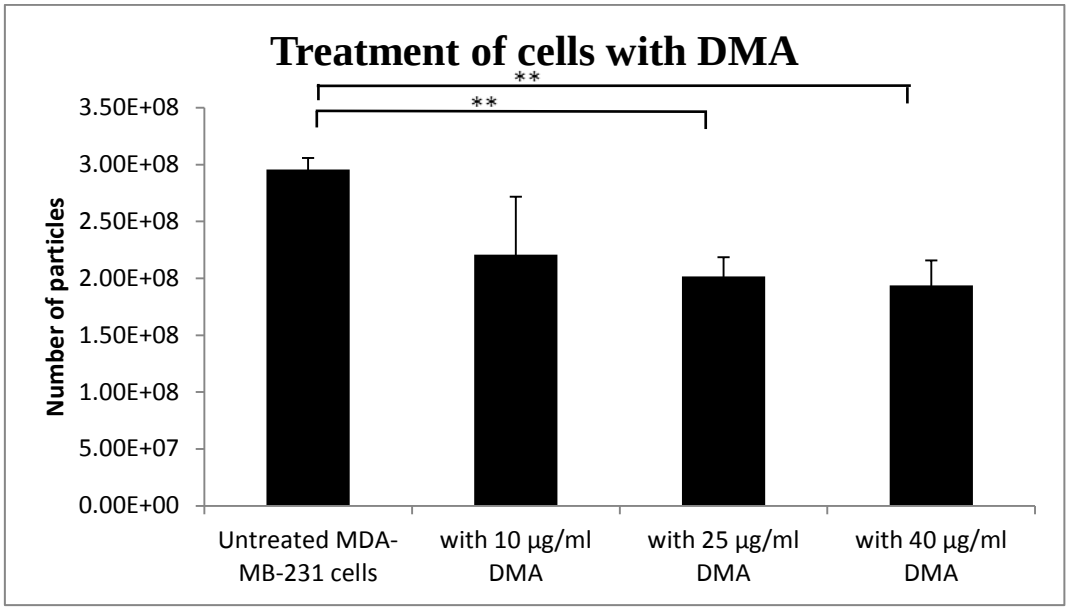

Figure 4.12: Treatment of MDA-MB-231 cells with DMA. Approximately 50,000 cells were seeded into each well of a six well plate. After cells reached approximately 50% confluency, different concentrations of DMA was added. Supernatant was collect after 24 hours, centrifuged at 300 x g and 10, 000 x g, then analysed by NTA. Error bars indicate standard deviation. ** P<0.01. Data are representative of three experiments. Results show that addition of 10 µg/ml DMA reduced exosome release, but this reduction was not statistically significant. Addition of 25 µg/ml and 40 µg/ml DMA significantly reduced exosome release as estimated by NTA.

Results show that treatment with 25 µg/ml and 40 µg/ml DMA significantly reduced exosomes release as measured by NTA (Figure 4.12).

Discussion

Since the emergence of NTA in 2006, it has been increasingly used in different fields of study such as nanoparticle synthesis and aggregation, toxicity and environment, drug delivery and micelles, exosomes and Pharma and vaccines, etc . For example, for nanoparticles synthesis and aggregation, some groups that used pulsed laser ablation to produce nanoparticles also used NTA to examine the particles size distribution (Suh et al., 2007). A recent paper has critically evaluated the ability of NTA to measure nanoparticles and protein aggregates. They have shown that NTA is very accurate in measuring both monodispersed and polydispersed samples and has better peak resolution when compared to DLS (dynamic light scattering) (Filipe et al., 2010).

The accuracy of Nanosight in measuring size and concentration.

First, the ability of NTA to measure size and concentration was determined by using polystyrene beads of known sizes supplied by Nanosight. The data suggested that although the detected sizes vary very slightly from the true sizes of the 200 nm and 400 nm beads, the results were still acceptably accurate. For measuring concentration, our data showed an almost straight line of the bead concentration at different dilutions. The Nanosight claims that the machine can measure concentration range from 10^8 to 10^9 particles/ml. It was found in this study that the most accurate sample concentration range is 2×10^8 to 1×10^9.

Supernatant from MDA-MB-231 and MCF7 after 300 x g and then 10, 000 x g

Supernatant collected from MDA-MB-231 cells were collected, centrifuged at 300 x g and 10, 000 x g, the supernatant was then analysed on NTA. The peak value of the MDA-MB-231 supernatant was 129 nm and the peak value for MCF7 supernatant was 159 nm.

Immunodepletion of exosomes/microvesicles using antibody-coupled magnetic beads.

CFSE and PE double staining described in the last chapter only labelled a relatively small percentage of the vesicles, so we further investigated the percentage of CD9 and CD63 positive vesicles by using secondary antibody-coated dynabeads coupled with either CD9 or CD63 primary antibody to pull down vesicles that were positive for either CD9 or CD63. Different amounts of antibodies were used and the supernatant that was depleted of either CD9 or CD63 positive vesicles were analysed on NTA. For CD9, 0.5 µl- 2 µl achieved better depletion compared to lower or higher concentrations of the antibody. It is possible using high concentrations of antibody may contaminate the supernatant with debris. For CD63, 5 µl seemed to have achieved the best depletion result.

Because non-specific binding of microvesicles to the beads exists, and it is hard to predict whether any exosomes would bind to the beads non-specifically and be excluded from the pre-cleared supernatant, it is hard to give a definite answer of the percentage of

CD9 or CD63 positive vesicles in our preparation by using this method. We could only conclude that at least 31.7 % of these vesicles were CD9 positive and at least 28.5% of these vesicles were CD63 positive (Figure 4.6). These data do vary from the result we obtained from the CFSE and PE double labelling experiment, which showed even weaker labelling (Figure 3.10). The discrepancy was not surprising as binding efficacy of different antibodies could vary.

Each protein is uniquely packed and loaded onto exosomes and also it has been reported that there might be different types of MVEs and exosomes. It is possible that not all thus necessarily contain CD9 or CD63 and exosomes should not be identified by a single molecular marker. CD9 has also been identified as present on other types of vesicles other than exosomes (Bobrie et al., 2012a) It is also possible the antibody to exosome ratio was not ideal and did not achieve the best binding efficacy.

Nanosight analysis of exosomes pulled down by CD9 and CD63 coupled-magnetic beads

An immunoaffinity method was used to pull down particles positive for either CD63 or CD9. NTA analysis of both populations of vesicles showed peak sizes of 131 nm, indicating that the sizes of exosomes purified by this method does not differ from the sizes of exosomes sedimented by sequential centrifugation. Of some note, however, purifying exosomes by immunoaffinity does not generate clinical grade exosomes as the acid elution of the exosomes from the beads and antibody may cause possible alterations of the surface of the exosomes.

NTA detection of apoptosis induced by Paclitaxel and Curcumin

Chemotherapeutic drugs exhibit their cytotoxic effect by inducing apoptosis in tumour cells. Chemotherapy may fail because the cancer cells become resistant to the therapeutic drugs. In the presence of toxic drugs, cancer cells can mutate and develop resistance to the drug, they can then divide and multiply and produce a tumour that is resistant to the drug. To overcome this problem, sometimes combinations of chemotherapeutic drugs are given at the same time, but multiple resistances can still occur. Thus, it is very important to know whether chemotherapeutic drugs being used can induce apoptosis in the tumour cells and the ability to detect apoptotic vesicles will be of great clinical significance.

It has been reported that Curcumin can sensitize tumour cells and make the therapeutic effect of Taxol more efficient in HeLa cells (Bava et al., 2005). We tested the ability of Taxol alone and Taxol in combination with Curcumin to induce apoptosis in MDA-MB-231 cells and tested whether NTA could detect apoptotic vesicles. For the supernatant from untreated cells or the supernatant from cells treated with DMSO, no large vesicles or very small amount of large vesicles were detected (possibly aggregates or microbubbles), and the peak sizes are between 120 nm to 150 nm, within the correct range of exosomes. In contrast, for supernatant from cells treated with either Taxol alone or Taxol with Curcumin, multiple peaks were detected. Apart from the main 'exosome' peak, another very noticeable peak with size between 180 nm to 250 nm constantly showed up with multiple experiments, indicating a different population of vesicles being secreted after the addition of these drugs. The percentage of apoptotic

vesicles were higher when treated with both drugs compared to the percentage of apoptotic vesicles induced by Taxol alone. This is consistent with the study by Bava et al, who illustrated that combining 5 nM Taxol with 5 μM curcumin enhances anticancer effects more efficiently than Taxol alone as demonstrated by increased cytotoxicity and reduced DNA synthesis in HeLa cells (Bava et al., 2005).

The vesicle formation in the cytoplasm of the apoptotic cells and enlargement of the cells was only observed when the cells were treated with a combination of 10 nM Taxol and 10 μM curcumin, indicating that a different mechanism may exist when high concentrations of Taxol and Curcumin was added. This will require further investigation. Flow cytometry also detected extra material after the addition of drugs, although the difference is not very significant. This could be due to the limitations of flow cytometry and insensitivity for detecting nanoparticles.

Multiple freeze/thaw does not affect exosome size.

It is very important to know whether multiple freezing and thawing would affect the stability of exosomes. Multiple freezing and thawing was achieved by snap freezing in dry ice and thawing in 37 °C water bath. Exosomes sizes did not change significantly after 6 times of freezing/thawing, indicating there is no obvious structural change or degradation. This is consistent with the study published by Sokolova et al, who examined the stability of exosomes during storage at -4 °C, -20 °C and 37 °C. They have found that exosomes sizes decreased at 4 °C and 37 °C, indicating a structural change or degradation (Sokolova et al., 2011). In contrast, another study demonstrated

that exosomes derived from IL-10-treated dendritic cells can supress inflammation and collagen-induced arthritis, and this suppressive effect is not just due to the delivery of the suppressive cytokine IL-10, but also requires the integrity of the exosome membrane. They have also shown by electron microscopy that multiple freeze/thawing using dry ice and water bath disrupted the exosomal membrane. Four freeze/thawing cycles disrupted the exosomes membrane and abrogate the suppressive effect (Kim et al., 2005). It has also been reported that the miRNAs present in exosomes from breast milk are very stable and are resistant to harsh conditions including multiple freeze/thawing (Zhou et al., 2012). Thus, it is unclear how exactly multiple freeze/thawing would affect the structure, function and contents of exosomes. Such information is, however, of critical importance if exosomes are to be used in clinical practice.

Comparison of MDA-MB-231 supernatant after 300 x g and then 10,000 x g and MDA-MB-231 exosomes purified by centrifugation and suspension in PBS.

Ultracentrifugation is the most widely used method for collecting exosomes, but it is unknown whether the 100, 000 x g ultracentrifugation and resuspending the 100, 000 x g pellet would cause the exosomes to form aggregates. The supernatants after 300 x g and then 10,000 x g and the 100, 000 x g pellet re-suspended in PBS were compared by using NTA. Very small amounts of large particles or aggregates were detected in the 100, 000 x g pellet re-suspended in PBS. We can conclude that the ultracentrifugation steps and re-suspension in PBS does not cause the significant formation of large number of aggregates.

NTA can detect increases in microvesicle release

Finding a rapid screening tool for increases in exosomes release will have significant clinical significance. NTA successfully detected increase in exosomes/microvesicles release from MCF7 cells induced by treatment with Tamoxifen and Thimerosal (Figure 4.11), indicating the possibility of using NTA as a cost effective, fast and reliable candidate.

Treatment of MDA-MB-231 cells with DMA

The ability to rapidly screen for drugs and agents that interfere specifically with exosome secretion may be of direct clinical importance. Decreasing exosome production using dimethyl amiloride has been reported to enhance the *in vivo* antitumor efficacy of the chemotherapeutic drug cyclophosphamide in 3 different mouse tumour models (Chalmin et al., 2010). It was also reported that treatment with 25 µg/ml DMA caused a significant 80% decrease in exosome release as evidenced by a decrease in CD63 expression in exosomal fractions examined by western blot (Sreekumar et al., 2010). Other groups have also reported that DMA reduced exosome release from cardiomyocytes by measuring the Acetylcholine esterase activity (Gupta and Knowlton, 2007; Zhang et al., 2012). Inhibition of exosomes released from tumour cells by using DMA has also been reported (Merendino et al., 2010).

We tested the ability of NTA to detect decreases in exosomes released from MDA-MB-231 cells after treatment with DMA. Adding 10 µg/ml has reduced

exosomes/microvesicles released by 25.4%, adding 25 μg/ml and 40 μg/ml decreased exosomes/microvesicles production by 31.8% and 34.5 %. Although the percentage of decrease is not consistent with Sreekumar et al' s group, who detected an 80% decrease, this could be due to different cell lines being used and different techniques being used to measure the decrease.

Chapter V: Rab27a and its effects on exosome release

Introduction

Rab27a belongs to the small GTPase Rab superfamily. It may be involved in protein transport and small GTPase mediated signal transduction. Rab27a has been shown to be involved in the exocytosis of secretory granules in melanocytes and cytotoxic T-cells. Rab27a is the only protein in the family whose loss of function is known to lead to disease, with Griscelli syndrome type 2 being an immunodeficiency genetic disorder that causes partial albinism. Patients with this disease have defects in cytotoxic T lymphocytes whose lytic granules fail to fuse with the plasma membrane and release their contents.

Rab27a regulates the transport of lysosome-related organelles, such as melanosome transport in melanocytes and lytic granule release in cytotoxic T cells. Rab27a has been shown to regulate the docking of vesicles with plasma membrane and the release of exosomes in HeLa cells. They have also noticed that multivesicular endosomes in the Rab27a knock down cells appear to be enlarged. Rab27a could be required for docking and vesicle fusion with each other instead of fusing with the plasma membrane when Rab27a has been knocked down. Alternatively, Rab27a could prevent fusion of the vesicles with each other and knocking it down caused formation of enlarged compartments whose physical sizes prevent them from fusing with the plasma

membrane (Ostrowski et al, 2010). Rab27a and Rab3a also regulate the docking step of dense-core vesicle exocytosis in neuroendocrine PC12 cells (Tsuboi a et al, 2006). Overexpression of RAB27A gene has also been shown to promote breast cancer cell invasiveness and the metastasis potential of the cancer by promoting the secretion of insulin-like growth factor-II (IGF- II) (Wang et al, 2008).

Ashen mice, which contain a splicing mutation in RAB27A, have been studied by a lot of groups. Ashen mice exhibit reduced intensity in coat colour, reduced number of platelet dense granules (Wilson et al., 2000) and defects in cytotoxic T cells which prevent them from killing the target cell.

Results

Rab27a shRNA treatment of MDA-MB-231 cells inhibits exosome release from MDA-MB-231 cells.

It has been reported that knocking down Rab27a in HeLa cells reduces exosome secretion (Ostrowski et al, 2010). Therefore we wanted to determine whether inhibiting Rab27a in MDA-MB-231 cells also resulted in a lowering of exosome secretion as analysed by NTA. Cells were stably transfected individually and with a *RAB27A*-targetting shRNA plasmid. Control and transfected cells were then lysed and analysed by immunoblotting (Figure 5.1 A), which revealed inhibition of Rab27a protein expression. Normalisation against actin with imageJ indicated that the knock down was approximately 50% (Figure 5.1 B).

A

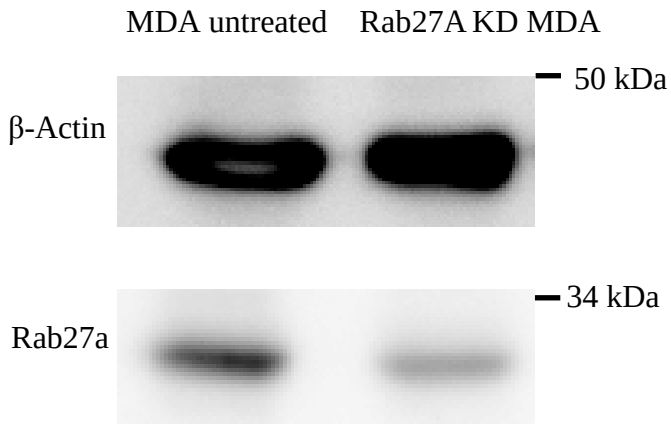

B

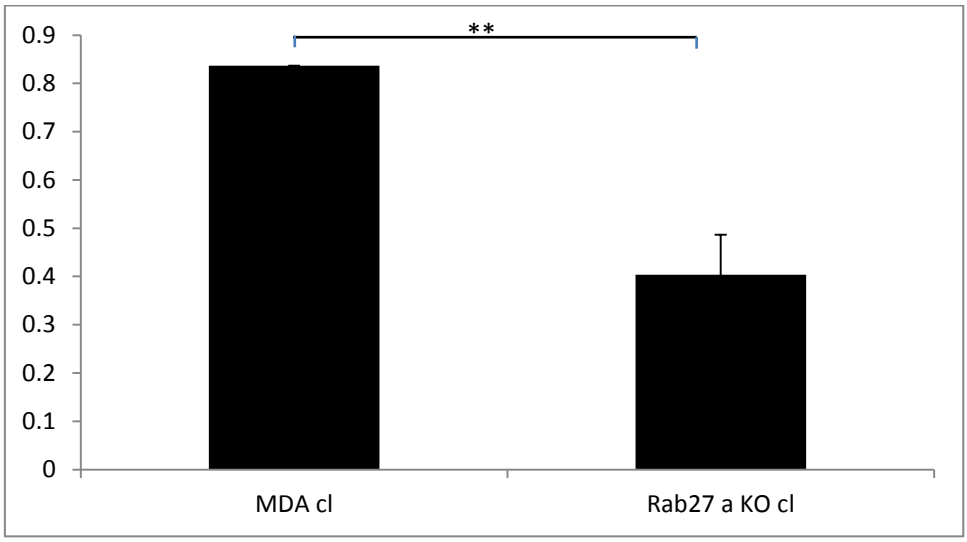

Figure 5.1: Transfecting MDA-MB-231 cells with Rab27a shRNA reduces the protein expression level. Cells were transfected with 1 µg of plasmid DNA and stable transfected cells were maintained in RPMI + 3 µg/ml Puromycin. **(A).** Cells were lysed and protein concentration was measured using the Bradford method. Equal amount of protein was loaded onto a 12% gel. Membranes were probed with the indicated antibodies. β-actin was also used to show equal loading. Results are representative of at three experiments. **(B).** Quantification of the band normalized with the corresponding β-actin band. Quantification was perfomed by using ImageJ from three experiments. Error bars indicate standard deviation. ** P< 0.01

To investigate whether inhibiting Rab27a also inhibits exosomes secretion in MDA-MB-231 cells and whether the decrease in exosome secretion was detectable by using NTA, the same number of control MDA–MB-231 cells and Rab27a KD cells were grown in a 6-well plate.

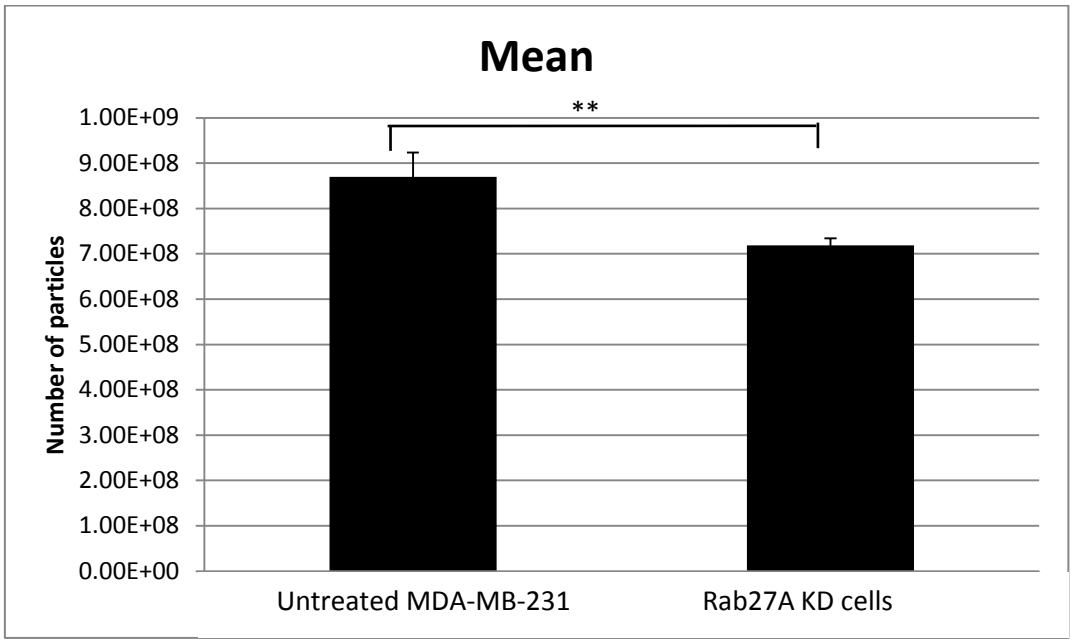

Figure 5.2: Exosome secretion comparison between untreated MDA-MB-231 cells and Rab27a knock down cells. Normal growth medium was replaced with serum free medium when both cell lines reached 90% confluency. Supernatant was then collected after 48 hours and was then ultracentrifuged at 300 x g for 10 minutes and 10,000 xg for 30 minutes. Pellet was diacarded and supernatant was compared on the Nanosight. Error bars indicate standard deviation. ** $P<0.01$

To confirm these findings, we decided to extend our observations and use more shRNA targetting Rab27a. 'SureSilencing shRNA plasmid for human Rab27a' (QIAGEN) was purchased which included 4 shRNA constructs which target the human RAB27A gene.

A negative scrambled shRNA construct was also supplied as a control. To confirm the plasmids supplied were the right size, plasmids were digested by *ScaI* (Figure 5.3).

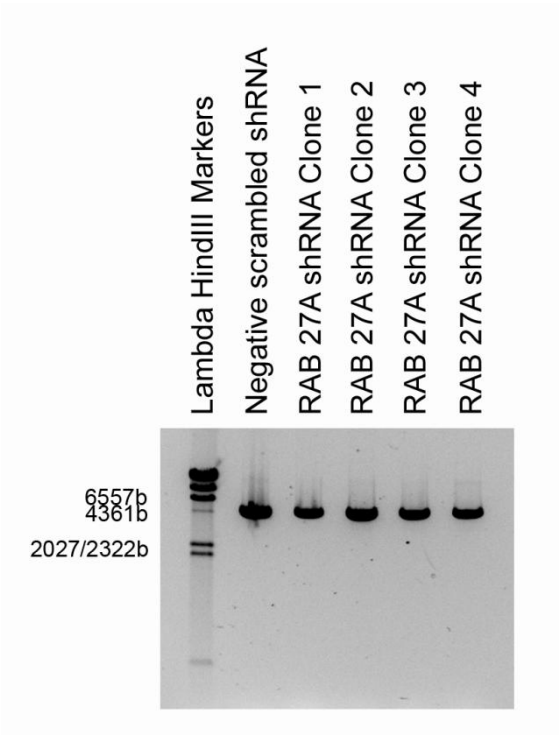

Figure 5.3: Sca 1 restriction digestion of the plasmid DNA. Purified plasmid DNA was checked by restriction digestion with *ScaI* which linearises the plasmid. Samples were analysed on 1 % agarose gels, at a constant voltage of 100 V for 45 minutes. DNA was visualised on an ultraviolet (UV) transilluminator.

The plasmids were confirmed to be the right size. MDA-MB-231 cells were then transfected using these shRNA plasmids. Cells were lysed and western blot was used to check the efficiency of inhibition of expression.

A

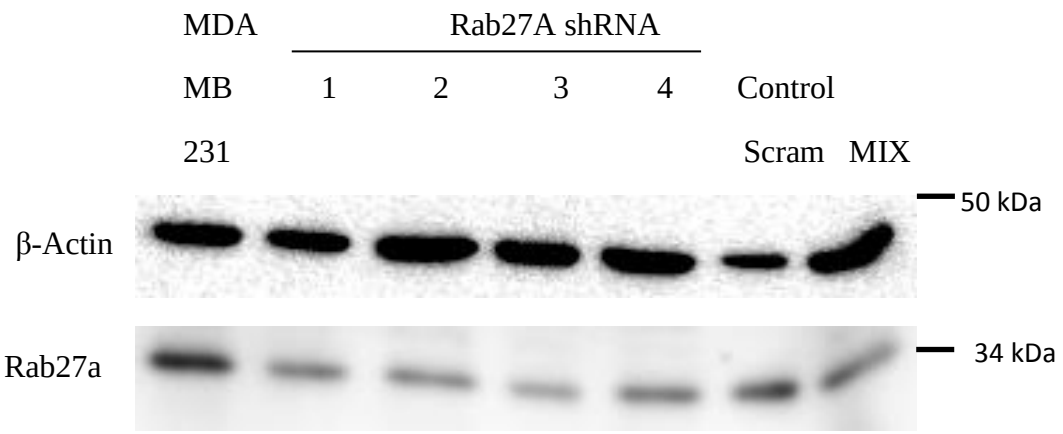

B

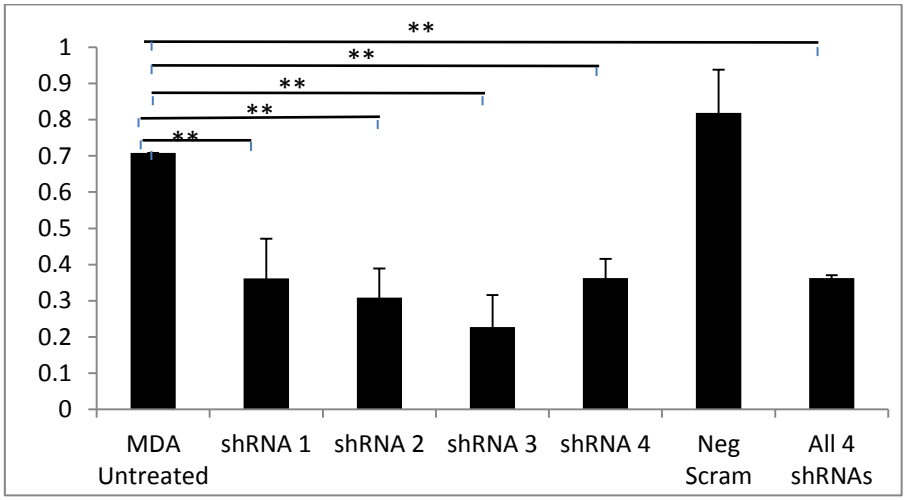

Figure 5.4: Transfecting MDA-MB-231 cells with Rab27a shRNA. Cells were transfected with 1 μg of 4 different types of shRNAs, a mixture of 4 shRNAs and a scrambled control. **(A)** Cells were lysed and protein concentration was measured using the Bradford method. Equal amount of protein was loaded onto a 12% gel. Membranes were probed with the indicated antibodies. β-actin was also used to show equal loading. Western blot result was representative of three experiments. **(B)** Quantification of the band normalized with the corresponding β-actin band. Quantification was performed by using ImageJ from three experiments. Error bars indicate standard deviation. ** P< 0.01

Immunoblotting again revealed efficient inhibition of Rab27a expression by all the ShRNA plasmids (Figure 5.4 A & B). Normalisation against actin analysed by using imageJ revealed that No.2 and No. 3 were more efficient compared to others, with No. 3 being the most efficient, when compared to control untransfected MDA-MB-231 cells and the negative scrambled construct (Figure 5. 4 B).

To further confirm the knock down of the Rab27a gene at the miRNA level, RNA was isolated from control MDA-MB-231 cells and Rab27a KD cells, RNA was then reverse-transcribed into cDNA and RT-PCR was performed. The expression level of the other Rab27 isoform, Rab27b, was also checked by PCR, based on a recent publication that indicated the possible inhibition of Rab27b in a similar system (Bobrie et al, 2012).

A

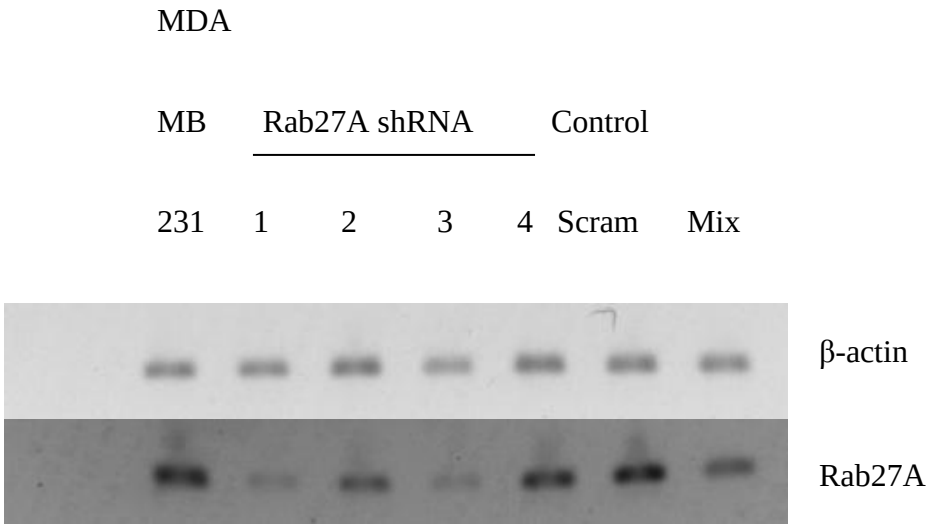

B

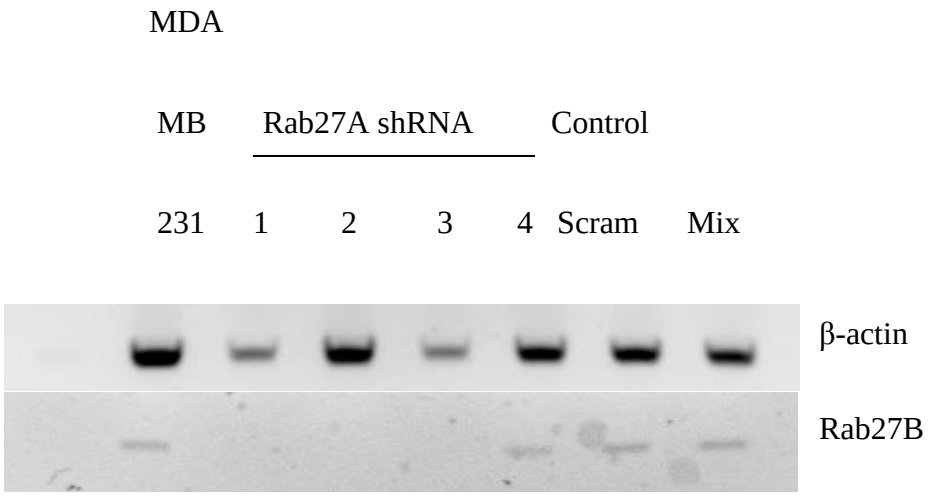

Figure 5.5: RT-PCR to check the knock down at the miRNA level. RNA was purified from untreated MDA-MB-231 cells and Rab27A shRNA transfected cells using RNeasy® Mini kit. 0.5 μg total RNA was used reverse-transcribed into cDNA. PCR was done using ReadyMix^{TM} Taq PCR Reaction Mix from Sigma. The RT-PCR

products were analysed by 2 % agarose gels, at a constant voltage of 100 V for 45 minutes. DNA was visualised on an ultraviolet (UV) transilluminator. **(A).** PCR for Rab27A. **(B).** PCR for Rab27B. Results are representative of at least three experiments.

RT-PCR results show that all shRNAs except No.4 gave knocked down Rab27A efficiently, these results are similar with the western blot data and have further confirmed the knock down at the mRNA level (Figure 5.5 A). Surprisingly, shRNA1, shRNA2 and shRNA3 also knocked down Rab27B completely, whereas shRNA4 and all 4 shRNA mixed together did not affect the Rab27B expression level (Figure 5.5B).

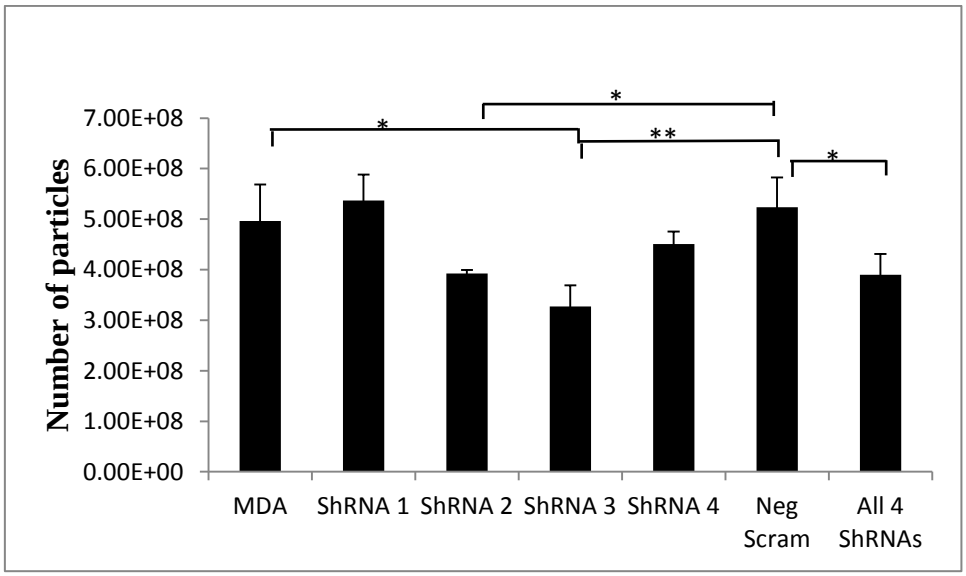

Figure 5.6: Exosome secretion comparison between untreated MDA-MB-231 cells and Rab27 knock down cells. Equal number of untreated and Rab27 KO MDA cells were seeded in a 6 well plate. After 24 hours, cell medium was replaced with serum free medium. After 24 hours, cell culture supernatant was collected and ultracentrifuged at 300 x g and then 10,000 xg for 30 minutes and analysed on the Nanosight. The concentration of microvesicles was compared. Results are representative of at least three experiments. Error bars indicate standard deviation. * $P<0.05$, ****** $P<0.01$

The cell supernatant from both control and transfected cells were ultracentrifuged at 300 x g and then 10, 000 x g and analysed by NTA. Lower number of exosomes were secreted from the Rab27 KD cells, with the exception of No.1, when compared to control cells. This could be because of loss of expression in the cells (Figure 5.6). Comparing exosome release from shRNA2, shRNA3 and mix to the scrambled control shRNA, all 3 were statistically different.

We further investigated that the decrease in the particle numbers were due to a reduction in exosome secretion. The total amount of secreted exosomes, was determined by measuring the total amount of protein in the 100,000 x g pellet.

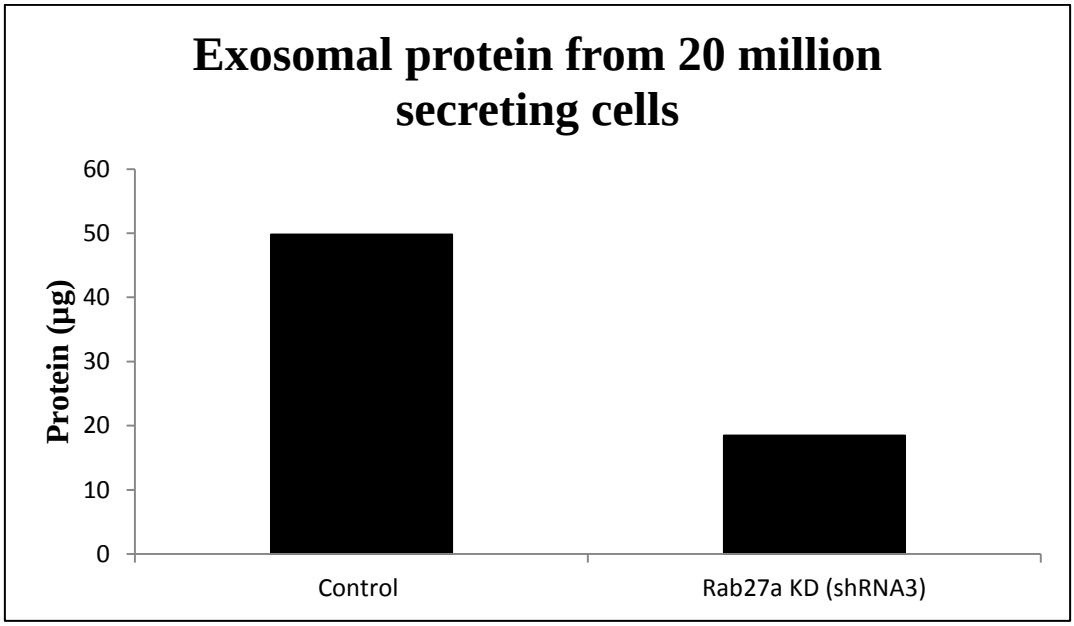

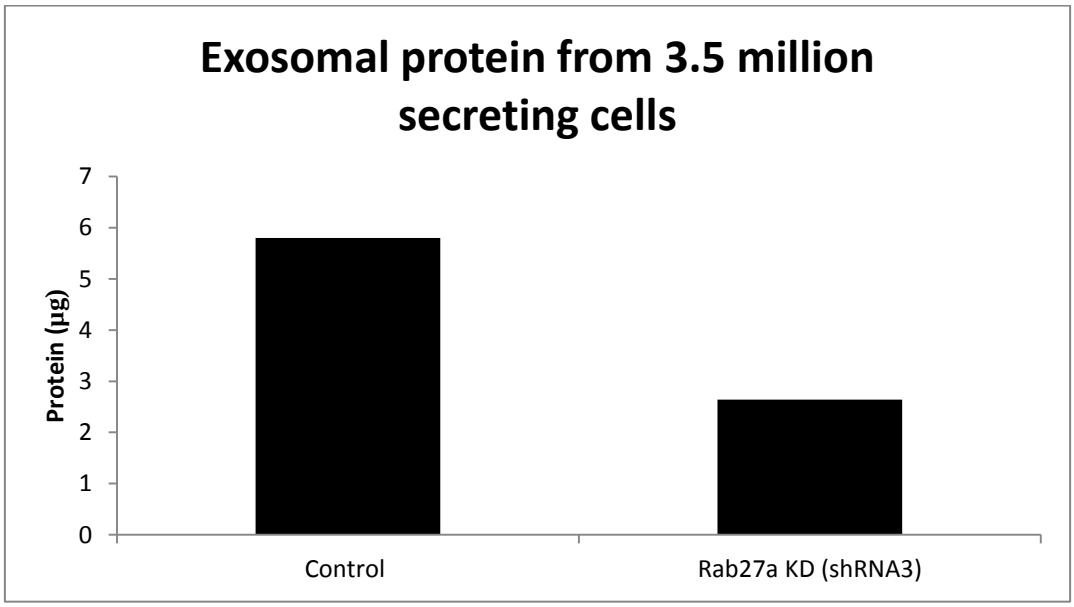

Figure 5.7: Total amounts of protein in the exosome pellets purified using our standard ultracentrifugation method. Cells were seeded in either two T150 cm^2 flasks with 10 million cells in each flask (for 20 million cells) or one T75 cm^2 flask (for 3.5 million cells). Medium were replaced with serum free medium as soon as cells attached. Supernatant was collected after 48 hours and spun to collect exosomes. Exosomal protein concentration was measured using Bradford method. Data are representative of two experiments.

Consistent with the Nanosight results, the total amount of protein in the exosome pellet from Rab27 KD cells were significantly reduced compared to the total amount of protein in the exosome pellet from untreated MDA-MB-232 cells (Figure 5.7). Typical exosome markers were also further analysed by immunoblotting. Briefly, exosomes/microvesicles were collected from the supernatant of the same number of control MDA-MB-231 and Rab27a KD secreting cells.

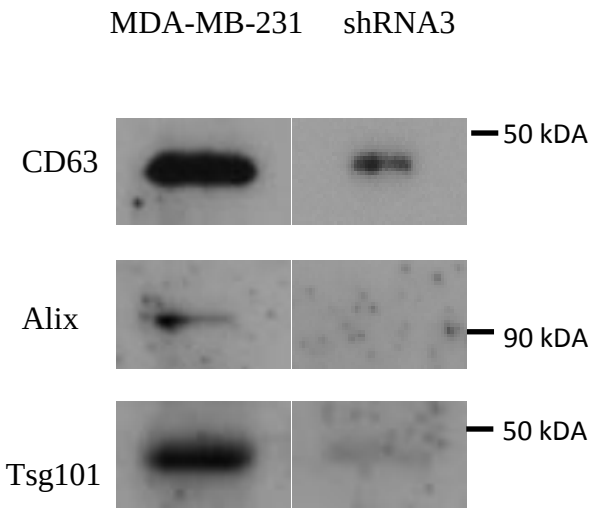

Figure 5.8: Characterisation of exosomal proteins by immunoblotting. 20 million control MDA-MB-231 cells and Rab27 KD cells were seeded and the medium was replaced with serum free medium after cells were attached. Exosomes were then analysed by immunoblotting for the comparison of typical exosomal markers Alix, Tsg101 and CD63. One representative experiment out of three is shown here.

Consistent with the NTA data, a reduction in the signals of typical exosomal markers (CD63, Alix and Tsg101) was observed from the immunoblotting results, indicating that exosome release was indeed reduced from Rab27 KD cells when compared with control cells (Figure 5.8).

It has been reported that knocking down Rab27a or Rab27b changes the morphology of MVBs in HeLa cells (Ostrowski et al., 2010). To investigate whether knocking down Rab27 in MDA-MB-231 cells have the same effect, MVBs were stained with a typical MVB marker CD63.

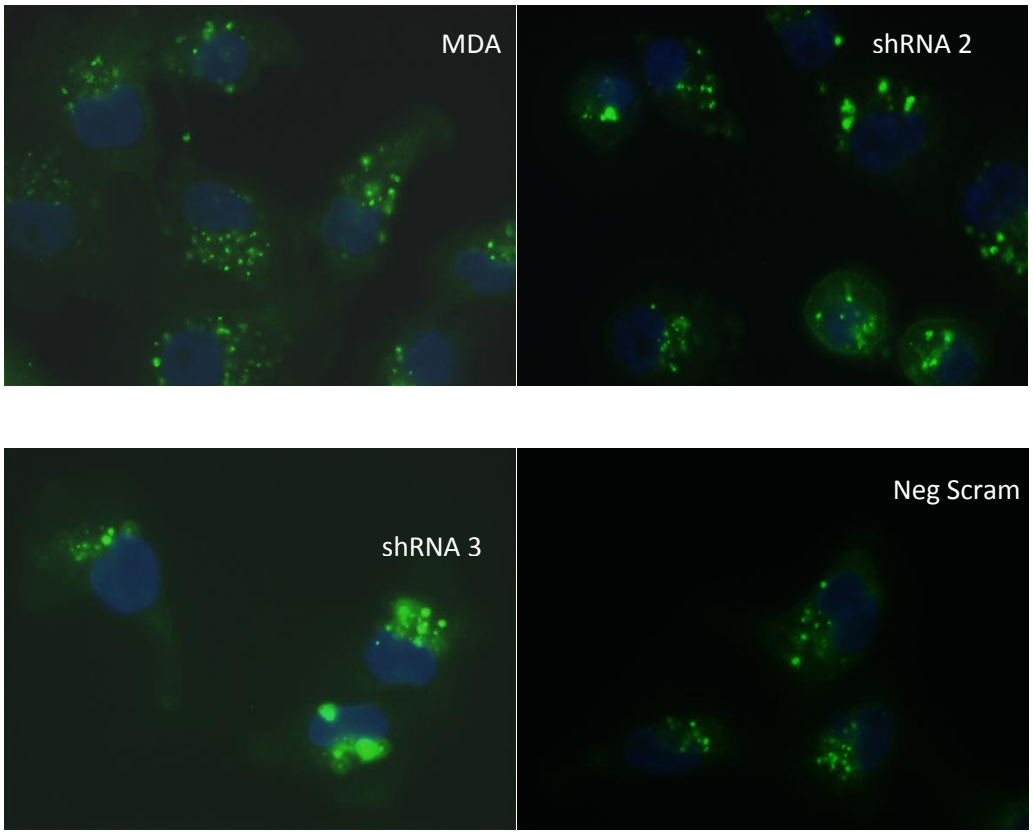

Figure 5.9: Immunofluorescence microscopy of control MDA cells and Rab27 knock down cells. A few drops of cells were seeded onto fluorodishes. After 24 hours, Cells were fixed with 4% paraformadehyde for 15 minutes at RT, washed 3 times with PBS containing 0.1M Glycine, and permeabilized with PBS containing 0.2% BSA and 0.05% Saponin. Cells were then incubated with anti-CD63 primary antibody and FITC anti-mouse secondary antibody, stained and visualized under a fluorescent microscope. This experiment was performed four times.

Immunofluorescenct microcopy images show that the MVBs in Rab27 KD cells appear enlarged when compared to the MVBs in the control MDA-MB-231 cells and the scrambled control cells (Figure 5.9). It is possible that Rab27a is required for the fusion of MVBs with plasma membrane and MVBs fuse with each other which lead to enlarged MVBs, or Rab27a prevents MVBs from fusing with each other and the lack of it cause MVBs to fuse together and the enlarged size impair their abilities to fuse with the plasma membrane (Ostrowski et al., 2010).

Knocking down Rab27 has reduced migration rate and invasiveness of MDA-MB-231.

It has been reported that tumour cells secrete exosomes which inhibit immune responses and promote their growth, or promote angiogenesis or migration to form metastases. We hypothesized that tumour secreted exosomes promotes changes in tumour behaviour, and that reduced secretion of exosomes should mean less growth and migration. We have shown that knocking down of Rab27 reduces the number of exosomes secreted by MDA-MB-231 cells. To test whether knocking down of Rab27 attenuates the cell's ability to grow and migrate, MDA-MB-231 cells were subject to a scratch assay.

A

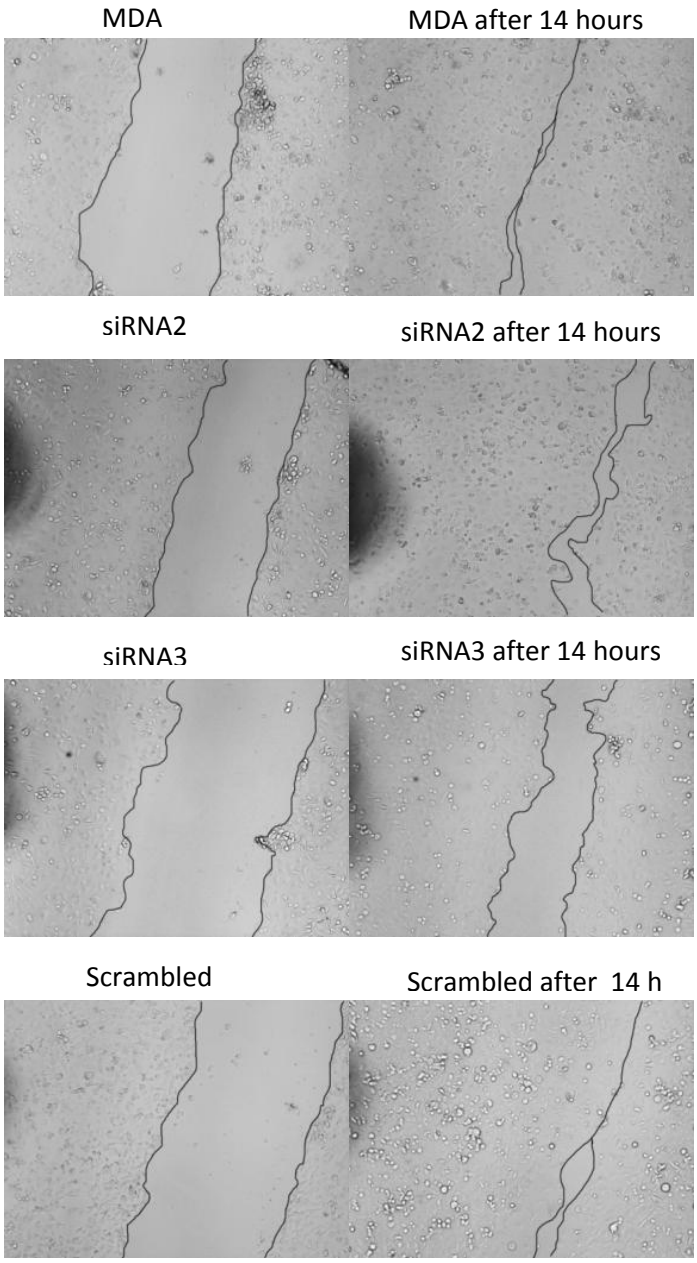
MDA
MDA after 14 hours
siRNA2
siRNA2 after 14 hours
siRNA3
siRNA3 after 14 hours
Scrambled
Scrambled after 14 h

B

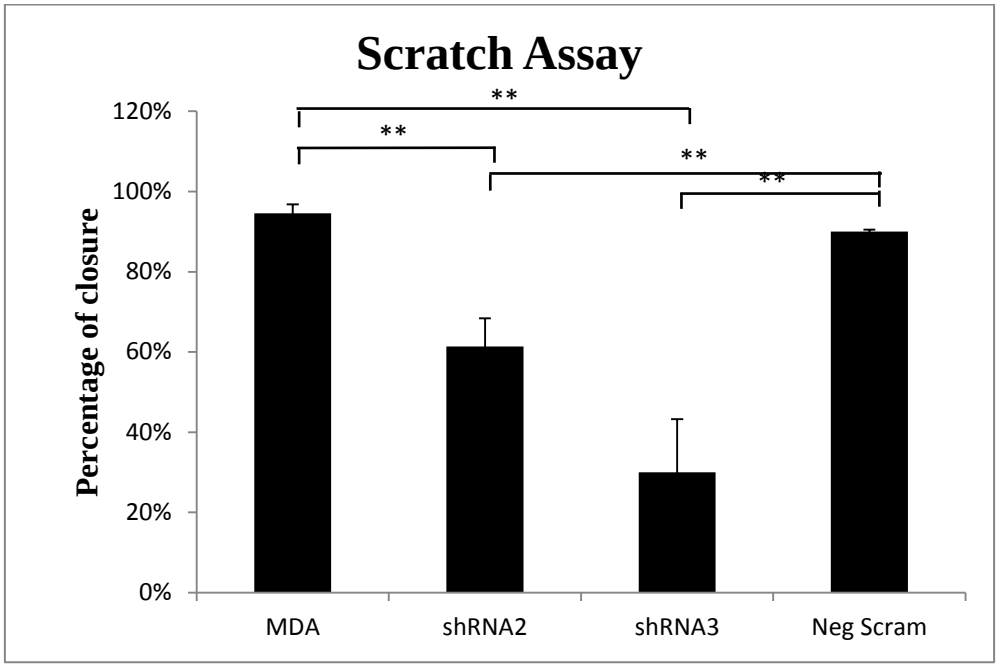

Figure 5.10: Scratch assay of MDA cells and Rab27 knock down cells. The same number of cells from each cell line was seeded into a 6 well plate. When the cells reached confluency after approximately 24 hours, the cell monolayer was scraped in a straight line to create a scratch with a P200 pipette tip. Cells were washed with media and fresh media was added. **(A).** Photos were taken at 0 hours and 14 hours and were compared. **(B).** Results of scratch assays were plotted as percentage of wound closure relative to hour 0. Error bars indicate standard deviation. Results are representative of four experiments. ** $P<0.01$

As expected, after 14 hours of scratching the plate, the gaps from MDA cells and control scrambled cells have almost closed completely (Figure 5.10A, first row and fourth row), whereas the gaps from the Rab27 knock down cells were still visible (Figure 5.10A, second and third row), with shRNA3 transfected cells showing the slowest closure (Figure 5.10A, third row). Results from three replicate experiments were plotted as percentage of wound closure relative to hour 0. The data revealed that

control Rab27 KD cells showed a deficit in growth and/or migration in comparison to control MDA-MB-231 cells and MDA-MB-231 cells containing scrambled shRNA, which had a percentage of closure of over 90%, whereas the percentage of wound healing for shRNA2 and shRNA3 were only approximately 60% and 30 % accordingly.

It has been reported that overexpression of Rab27A may be related to the invasiveness of breast cancer. To determine whether knocking down of Rab27 would impact on cell's growth and invasive potential and whether this reduction is due to the reduction of exosome secretion, untreated MDA cells, two of the transfected lines and the scrambled control were tested in the matrigel invasion assay.

A

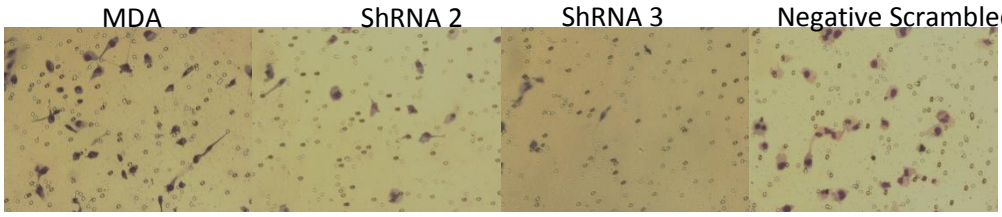
MDA
ShRNA 2
ShRNA 3
Negative Scrambled

B

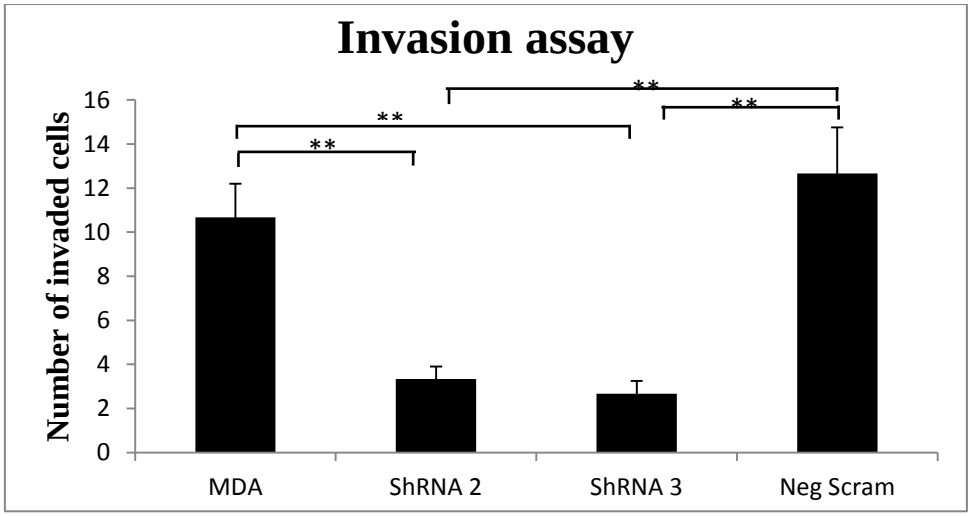
Invasion assay
Number of invaded cells
16
14
12
10
8
6
4
2
0
**
**
**
**
MDA
ShRNA 2
ShRNA 3
Neg Scram

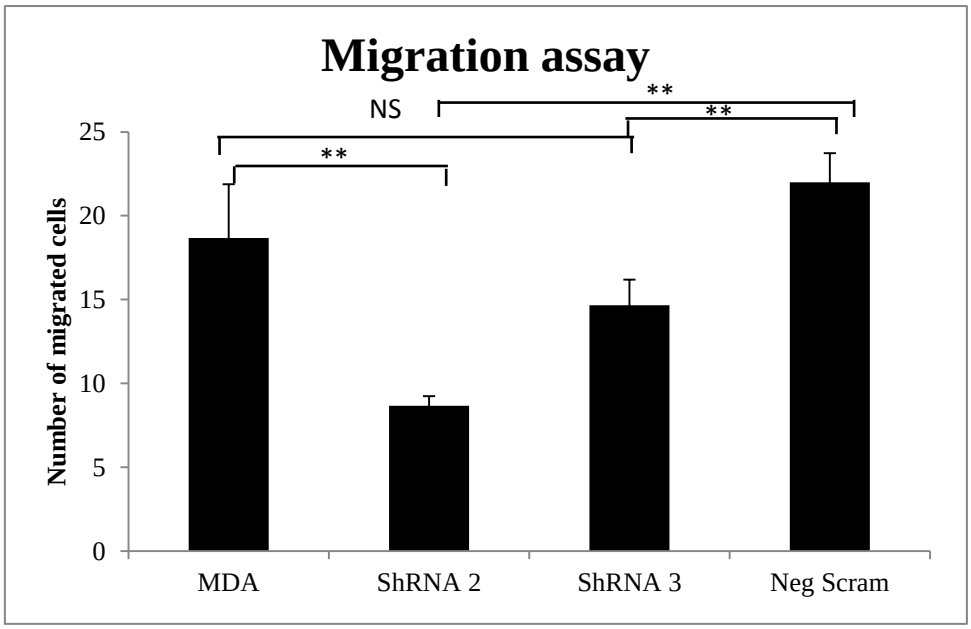
Migration assay
Number of migrated cells
25
20
15
10
5
0
NS
**
**
**
MDA
ShRNA 2
ShRNA 3
Neg Scram

C

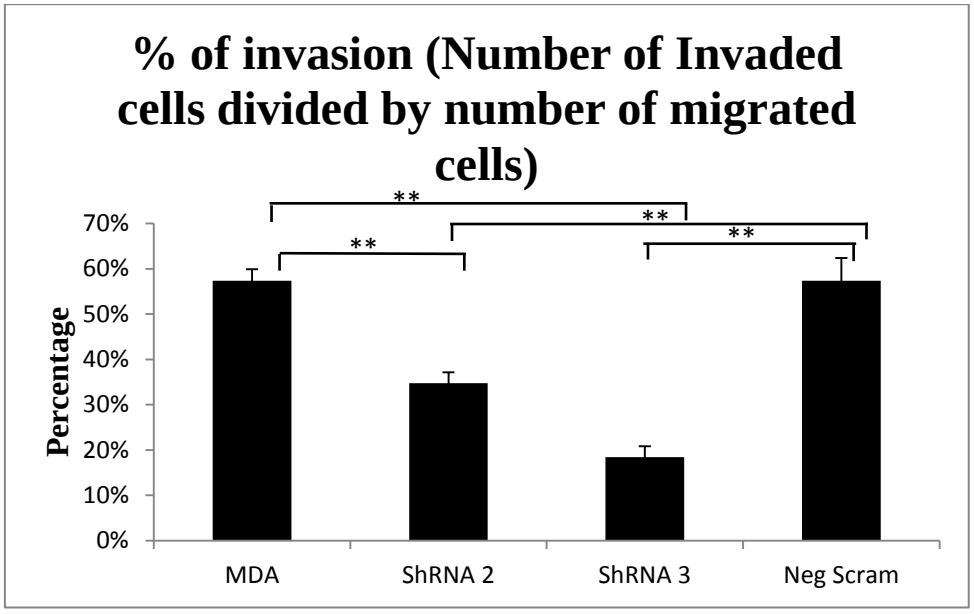

Figure 5.11: Matrigel Invasion assay results for untreated MDA cells and Rab27 knock down cells. Matrigel coated inserts was pre-treated according to manufacturer's instructions. 0.75 ml RPMI with 10% FCS and PSG were added to the bottom of the wells as chemoattractant. 2.5 x 10^4 cells in serum-free RPMI + 0.1% BSA were seeded into the control inserts and Matrigel-coated inserts. After 22 hours of incubation, cells on top of the inserts were scrubbed off and cells that migrated/invaded through the inserts were stained and counted. **(A).** These are the cells that invaded through the Matrigel coated inserts. **(B).** These are the cells that migrated through the control inserts. **(C).** Percentage of invasion was calculated according to the equation stated in the materials and methods section. Result was representative for three experiments. Error bars indicate standard deviation. ** $P<0.01$

The number of cells that migrated through the control inserts and invaded through the Matrigel coated inserts vary between untreated MDA cells and Rab27 KD cells. Slightly less RAB27 knock down cells migrated through the normal control inserts (Figure 5.11B), but dramatically less RAb27 knock down cells invaded through the matrigel inserts compared to untreated MDA cells and control scrambled cells (Figure 5.11 A).

Percentage of invasion was calculated as number of invaded cells divided by number of migrated cells.

ShRNA 3 shows the lowest number of invaded cells (Figure 5.11A). Thus, the knocking down of RAB27 has dramatically reduced the cell's ability to invade. Knocking down of RAB27 also affected the cell's ability to migrate (Figure 5.11B), but the affect is not as dramatic. In order to investigate whether the cloning efficiency of tumour cells changed as well as the reduced ability of the cells to migrate and invade and whether this was due to a reduced number of exosomes released in the knock down cells, we performed an anchorage independent colony assay.

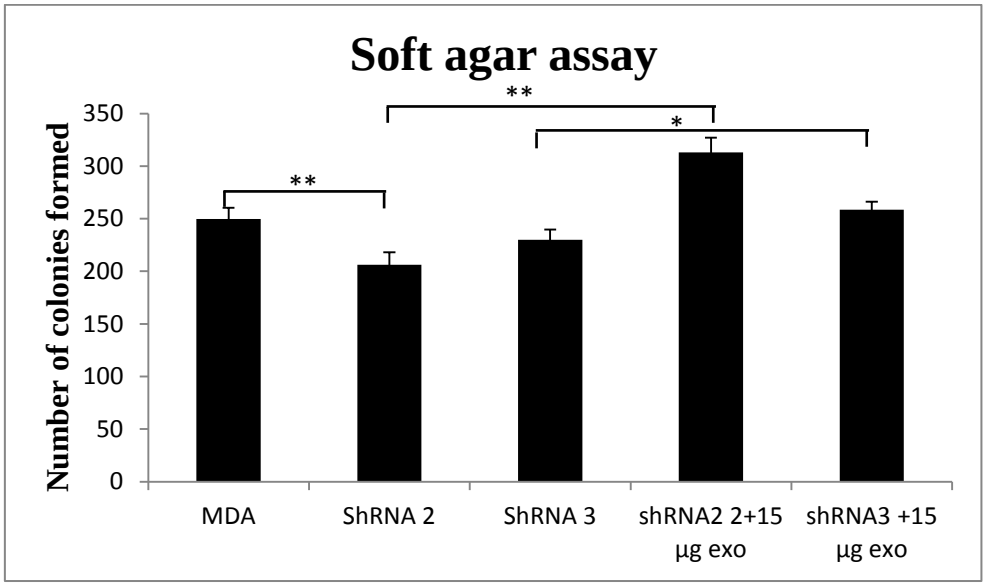

Figure 5.12: **Soft agar assay of control MDA cells and Rab27 knock down cells.** 5% agar was melted and mixed with RPMI to make 0.5% agar. 2 ml was added to each well of all the 6 well plates as the bottom layer. It was left to set for about 1 hour. Stock concentration of 10,000 cells/ml was prepared. 3% agar was mixed with RPMI and 1 ml of cell. 2 ml of the mixture was added to each well to make the top layer. 15 µg of exosomes were added to each of the wells of shRNA2 and shRNA 3 cells. Experiment was done in triplicates. * $P<0.05$, ** $P<0.01$

ShRNA2 and shRNA3 targeted cells formed fewer colonies compared to control MDA-MB-231 cells, however supplementation with 15 μg MDA-MB-231 derived exosomes increased the number of colonies formed (Figure 5.12).

Discussion

Rab27a shRNAs treatment of MDA-MB-231 cells inhibits exosome release from MDA-MB-231 cells.

We used a single shRNA construct from Santa Cruz and SureSilencing shRNA plasmids for human Rab27a from Qiagen, which included 4 shRNA constructs which target the human RAB27a gene. A negative scrambled shRNA construct was also supplied as a control. Plasmids were digested by *ScaI* and were confirmed to be the right size. Western blot was used to check the knock down of Rab27a and normalisation against β-actin showed confirmed knocking down of Rab27a. RT-PCR was used to check the knock down at the mRNA level and surprisingly, although Rab27a was knocked down at the mRNA level, shRNA No.1, No.2 and No.3 also knocked down Rab27b completely. A recent study from Thery's group also reported that only 2 out of 5 shRNAs they used that were designed to target Rab27a, inhibited this gene without affecting Rab27b (Bobrie et al., 2012a). Thus our data is in accordance with this observation.

We then examined whether knocking down Rab27a affects exosome release from MDA-MB-231 cells and whether this decrease in exosome release could be detected by NTA. NTA analysis of the cell conditioned supernatants, post 10,000 x g spin, revealed lower numbers of exosomes in all the shRNA constructs expressing cells, with the exception of no.1 (shRNA 1 treated cells were looking very unhealthy and apoptotic).

Comparing exosome release from shRNA2, shRNA3 and mix to the scrambled control shRNA, all 3 were statistically different.

We needed to confirm that the decrease in particle production was due to decreases in exosomes released and not decreases in other populations of microvesicles, so the Bradford method was then used to confirm that the amount of exosomal protein was decreased when comparing the exosomes secreted from the same number of untreated cells and shRNA3 treated cells. Western blot was also used to confirm that the intensity of the bands of typical exosome markers was decreased. These data suggest that inhibiting the expression of Rab27a (and Rab27b) inhibited the release of exosomes from MDA-MB-231 cells and shRNA2 and shRNA3 seem to be the most efficient, possibly because shRNA2 and shRNA3 not only targeted Rab27a, but also inhibited Rab27b, thus enhancing the effect, as Rab27b was also reported to inhibit exosomes release from HeLa cells (Ostrowski et al., 2010). A very recent study by the same group demonstrated that inhibition of Rab27b did not affect the secretion of exosomes by the two murine carcinomas used in the study as it did in HeLa cells, suggesting that Rab27 proteins are not universal regulators of exosomes secretion (Bobrie et al., 2012b). Nevertheless, our data showed that Rab27 proteins do play a role in the regulation of exosomes secretion from breast cancer MDA-MB-231 cell line.

Immunofluorescence also revealed that multivesicular bodies were enlarged and the distribution was more ‘peri-nuclear’, rather than distributed more evenly in the cytoplasm in the control cells. This is consistent with the study published by Ostrowski et, al, who demonstrated that inhibition of Rab27a lead to enlarged multivesicular

bodies and inhibition of Rab27b causing the multivesicular bodies to distribute in the peri-nuclear regions (Ostrowski et al., 2010). Because our shRNAs inhibited the expression of both Rab27a and Rab27b, so both effects were observed in this study.

Knocking down The Rab27 family has reduced migration rate and invasiveness of MDA-MB-231.

It is still unclear whether the constant production of tumour cell-derived exosomes is beneficial or harmful for their own survival *in vivo*. Pancreatic tumour cell-derived exosomes have been shown to decrease tumour cell proliferation and induce apoptosis (Ristorcelli et al., 2008). On the other hand, tumour cell-derived exosomes have also been shown by most studies to promote cancer cell growth. It was shown that tumour-derived exosomes contribute to the growth of tumours by blocking the activation of NK cells (Liu et al., 2006). Gastric cancer exosomes have been shown to promote cancer cell proliferation through activation of the PI3K/Akt and MAPK/ERK pathway (Qu et al., 2009a).

We checked whether knocking down the Rab27 family affected the cell's ability to grow by performing a scratch assay. The result of the scratch assay indicates that when the Rab27 family genes were knocked down, cells migrated at a slower rate. To test whether the knock down cells have attenuated ability to invade, a matrigel invasion assay was performed. Consistent with the scratch assay, fewer knock down cells migrated through the control inserts towards chemoattractants, and dramatically lower number of knock down cells invaded through the matrigel coated inserts.

Since our data suggest that knocking down the Rab27 family was associated with a decrease in the release of exosomes, and also associated with the reduced ability of the MDA-MB-231 cells to migrate and invade, we hypothesized that the reduced ability of the cells to migrate and invade could be due to, or at least partly due to decreased number of exosomes secreted by the knock down cells. Behaviour of the untreated MDA-MB-231 cells and the Rab27 family knock down cells were investigated further by performing a soft agar assay. The knock down cells produced a smaller number of anchorage-independent colonies compared to the untreated cells and supplement of the medium with MDA-MB-231-derived exosomes restores the colony formation. Thus, it is possible that the ability of MDA-MB-231 to migrate, invade and form colonies could be driven by the release of exosomes and a decrease in exosomes released would attenuate the cell's ability to migrate, invade and metastasize. This would need to be further investigated and we do not exclude the possibility of involvement of other factors. Thus, the exosome pathway is a valid target to attempt to disrupt the behaviour of tumour cells.

Our results, together with the very recent study showing that reducing the expression of RAB27A decreased tumour growth and metastasis (Peinado et al., 2012), and the study by Wang et al showing that overexpression of RAB27A correlates with breast cancer invasiveness and metastasis (Wang et al., 2008), indicate that RAB27A should be considered as a potential therapeutic target in cancer.

Summary

The results we obtained in this chapter demonstrated that knocking down the Rab27 family genes reduced exosomes released by in MDA-MB-231 cells and NTA is capable of rapidly detecting this decrease. The fact that knocking down Rab27 family reduced the cell's ability to migrate, invade and form anchorage independent colonies, and adding MDA-MB-231 cells-derived exosomes restored the knock down cells' ability to form colonies leads to the conclusion that MDA-MB-231 cell derived exosomes may play a role in the migration, invasion and metastasize of the cells. However, further investigation is needed to define the mechanism by which exosomes influence these changes in tumour behaviour.

Chapter VII: conclusions and future work

Although interest in exosomes has expanded greatly in recent years, the biogenesis, composition and functions of exosomes are still less than perfectly clear. Characterisation of these fascinating vesicles will contribute to the understanding of how they behave. The aim of my project is to further characterise the exosomes/microvesicles secreted from MDA-MB-231 and MCF7 breast cancer cell lines. In this study, we have used flow cytometry, western blot and NTA to characterise exosomes. In the first chapter of results, we have shown that MDA-MB-231 and MCF7 breast cancer cell-derived exosomes were capable of inducing apoptosis of Jurkat T cells, supporting the theory of immunosuppressive functions of tumour-derived exosomes. We have also successfully used electroporation to transfer Rab27a siRNA into MDA-MB-231 cell-derived exosomes, and these exosomes were capable of delivering the encapsulated siRNA into MDA-MB-231 cells and knocking down the Rab27A gene.

Secondly, NTA was used to characterise the exosomes. NTA was shown be very accurate at rapidly measuring size and concentration of particles. The ability of NTA to detect apoptotic vesicles may be of great clinical significance.

In the final chapter of results, Data show that knocking down the Rab27 family reduced the number of exosomes released from MDA-MB-231 cells, and reduced the cell's ability to proliferate and invade. Adding exosomes back to Rab27a/b knock down cells restored the cell's ability to form colonies, highlighting the role of exosomes and the

Rab27 family in metastasis and invasiveness of tumour cells. Thus, the exosome pathway is a valid target to attempt to disrupt the behaviour of tumour cells and Rab27 family could be potential a therapeutic target. NTA was capable of rapidly detecting decreases in exosomes released following DMA treatment of MDA-MB-231 cells and Rab27 knock down cells. Thus, this technique is likely to be of significant use in the monitoring of any fluctuation of exosome release (eg, after drug treatment in patients) and further characterisation of exosomes.

The data presented in this thesis will contribute to the continued research and characterisation of exosomes.

Studying of Microvesicles using Flow Cytometry, Western Blot and Lipidomics.

In this chapter, exosomes were shown to be present in our preparation by using flow cytometry (Figure 3.4), western blot (Figure 3.2) and electron microscopy (Figure 3.3). Annexin V staining revealed that MDA-MB-231 and MCF7-derived exosomes caused apoptosis of Jurkat T cells (Figure 3.6), PI staining confirmed that MDA-MB-231 and MCF7 conditioned medium and exosomes derived from both tumour lines induced Jurkat T cell apoptosis (Figure 3.7 and Figure 3.8). It has been reported that the Cbl family of ubiquitin ligases might pay a role in regulation of gastric cancer exosome-induced apoptosis of Jurkat T cells by increasing PI3K proteasome degradation, inactivation of PI3K/Akt signalling, therefore mediating some effects of caspase

activation (Qu et al., 2009b). It will be very interesting to find out the underlying molecular mechanism of the Jurkat cell apoptosis induced by breast cancer tumour cells observed in my study.

CFSE and PE double staining were used to investigate the percentage of CD9 and CD63-positive vesicles preparation. We have shown that CD9 and CD63 have a different subcellular distribution (Figure 3.9) and CD63 and CD9 did not label the same percentage of vesicles (Figure 3.10). This could be due to in-sufficient binding efficacy of the antibodies or indicating sub-population of exosomes. In fact, CD9, which was previously considered as a reliable exosome marker, has been reported to present on vesicles other than exosomes and subpopulations of exosomes have also been suggested. There is still not a standardised protocol for isolating exosomes. 'Exoquick', the new product that claimed to isolate exosomes rapidly, was reported to isolate vesicles rich in CD9 and not CD63, hence the vesicles were unlikely to be exosomes (Bobrie et al., 2012a). It will be very interesting to further investigate whether any other of the typical exosome markers are just specific for exosomes and such findings would help develop a standardized protocol or new products for isolating exosomes.

We have successfully transferred Rab27a and Erap1 siRNAs into exosomes, which then delivered the siRNAs into cells and knocked down the expression (Figure 3.12). Exosomes have more advantages over existing gene delivery vectors. Delivery of siRNA into the brain by using genetically engineered immature dendritic cells-derived exosomes (Alvarez-Erviti et al., 2011) and using plasma cell-derived exosomes into monocytes and lymphocytes have been reported (Wahlgren et al., 2012). In our study, it

was not known whether the siRNAs were encapsulated in exosomes or were 'attached' to the outside of the exosomes. RNase treatment should be used in the future to ensure that the exosomes were indeed encapsulated in the exosomes. In the future, it will also be very interesting to transfer siRNAs into cells to knock down a therapeutic target of a specific disease. It will also be fascinating to isolate exosomes from dendritic cells from blood and engineer the exosomes to target different tissues and test the delivery of siRNA *in vivo*. This will contribute to the development of exosomes as drug delivery vehicles.

we have shown that exosomes derived from MDA-MB-231 cells and the parental cells have very different lipid composition (figure 6.1). These preliminary data compliment with other lipidomics studies of exosomes and will contribute to the characterisation of exosomes. Some lipids were not able to be identified due to limited amount of exosomal material, thus, it will be very interesting to collect larger amount of exosomes to be analysed in the future. It will also be intriguing to investigate whether the DMA-treated MDA-MB-231 cells and the Rab27a shRNA expressing cells show any differences in the lipid composition compared to untreated MDA-MB-231 cells. It will also be very interesting to compare the lipid composition of exosomes and MVBs.

Nanoparticle tracking analysis with Nanosight.

We have analysed the accuracy of NTA in measuring size and concentration (Figure 4.3) and the data suggested that NTA is very accurate in measuring both size and

concentration. We then analysed supernatant from MDA-MB-231 cells and MCF7 cells and exosome size was estimated by NTA (Figure 4.4).

Immunodepletion method was then used to try to deplete either CD9 or CD63 positive vesicles. The results vary slightly compared to that from the CFSE and PE double staining described in the last chapter, which also stained CD9 or CD63 positive vesicles. Using the immunodepletion method with magnetic dynabeads depleted 31.7 % of vesicles using anti-CD9 antibody and 28.5 % vesicles using anti-CD63 antibody compared to pre-cleared supernatant. Vesicles pulled down by both antibodies had a peak size of 131 nm, which was consistent with the neat supernatant. These data could suggest that only a small percentage of our preparation was exosomes, the rest was microvesicles; or the antibodies did not bind to all exosomes due to a low concentration of antibodies, etc; or there maybe subpopulations of exosomes that do not express CD9 or CD63. These data would contribute to the characterisation of exosomes and microvesicles and as suggested in the last chapter, it will be very interesting to investigate whether the typical exosomes markers are specific for exosomes. It will also be interesting to use fluorescent antibodies (CD9 or CD63) to label our preparation and to use NTA to detect the fluorescence.

The NTA's ability to detect apototic vesicles was then investigated. It has been reported that a combination of Taxol and Curcumin achieved better anticancer effects compare to Taxol alone (Bava et al., 2005). Therefore it would be intriguing if NTA is able to detect apoptotic vesicles induced by Taxol and Curcumin. By using the EDR mode, NTA was able to detect the very distinguishable extra population of vesicles which range from approximately 180 nm to 300 nm (Figure 4.8). This may contribute to the

monitor of the effect of therapeutic drugs on patients' tumour cells, eg, whether the drug can cause apoptosis of the tumour cells. It will be fascinating if we could label the tumour cell-derived exosomes and apoptotic vesicles and distinguish them from normal cells-derived exosomes and microvesicles, this will enable us to monitor whether therapeutic drugs are specific and are efficient in causing tumour cell apoptosis without affecting normal cells excessively.

Multiple freezing and thawing does not affect the exosomes size, indicating that this method is well-suited for storing exosomes (Figure 4.9). Because the snap freezing-thawing method was used in this study, it will be interesting in the future to see whether freezing for a long period of time and then multiple freeze/thawing would affect the exosomes' sizes. We have shown that resuspending the 100, 000 x g pellet in PBS does not cause the exosomes to clump together (Figure 4.10). We have also shown NTA is capable of detecting increases in exosomes released following treatment with Tamoxifen and Thimerosal to MCF 7 cells.

Rab27A and its effects on exosome release and cell's invasive potential, etc.

In this chapter we have shown that by transfecting cells with Rab27a shRNA, cells showed reduced exosome release (Figure 5.6). Western blot confirmed the knock down of Rab27a (Figure 5.1 and Figure 5.4). RT-PCR data suggested that No.1, No.2 and No 3 shRNA also inhibited Rab27b expression (Figure 5.5). The reduction in exosome released was confirmed by measuring the amount of protein present in exosomes

secreted from same number of control cells and Rab27a knock down cells using the Bradford method (Figure 5.7), and also by measuring the quantity of typical exosome markers CD63, Alix and tsg101 present in exosomes secreted from same number of control and knock down cells using western blot (Figure 5.8) and all the data suggested that inhibiting Rab27a/Rab27b expression reduced exosome release.

The scratch assay, invasion assay and cloning in soft agar indicated that inhibition of Rab27 affected the cells' ability to migrate, invade and form anchorage-independent colonies. The cells' abilities to form colonies were restored after the addition of exosomes back to Rab27a knock down cells. It has only been reported previously that breast carcinoma cells's ability to form colonies was dependent on exosomes derived from fetal bovine serum (Ochieng et al., 2009), so the data presented in this study will contribute to the understanding of the functions of breast cancer cell-derived exosomes.

These data suggest that the exosome pathway is an important pathway in tumour cells' migration and metastasis and thus a valid pathway to target to disrupt tumour cells' properties. Our data also suggest that NTA is a rapid tool for screening of drug inhibition of exosome release.

It will be very interesting in the future to compare therapeutic drug-induced vesicle release in tumour and normal cells.

References

Abusamra, A.J., Zhong, Z., Zheng, X., Li, M., Ichim, T.E., Chin, J.L., and Min, W.P. (2005). Tumor exosomes expressing Fas ligand mediate CD8+ T-cell apoptosis. Blood Cells, Molecules & Diseases *35*, 169-173.

Admyre, C., Johansson, S.M., Paulie, S., and Gabrielsson, S. (2006). Direct exosome stimulation of peripheral human T cells detected by ELISPOT. European Journal of Immunology *36*, 1772-1781.

Admyre, C., Johansson, S.M., Qazi, K.R., Filen, J.J., Lahesmaa, R., Norman, M., Neve, E.P., Scheynius, A., and Gabrielsson, S. (2007). Exosomes with immune modulatory features are present in human breast milk. Journal of Immunology *179*, 1969-1978.

Admyre, C., Telemo, E., Almqvist, N., Lotvall, J., Lahesmaa, R., Scheynius, A., and Gabrielsson, S. (2008). Exosomes - nanovesicles with possible roles in allergic inflammation. Allergy *63*, 404-408.

Al-Nedawi, K., Meehan, B., Micallef, J., Lhotak, V., May, L., Guha, A., and Rak, J. (2008). Intercellular transfer of the oncogenic receptor EGFRvIII by microvesicles derived from tumour cells. Nature Cell Biology *10*, 619-624.

Alvarez-Erviti, L., Seow, Y., Yin, H., Betts, C., Lakhal, S., and Wood, M.J. (2011). Delivery of siRNA to the mouse brain by systemic injection of targeted exosomes. Nature Biotechnology *29*, 341-345.

Andersen, M.H., Berglund, L., Rasmussen, J.T., and Petersen, T.E. (1997). Bovine PAS-6/7 binds alpha v beta 5 integrins and anionic phospholipids through two domains. Biochemistry *36*, 5441-5446.

Andreola, G., Rivoltini, L., Castelli, C., Huber, V., Perego, P., Deho, P., Squarcina, P., Accornero, P., Lozupone, F., Lugini, L., *et al.* (2002). Induction of lymphocyte apoptosis by tumor cell secretion of FasL-bearing microvesicles. The Journal of Experimental Medicine *195*, 1303-1316.

Baietti, M.F., Zhang, Z., Mortier, E., Melchior, A., Degeest, G., Geeraerts, A., Ivarsson, Y., Depoortere, F., Coomans, C., Vermeiren, E., *et al.* (2012). Syndecan-syntenin-ALIX regulates the biogenesis of exosomes. Nature Cell Biology *14*, 677-685.

Baj-Krzyworzeka, M., Majka, M., Pratico, D., Ratajczak, J., Vilaire, G., Kijowski, J., Reca, R., Janowska-Wieczorek, A., and Ratajczak, M.Z. (2002). Platelet-derived microparticles stimulate proliferation, survival, adhesion, and chemotaxis of hematopoietic cells. Experimental Hematology *30*, 450-459.

Baj-Krzyworzeka, M., Szatanek, R., Weglarczyk, K., Baran, J., and Zembala, M. (2007). Tumour-derived microvesicles modulate biological activity of human monocytes. Immunology Letters *113*, 76-82.

Bava, S.V., Puliappadamba, V.T., Deepti, A., Nair, A., Karunagaran, D., and Anto, R.J. (2005). Sensitization of taxol-induced apoptosis by curcumin involves down-regulation of nuclear

factor-kappaB and the serine/threonine kinase Akt and is independent of tubulin polymerization. The Journal of Biological Chemistry *280*, 6301-6308.

Bhatnagar, S., and Schorey, J.S. (2007). Exosomes released from infected macrophages contain Mycobacterium avium glycopeptidolipids and are proinflammatory. The Journal of Biological Chemistry *282*, 25779-25789.

Bobrie, A., Colombo, M., Krumeich, S., Raposo, G., and Théry, C. (2012a). Diverse subpopulations of vesicles secreted by different intracellular mechanisms are present in exosome preparations obtained by differential ultracentrifugation. Journal of Extracellular Vesicles *1*.

Bobrie, A., Colombo, M., Raposo, G., and Thery, C. (2011). Exosome secretion: molecular mechanisms and roles in immune responses. Traffic *12*, 1659-1668.

Bobrie, A., Krumeich, S., Reyal, F., Recchi, C., Moita, L.F., Seabra, M.C., Ostrowski, M., and Thery, C. (2012b). Rab27a supports exosome-dependent and -independent mechanisms that modify the tumor microenvironment and can promote tumor progression. Cancer research.

Buschow, S.I., Nolte-'t Hoen, E.N., van Niel, G., Pols, M.S., ten Broeke, T., Lauwen, M., Ossendorp, F., Melief, C.J., Raposo, G., Wubbolts, R., *et al.* (2009). MHC II in dendritic cells is targeted to lysosomes or T cell-induced exosomes via distinct multivesicular body pathways. Traffic *10*, 1528-1542.

Caby, M.P., Lankar, D., Vincendeau-Scherrer, C., Raposo, G., and Bonnerot, C. (2005). Exosomal-like vesicles are present in human blood plasma. International Immunology *17*, 879-887.

Cai, Z., Yang, F., Yu, L., Yu, Z., Jiang, L., Wang, Q., Yang, Y., Wang, L., Cao, X., and Wang, J. (2012). Activated T Cell Exosomes Promote Tumor Invasion via Fas Signaling Pathway. Journal of Immunology.

Cantin, R., Diou, J., Belanger, D., Tremblay, A.M., and Gilbert, C. (2008). Discrimination between exosomes and HIV-1: purification of both vesicles from cell-free supernatants. Journal of Immunological Methods *338*, 21-30.

Chalmin, F., Ladoire, S., Mignot, G., Vincent, J., Bruchard, M., Remy-Martin, J.P., Boireau, W., Rouleau, A., Simon, B., Lanneau, D., *et al.* (2010). Membrane-associated Hsp72 from tumor-derived exosomes mediates STAT3-dependent immunosuppressive function of mouse and human myeloid-derived suppressor cells. The Journal of Clinical Investigation *120*, 457-471.

Chaput, N., and Thery, C. (2011). Exosomes: immune properties and potential clinical implementations. Seminars in Immunopathology *33*, 419-440.

Clayton, A., Mitchell, J.P., Court, J., Linnane, S., Mason, M.D., and Tabi, Z. (2008). Human tumor-derived exosomes down-modulate NKG2D expression. Journal of Immunology *180*, 7249-7258.

Clayton, A., Mitchell, J.P., Court, J., Mason, M.D., and Tabi, Z. (2007). Human tumor-derived exosomes selectively impair lymphocyte responses to interleukin-2. Cancer Research *67*, 7458-7466.

Cocucci, E., Racchetti, G., and Meldolesi, J. (2009). Shedding microvesicles: artefacts no more. Trends in Cell Biology *19*, 43-51.

Cramer, E.M., Berger, G., and Berndt, M.C. (1994). Platelet alpha-granule and plasma membrane share two new components: CD9 and PECAM-1. Blood *84*, 1722-1730.

Dai, S., Wei, D., Wu, Z., Zhou, X., Wei, X., Huang, H., and Li, G. (2008). Phase I clinical trial of autologous ascites-derived exosomes combined with GM-CSF for colorectal cancer. Molecular Therapy : The Journal of the American Society of Gene Therapy *16*, 782-790.

Eken, C., Gasser, O., Zenhaeusern, G., Oehri, I., Hess, C., and Schifferli, J.A. (2008). Polymorphonuclear neutrophil-derived ectosomes interfere with the maturation of monocyte-derived dendritic cells. Journal of Immunology *180*, 817-824.

Elsner, L., Muppala, V., Gehrmann, M., Lozano, J., Malzahn, D., Bickeboller, H., Brunner, E., Zientkowska, M., Herrmann, T., Walter, L., *et al.* (2007). The heat shock protein HSP70 promotes mouse NK cell activity against tumors that express inducible NKG2D ligands. Journal of Immunology *179*, 5523-5533.

Escrevente, C., Keller, S., Altevogt, P., and Costa, J. (2011). Interaction and uptake of exosomes by ovarian cancer cells. BMC Cancer *11*, 108.

Escudier, B., Dorval, T., Chaput, N., Andre, F., Caby, M.P., Novault, S., Flament, C., Leboulaire, C., Borg, C., Amigorena, S., *et al.* (2005). Vaccination of metastatic melanoma patients with autologous dendritic cell (DC) derived-exosomes: results of thefirst phase I clinical trial. Journal of Translational Medicine *3*, 10.

Fader, C.M., and Colombo, M.I. (2009). Autophagy and multivesicular bodies: two closely related partners. Cell Death and Differentiation *16*, 70-78.

Fader, C.M., Sanchez, D., Furlan, M., and Colombo, M.I. (2008). Induction of autophagy promotes fusion of multivesicular bodies with autophagic vacuoles in k562 cells. Traffic *9*, 230-250.

Feng, D., Zhao, W.L., Ye, Y.Y., Bai, X.C., Liu, R.Q., Chang, L.F., Zhou, Q., and Sui, S.F. (2010). Cellular internalization of exosomes occurs through phagocytosis. Traffic *11*, 675-687.

Fevrier, B., Vilette, D., Laude, H., and Raposo, G. (2005). Exosomes: a bubble ride for prions? Traffic *6*, 10-17.

Filipe, V., Hawe, A., and Jiskoot, W. (2010). Critical evaluation of Nanoparticle Tracking Analysis (NTA) by NanoSight for the measurement of nanoparticles and protein aggregates. Pharmaceutical Research *27*, 796-810.

Fortin, J.F., Cantin, R., and Tremblay, M.J. (1998). T cells expressing activated LFA-1 are more susceptible to infection with human immunodeficiency virus type 1 particles bearing host-encoded ICAM-1. Journal of Vvirology *72*, 2105-2112.

Gastpar, R., Gehrmann, M., Bausero, M.A., Asea, A., Gross, C., Schroeder, J.A., and Multhoff, G. (2005). Heat shock protein 70 surface-positive tumor exosomes stimulate migratory and cytolytic activity of natural killer cells. Cancer Research *65*, 5238-5247.

Gesierich, S., Berezovskiy, I., Ryschich, E., and Zoller, M. (2006). Systemic induction of the angiogenesis switch by the tetraspanin D6.1A/CO-029. Cancer Research *66*, 7083-7094.

Giri, P.K., and Schorey, J.S. (2008). Exosomes derived from M. Bovis BCG infected macrophages activate antigen-specific CD4+ and CD8+ T cells in vitro and in vivo. PloS One *3*, e2461.

Graner, M.W., Alzate, O., Dechkovskaia, A.M., Keene, J.D., Sampson, J.H., Mitchell, D.A., and Bigner, D.D. (2009). Proteomic and immunologic analyses of brain tumor exosomes. FASEB Journal : Official Publication of the Federation of American Societies for Experimental Biology *23*, 1541-1557.

Grootjans, J.J., Zimmermann, P., Reekmans, G., Smets, A., Degeest, G., Durr, J., and David, G. (1997). Syntenin, a PDZ protein that binds syndecan cytoplasmic domains. Proceedings of the National Academy of Sciences of the United States of America *94*, 13683-13688.

Guo, S., Tschammer, N., Mohammed, S., and Guo, P. (2005). Specific delivery of therapeutic RNAs to cancer cells via the dimerization mechanism of phi29 motor pRNA. Human Gene Therapy *16*, 1097-1109.

Gupta, S., and Knowlton, A.A. (2007). HSP60 trafficking in adult cardiac myocytes: role of the exosomal pathway. American Journal of Physiology Heart and Circulatory Physiology *292*, H3052-3056.

Hanayama, R., Tanaka, M., Miwa, K., Shinohara, A., Iwamatsu, A., and Nagata, S. (2002). Identification of a factor that links apoptotic cells to phagocytes. Nature *417*, 182-187.

Hao, S., Bai, O., Yuan, J., Qureshi, M., and Xiang, J. (2006). Dendritic cell-derived exosomes stimulate stronger CD8+ CTL responses and antitumor immunity than tumor cell-derived exosomes. Cellular & Molecular Immunology *3*, 205-211.

Harding, C., Heuser, J., and Stahl, P. (1983). Receptor-mediated endocytosis of transferrin and recycling of the transferrin receptor in rat reticulocytes. The Journal of Cell Biology *97*, 329-339.

Hedlund, M., Stenqvist, A.C., Nagaeva, O., Kjellberg, L., Wulff, M., Baranov, V., and Mincheva-Nilsson, L. (2009). Human placenta expresses and secretes NKG2D ligands via exosomes that down-modulate the cognate receptor expression: evidence for immunosuppressive function. Journal of Immunology *183*, 340-351.

Hegmans, J.P., Bard, M.P., Hemmes, A., Luider, T.M., Kleijmeer, M.J., Prins, J.B., Zitvogel, L., Burgers, S.A., Hoogsteden, H.C., and Lambrecht, B.N. (2004). Proteomic analysis of exosomes secreted by human mesothelioma cells. The American Journal of Pathology *164*, 1807-1815.

Herrero-Turrion, M.J., Calafat, J., Janssen, H., Fukuda, M., and Mollinedo, F. (2008). Rab27a regulates exocytosis of tertiary and specific granules in human neutrophils. Journal of Immunology *181*, 3793-3803.

Hood, J.L., Pan, H., Lanza, G.M., and Wickline, S.A. (2009). Paracrine induction of endothelium by tumor exosomes. Laboratory Investigation; A Journal of Technical Methods and Pathology *89*, 1317-1328.

Hood, J.L., San, R.S., and Wickline, S.A. (2011). Exosomes released by melanoma cells prepare sentinel lymph nodes for tumor metastasis. Cancer Research *71*, 3792-3801.

Horwitz, S.B. (1994). Taxol (paclitaxel): mechanisms of action. Annals of Oncology : Official Journal of the European Society for Medical Oncology / ESMO *5 Suppl 6*, S3-6.

Hsu, C., Morohashi, Y., Yoshimura, S., Manrique-Hoyos, N., Jung, S., Lauterbach, M.A., Bakhti, M., Gronborg, M., Mobius, W., Rhee, J., *et al.* (2010). Regulation of exosome secretion by Rab35 and its GTPase-activating proteins TBC1D10A-C. The Journal of Cell Biology *189*, 223-232.

Ichim, T.E., Zhong, Z., Kaushal, S., Zheng, X., Ren, X., Hao, X., Joyce, J.A., Hanley, H.H., Riordan, N.H., Koropatnick, J., *et al.* (2008). Exosomes as a tumor immune escape mechanism: possible therapeutic implications. Journal of Translational Medicine *6*, 37.

Janiszewski, M., Do Carmo, A.O., Pedro, M.A., Silva, E., Knobel, E., and Laurindo, F.R. (2004). Platelet-derived exosomes of septic individuals possess proapoptotic NAD(P)H oxidase activity: A novel vascular redox pathway. Critical Care Mmedicine *32*, 818-825.

Johnstone, R.M., Adam, M., Hammond, J.R., Orr, L., and Turbide, C. (1987). Vesicle formation during reticulocyte maturation. Association of plasma membrane activities with released vesicles (exosomes). Journal of Biological Chemistry *262*, 9412-9420.

Kao, J., Salari, K., Bocanegra, M., Choi, Y.L., Girard, L., Gandhi, J., Kwei, K.A., Hernandez-Boussard, T., Wang, P., Gazdar, A.F., *et al.* (2009). Molecular profiling of breast cancer cell lines defines relevant tumor models and provides a resource for cancer gene discovery. PloS One *4*, e6146.

Kim, S.H., Lechman, E.R., Bianco, N., Menon, R., Keravala, A., Nash, J., Mi, Z., Watkins, S.C., Gambotto, A., and Robbins, P.D. (2005). Exosomes derived from IL-10-treated dendritic cells can suppress inflammation and collagen-induced arthritis. Journal of Immunology *174*, 6440-6448.

Klibi, J., Niki, T., Riedel, A., Pioche-Durieu, C., Souquere, S., Rubinstein, E., Le Moulec, S., Guigay, J., Hirashima, M., Guemira, F., *et al.* (2009). Blood diffusion and Th1-suppressive effects of galectin-9-containing exosomes released by Epstein-Barr virus-infected nasopharyngeal carcinoma cells. Blood *113*, 1957-1966.

Lamparski, H.G., Metha-Damani, A., Yao, J.Y., Patel, S., Hsu, D.H., Ruegg, C., and Le Pecq, J.B. (2002). Production and characterization of clinical grade exosomes derived from dendritic cells. Journal of Immunological Methods *270*, 211-226.

Laulagnier, K., Motta, C., Hamdi, S., Roy, S., Fauvelle, F., Pageaux, J.F., Kobayashi, T., Salles, J.P., Perret, B., Bonnerot, C., *et al.* (2004). Mast cell- and dendritic cell-derived exosomes display a specific lipid composition and an unusual membrane organization. The Biochemical Journal *380*, 161-171.

Lenassi, M., Cagney, G., Liao, M., Vaupotic, T., Bartholomeeusen, K., Cheng, Y., Krogan, N.J., Plemenitas, A., and Peterlin, B.M. (2010). HIV Nef is secreted in exosomes and triggers apoptosis in bystander CD4+ T cells. Traffic *11*, 110-122.

Li, C.I., Uribe, D.J., and Daling, J.R. (2005). Clinical characteristics of different histologic types of breast cancer. British Journal of Cancer *93*, 1046-1052.

Liu, C., Yu, S., Zinn, K., Wang, J., Zhang, L., Jia, Y., Kappes, J.C., Barnes, S., Kimberly, R.P., Grizzle, W.E., *et al.* (2006). Murine mammary carcinoma exosomes promote tumor growth by suppression of NK cell function. Journal of Immunology *176*, 1375-1385.

Liu, Y., Xiang, X., Zhuang, X., Zhang, S., Liu, C., Cheng, Z., Michalek, S., Grizzle, W., and Zhang, H.G. (2010). Contribution of MyD88 to the tumor exosome-mediated induction of myeloid derived suppressor cells. The American Journal of Pathology *176*, 2490-2499.

Luketic, L., Delanghe, J., Sobol, P.T., Yang, P., Frotten, E., Mossman, K.L., Gauldie, J., Bramson, J., and Wan, Y. (2007). Antigen presentation by exosomes released from peptide-pulsed dendritic cells is not suppressed by the presence of active CTL. Journal of Immunology *179*, 5024-5032.

Mack, M., Kleinschmidt, A., Bruhl, H., Klier, C., Nelson, P.J., Cihak, J., Plachy, J., Stangassinger, M., Erfle, V., and Schlondorff, D. (2000). Transfer of the chemokine receptor CCR5 between cells by membrane-derived microparticles: a mechanism for cellular human immunodeficiency virus 1 infection. Nature Mmedicine *6*, 769-775.

Mallegol, J., Van Niel, G., Lebreton, C., Lepelletier, Y., Candalh, C., Dugave, C., Heath, J.K., Raposo, G., Cerf-Bensussan, N., and Heyman, M. (2007). T84-intestinal epithelial exosomes bear MHC class II/peptide complexes potentiating antigen presentation by dendritic cells. Gastroenterology *132*, 1866-1876.

Marleau, A.M., Chen, C.S., Joyce, J.A., and Tullis, R.H. (2012). Exosome removal as a therapeutic adjuvant in cancer. Journal of Translational Medicine *10*, 134.

Matsuo, H., Chevallier, J., Mayran, N., Le Blanc, I., Ferguson, C., Faure, J., Blanc, N.S., Matile, S., Dubochet, J., Sadoul, R., *et al.* (2004). Role of LBPA and Alix in multivesicular liposome formation and endosome organization. Science *303*, 531-534.

Merendino, A.M., Bucchieri, F., Campanella, C., Marciano, V., Ribbene, A., David, S., Zummo, G., Burgio, G., Corona, D.F., Conway de Macario, E., *et al.* (2010). Hsp60 is actively secreted by human tumor cells. PloS One *5*, e9247.

Mincheva-Nilsson, L., Nagaeva, O., Chen, T., Stendahl, U., Antsiferova, J., Mogren, I., Hernestal, J., and Baranov, V. (2006). Placenta-derived soluble MHC class I chain-related molecules down-regulate NKG2D receptor on peripheral blood mononuclear cells during human pregnancy: a possible novel immune escape mechanism for fetal survival. Journal of Immunology *176*, 3585-3592.

Mitsiades, C.S., Poulaki, V., Fanourakis, G., Sozopoulos, E., McMillin, D., Wen, Z., Voutsinas, G., Tseleni-Balafouta, S., and Mitsiades, N. (2006). Fas signaling in thyroid carcinomas is diverted from apoptosis to proliferation. Clinical cancer research : an official journal of the American Association for Cancer Research *12*, 3705-3712.

Mittelbrunn, M., Gutierrez-Vazquez, C., Villarroya-Beltri, C., Gonzalez, S., Sanchez-Cabo, F., Gonzalez, M.A., Bernad, A., and Sanchez-Madrid, F. (2011). Unidirectional transfer of microRNA-loaded exosomes from T cells to antigen-presenting cells. Nature Communications *2*, 282.

Miyanishi, M., Tada, K., Koike, M., Uchiyama, Y., Kitamura, T., and Nagata, S. (2007). Identification of Tim4 as a phosphatidylserine receptor. Nature *450*, 435-439.

Monleon, I., Martinez-Lorenzo, M.J., Monteagudo, L., Lasierra, P., Taules, M., Iturralde, M., Pineiro, A., Larrad, L., Alava, M.A., Naval, J., *et al.* (2001). Differential secretion of Fas ligand- or APO2 ligand/TNF-related apoptosis-inducing ligand-carrying microvesicles during activation-induced death of human T cells. Journal of Immunology *167*, 6736-6744.

Montecalvo, A., Shufesky, W.J., Stolz, D.B., Sullivan, M.G., Wang, Z., Divito, S.J., Papworth, G.D., Watkins, S.C., Robbins, P.D., Larregina, A.T., *et al.* (2008). Exosomes as a short-range mechanism to spread alloantigen between dendritic cells during T cell allorecognition. Journal of Immunology *180*, 3081-3090.

Morse, M.A., Garst, J., Osada, T., Khan, S., Hobeika, A., Clay, T.M., Valente, N., Shreeniwas, R., Sutton, M.A., Delcayre, A., *et al.* (2005). A phase I study of dexosome immunotherapy in patients with advanced non-small cell lung cancer. Journal of Translational Medicine *3*, 9.

Muntasell, A., Berger, A.C., and Roche, P.A. (2007). T cell-induced secretion of MHC class II-peptide complexes on B cell exosomes. The EMBO journal *26*, 4263-4272.

Nieuwland, R., van der Post, J.A., Lok, C.A., Kenter, G., and Sturk, A. (2010). Microparticles and exosomes in gynecologic neoplasias. Seminars in Thrombosis and Hemostasis *36*, 925-929.

Nolte-'t Hoen, E.N., Buschow, S.I., Anderton, S.M., Stoorvogel, W., and Wauben, M.H. (2009). Activated T cells recruit exosomes secreted by dendritic cells via LFA-1. Blood *113*, 1977-1981.

Ochieng, J., Pratap, S., Khatua, A.K., and Sakwe, A.M. (2009). Anchorage-independent growth of breast carcinoma cells is mediated by serum exosomes. Experimental Cell Research *315*, 1875-1888.

Ohshima, K., Inoue, K., Fujiwara, A., Hatakeyama, K., Kanto, K., Watanabe, Y., Muramatsu, K., Fukuda, Y., Ogura, S., Yamaguchi, K., *et al.* (2010). Let-7 microRNA family is selectively secreted into the extracellular environment via exosomes in a metastatic gastric cancer cell line. PloS One *5*, e13247.

Ostrowski, M., Carmo, N.B., Krumeich, S., Fanget, I., Raposo, G., Savina, A., Moita, C.F., Schauer, K., Hume, A.N., Freitas, R.P., *et al.* (2010). Rab27a and Rab27b control different steps of the exosome secretion pathway. Nature Cell Biology *12*, 19-30; sup pp 11-13.

Pan, B.T., Teng, K., Wu, C., Adam, M., and Johnstone, R.M. (1985). Electron microscopic evidence for externalization of the transferrin receptor in vesicular form in sheep reticulocytes. Journal of Cell Biology *101*, 942-948.

Parolini, I., Federici, C., Raggi, C., Lugini, L., Palleschi, S., De Milito, A., Coscia, C., Iessi, E., Logozzi, M., Molinari, A., *et al.* (2009). Microenvironmental pH is a key factor for exosome traffic in tumor cells. The Journal of Biological Chemistry *284*, 34211-34222.

Peche, H., Heslan, M., Usal, C., Amigorena, S., and Cuturi, M.C. (2003). Presentation of donor major histocompatibility complex antigens by bone marrow dendritic cell-derived exosomes modulates allograft rejection. Transplantation *76*, 1503-1510.

Pegtel, D.M., Cosmopoulos, K., Thorley-Lawson, D.A., van Eijndhoven, M.A., Hopmans, E.S., Lindenberg, J.L., de Gruijl, T.D., Wurdinger, T., and Middeldorp, J.M. (2010). Functional delivery of viral miRNAs via exosomes. Proceedings of the National Academy of Sciences of the United States of America *107*, 6328-6333.

Peinado, H., Aleckovic, M., Lavotshkin, S., Matei, I., Costa-Silva, B., Moreno-Bueno, G., Hergueta-Redondo, M., Williams, C., Garcia-Santos, G., Ghajar, C., *et al.* (2012). Melanoma exosomes educate bone marrow progenitor cells toward a pro-metastatic phenotype through MET. Nature Medicine *18*, 883-891.

Pisitkun, T., Shen, R.F., and Knepper, M.A. (2004). Identification and proteomic profiling of exosomes in human urine. Proceedings of the National Academy of Sciences of the United States of America *101*, 13368-13373.

Pols, M.S., and Klumperman, J. (2009). Trafficking and function of the tetraspanin CD63. Experimental Cell Research *315*, 1584-1592.

Poutsiaka, D.D., Schroder, E.W., Taylor, D.D., Levy, E.M., and Black, P.H. (1985). Membrane vesicles shed by murine melanoma cells selectively inhibit the expression of Ia antigen by macrophages. Journal of Immunology *134*, 138-144.

Prado, N., Marazuela, E.G., Segura, E., Fernandez-Garcia, H., Villalba, M., Thery, C., Rodriguez, R., and Batanero, E. (2008). Exosomes from bronchoalveolar fluid of tolerized mice prevent allergic reaction. Journal of Immunology *181*, 1519-1525.

Qu, J.L., Qu, X.J., Zhao, M.F., Teng, Y.E., Zhang, Y., Hou, K.Z., Jiang, Y.H., Yang, X.H., and Liu, Y.P. (2009a). Gastric cancer exosomes promote tumour cell proliferation through PI3K/Akt and MAPK/ERK activation. Digestive and Liver Disease : Official Journal of the Italian Society of Gastroenterology and the Italian Association for the Study of the Liver *41*, 875-880.

Qu, J.L., Qu, X.J., Zhao, M.F., Teng, Y.E., Zhang, Y., Hou, K.Z., Jiang, Y.H., Yang, X.H., and Liu, Y.P. (2009b). The role of cbl family of ubiquitin ligases in gastric cancer exosome-induced apoptosis of Jurkat T cells. Acta Oncologica *48*, 1173-1180.

Rabinowits, G., Gercel-Taylor, C., Day, J.M., Taylor, D.D., and Kloecker, G.H. (2009). Exosomal microRNA: a diagnostic marker for lung cancer. Clinical Lung Cancer *10*, 42-46.

Raposo, G., Nijman, H.W., Stoorvogel, W., Liejendekker, R., Harding, C.V., Melief, C.J., and Geuze, H.J. (1996). B lymphocytes secrete antigen-presenting vesicles. The Journal of Experimental Medicine *183*, 1161-1172.

Ristorcelli, E., Beraud, E., Verrando, P., Villard, C., Lafitte, D., Sbarra, V., Lombardo, D., and Verine, A. (2008). Human tumor nanoparticles induce apoptosis of pancreatic cancer cells. FASEB Journal : Official Publication of the Federation of American Societies for Experimental Biology *22*, 3358-3369.

Ronquist, G., and Brody, I. (1985). The prostasome: its secretion and function in man. Biochimica Et Biophysica Acta *822*, 203-218.

Runz, S., Keller, S., Rupp, C., Stoeck, A., Issa, Y., Koensgen, D., Mustea, A., Sehouli, J., Kristiansen, G., and Altevogt, P. (2007). Malignant ascites-derived exosomes of ovarian carcinoma patients contain CD24 and EpCAM. Gynecologic Oncology *107*, 563-571.

Safaei, R., Larson, B.J., Cheng, T.C., Gibson, M.A., Otani, S., Naerdemann, W., and Howell, S.B. (2005). Abnormal lysosomal trafficking and enhanced exosomal export of cisplatin in drug-resistant human ovarian carcinoma cells. Molecular Cancer Therapeutics *4*, 1595-1604.

Salzer, U., Hinterdorfer, P., Hunger, U., Borken, C., and Prohaska, R. (2002). Ca(++)-dependent vesicle release from erythrocytes involves stomatin-specific lipid rafts, synexin (annexin VII), and sorcin. Blood *99*, 2569-2577.

Savina, A., Fader, C.M., Damiani, M.T., and Colombo, M.I. (2005). Rab11 promotes docking and fusion of multivesicular bodies in a calcium-dependent manner. Traffic *6*, 131-143.

Savina, A., Furlan, M., Vidal, M., and Colombo, M.I. (2003). Exosome release is regulated by a calcium-dependent mechanism in K562 cells. The Journal of Biological Chemistry *278*, 20083-20090.

Schnitt, S.J. (2010). Classification and prognosis of invasive breast cancer: from morphology to molecular taxonomy. Modern Pathology : an Official Journal of the United States and Canadian Academy of Pathology, Inc *23 Suppl 2*, S60-64.

Segura, E., Guerin, C., Hogg, N., Amigorena, S., and Thery, C. (2007). CD8+ dendritic cells use LFA-1 to capture MHC-peptide complexes from exosomes in vivo. Journal of Immunology *179*, 1489-1496.

Segura, E., Nicco, C., Lombard, B., Veron, P., Raposo, G., Batteux, F., Amigorena, S., and Thery, C. (2005). ICAM-1 on exosomes from mature dendritic cells is critical for efficient naive T-cell priming. Blood *106*, 216-223.

Simhadri, V.R., Reiners, K.S., Hansen, H.P., Topolar, D., Simhadri, V.L., Nohroudi, K., Kufer, T.A., Engert, A., and Pogge von Strandmann, E. (2008). Dendritic cells release HLA-B-associated transcript-3 positive exosomes to regulate natural killer function. PloS One *3*, e3377.

Skog, J., Wurdinger, T., van Rijn, S., Meijer, D.H., Gainche, L., Sena-Esteves, M., Curry, W.T., Jr., Carter, B.S., Krichevsky, A.M., and Breakefield, X.O. (2008). Glioblastoma microvesicles transport RNA and proteins that promote tumour growth and provide diagnostic biomarkers. Nature Cell Biology *10*, 1470-1476.

Sokolova, V., Ludwig, A.K., Hornung, S., Rotan, O., Horn, P.A., Epple, M., and Giebel, B. (2011). Characterisation of exosomes derived from human cells by nanoparticle tracking analysis and scanning electron microscopy. Colloids and Surfaces B, Biointerfaces *87*, 146-150.

Sprague, D.L., Elzey, B.D., Crist, S.A., Waldschmidt, T.J., Jensen, R.J., and Ratliff, T.L. (2008). Platelet-mediated modulation of adaptive immunity: unique delivery of CD154 signal by platelet-derived membrane vesicles. Blood *111*, 5028-5036.

Sreekumar, P.G., Kannan, R., Kitamura, M., Spee, C., Barron, E., Ryan, S.J., and Hinton, D.R. (2010). alphaB crystallin is apically secreted within exosomes by polarized human retinal pigment epithelium and provides neuroprotection to adjacent cells. PloS One *5*, e12578.

Stein, J.M., and Luzio, J.P. (1991). Ectocytosis caused by sublytic autologous complement attack on human neutrophils. The sorting of endogenous plasma-membrane proteins and lipids into shed vesicles. The Biochemical Journal *274 (Pt 2)*, 381-386.

Stoeck, A., Keller, S., Riedle, S., Sanderson, M.P., Runz, S., Le Naour, F., Gutwein, P., Ludwig, A., Rubinstein, E., and Altevogt, P. (2006). A role for exosomes in the constitutive and stimulus-induced ectodomain cleavage of L1 and CD44. The Biochemical Journal *393*, 609-618.

Subra, C., Laulagnier, K., Perret, B., and Record, M. (2007). Exosome lipidomics unravels lipid sorting at the level of multivesicular bodies. Biochimie *89*, 205-212.

Suh, D.H., Chang, K.Y., Son, H.C., Ryu, J.H., Lee, S.J., and Song, K.Y. (2007). Radiofrequency and 585-nm pulsed dye laser treatment of striae distensae: a report of 37 Asian patients. Dermatologic Surgery : Official Publication for American Society for Dermatologic Surgery [et al] *33*, 29-34.

Sun, D., Zhuang, X., Xiang, X., Liu, Y., Zhang, S., Liu, C., Barnes, S., Grizzle, W., Miller, D., and Zhang, H.G. (2010). A novel nanoparticle drug delivery system: the anti-inflammatory activity of curcumin is enhanced when encapsulated in exosomes. Molecular Therapy : the journal of the American Society of Gene Therapy *18*, 1606-1614.

Szajnik, M., Czystowska, M., Szczepanski, M.J., Mandapathil, M., and Whiteside, T.L. (2010). Tumor-derived microvesicles induce, expand and up-regulate biological activities of human regulatory T cells (Treg). PloS One *5*, e11469.

Taylor, D.D., Akyol, S., and Gercel-Taylor, C. (2006). Pregnancy-associated exosomes and their modulation of T cell signaling. Journal of Immunology *176*, 1534-1542.

Taylor, D.D., and Gercel-Taylor, C. (2008). MicroRNA signatures of tumor-derived exosomes as diagnostic biomarkers of ovarian cancer. Gynecologic Oncology *110*, 13-21.

Thery, C. (2011). Exosomes: secreted vesicles and intercellular communications. F1000 Biology Reports *3*, 15.

Thery, C., Amigorena, S., Raposo, G., and Clayton, A. (2006). Isolation and characterization of exosomes from cell culture supernatants and biological fluids. Current protocols in cell biology *Chapter 3*, Unit 3 22.

Thery, C., Boussac, M., Veron, P., Ricciardi-Castagnoli, P., Raposo, G., Garin, J., and Amigorena, S. (2001). Proteomic analysis of dendritic cell-derived exosomes: a secreted subcellular compartment distinct from apoptotic vesicles. Journal of Immunology *166*, 7309-7318.

Thery, C., Duban, L., Segura, E., Veron, P., Lantz, O., and Amigorena, S. (2002). Indirect activation of naive CD4+ T cells by dendritic cell-derived exosomes. Nature Immunology *3*, 1156-1162.

Thery, C., Ostrowski, M., and Segura, E. (2009). Membrane vesicles as conveyors of immune responses. Nature Reviews Immunology *9*, 581-593.

Tian, T., Wang, Y., Wang, H., Zhu, Z., and Xiao, Z. (2010). Visualizing of the cellular uptake and intracellular trafficking of exosomes by live-cell microscopy. Journal of Cellular Biochemistry *111*, 488-496.

Torregrosa Paredes, P., Esser, J., Admyre, C., Nord, M., Rahman, Q.K., Lukic, A., Radmark, O., Gronneberg, R., Grunewald, J., Eklund, A., *et al.* (2012). Bronchoalveolar lavage fluid exosomes contribute to cytokine and leukotriene production in allergic asthma. Allergy.

Trajkovic, K., Hsu, C., Chiantia, S., Rajendran, L., Wenzel, D., Wieland, F., Schwille, P., Brugger, B., and Simons, M. (2008). Ceramide triggers budding of exosome vesicles into multivesicular endosomes. Science *319*, 1244-1247.

Tullis, R.H., Duffin, R.P., Handley, H.H., Sodhi, P., Menon, J., Joyce, J.A., and Kher, V. (2009). Reduction of hepatitis C virus using lectin affinity plasmapheresis in dialysis patients. Blood Purification *27*, 64-69.

Valadi, H., Ekstrom, K., Bossios, A., Sjostrand, M., Lee, J.J., and Lotvall, J.O. (2007). Exosome-mediated transfer of mRNAs and microRNAs is a novel mechanism of genetic exchange between cells. Nature Cell Biology *9*, 654-659.

van den Boorn, J.G., Schlee, M., Coch, C., and Hartmann, G. (2011). SiRNA delivery with exosome nanoparticles. Nature Biotechnology *29*, 325-326.

van Niel, G., Raposo, G., Candalh, C., Boussac, M., Hershberg, R., Cerf-Bensussan, N., and Heyman, M. (2001). Intestinal epithelial cells secrete exosome-like vesicles. Gastroenterology *121*, 337-349.

Veron, P., Segura, E., Sugano, G., Amigorena, S., and Thery, C. (2005). Accumulation of MFG-E8/lactadherin on exosomes from immature dendritic cells. Blood cells, Molecules & Diseases *35*, 81-88.

Viaud, S., Ploix, S., Lapierre, V., Thery, C., Commere, P.H., Tramalloni, D., Gorrichon, K., Virault-Rocroy, P., Tursz, T., Lantz, O., *et al.* (2011). Updated technology to produce highly immunogenic dendritic cell-derived exosomes of clinical grade: a critical role of interferon-gamma. Journal of Immunotherapy *34*, 65-75.

Viaud, S., Terme, M., Flament, C., Taieb, J., Andre, F., Novault, S., Escudier, B., Robert, C., Caillat-Zucman, S., Tursz, T., *et al.* (2009). Dendritic cell-derived exosomes promote natural killer cell activation and proliferation: a role for NKG2D ligands and IL-15Ralpha. PloS One *4*, e4942.

Vidal, M., Sainte-Marie, J., Philippot, J.R., and Bienvenue, A. (1989). Asymmetric distribution of phospholipids in the membrane of vesicles released during in vitro maturation of guinea pig reticulocytes: evidence precluding a role for "aminophospholipid translocase". Journal of Cellular Physiology *140*, 455-462.

Wada, J., Onishi, H., Suzuki, H., Yamasaki, A., Nagai, S., Morisaki, T., and Katano, M. (2010). Surface-bound TGF-beta1 on effusion-derived exosomes participates in maintenance of number and suppressive function of regulatory T-cells in malignant effusions. Anticancer Research *30*, 3747-3757.

Wahlgren, J., Karlson, T.D., Brisslert, M., Vaziri Sani, F., Telemo, E., Sunnerhagen, P., and Valadi, H. (2012). Plasma exosomes can deliver exogenous short interfering RNA to monocytes and lymphocytes. Nucleic Acids Research.

Wang, J.S., Wang, F.B., Zhang, Q.G., Shen, Z.Z., and Shao, Z.M. (2008). Enhanced expression of Rab27A gene by breast cancer cells promoting invasiveness and the metastasis potential by secretion of insulin-like growth factor-II. Molecular Cancer Research : MCR *6*, 372-382.

Webber, J., Steadman, R., Mason, M.D., Tabi, Z., and Clayton, A. (2010). Cancer exosomes trigger fibroblast to myofibroblast differentiation. Cancer Research *70*, 9621-9630.

Wilson, S.M., Yip, R., Swing, D.A., O'Sullivan, T.N., Zhang, Y., Novak, E.K., Swank, R.T., Russell, L.B., Copeland, N.G., and Jenkins, N.A. (2000). A mutation in Rab27a causes the

vesicle transport defects observed in ashen mice. Proceedings of the National Academy of Sciences of the United States of America *97*, 7933-7938.

Winau, F., Weber, S., Sad, S., de Diego, J., Hoops, S.L., Breiden, B., Sandhoff, K., Brinkmann, V., Kaufmann, S.H., and Schaible, U.E. (2006). Apoptotic vesicles crossprime CD8 T cells and protect against tuberculosis. Immunity *24*, 105-117.

Wolfers, J., Lozier, A., Raposo, G., Regnault, A., Thery, C., Masurier, C., Flament, C., Pouzieux, S., Faure, F., Tursz, T., *et al.* (2001). Tumor-derived exosomes are a source of shared tumor rejection antigens for CTL cross-priming. Nature Medicine *7*, 297-303.

Wollert, T., and Hurley, J.H. (2010). Molecular mechanism of multivesicular body biogenesis by ESCRT complexes. Nature *464*, 864-869.

Wubbolts, R., Leckie, R.S., Veenhuizen, P.T., Schwarzmann, G., Mobius, W., Hoernschemeyer, J., Slot, J.W., Geuze, H.J., and Stoorvogel, W. (2003). Proteomic and biochemical analyses of human B cell-derived exosomes. Potential implications for their function and multivesicular body formation. The Journal of Biological Chemistry *278*, 10963-10972.

Xiang, X., Liu, Y., Zhuang, X., Zhang, S., Michalek, S., Taylor, D.D., Grizzle, W., and Zhang, H.G. (2010). TLR2-mediated expansion of MDSCs is dependent on the source of tumor exosomes. The American Journal of Pathology *177*, 1606-1610.

Xiang, X., Poliakov, A., Liu, C., Liu, Y., Deng, Z.B., Wang, J., Cheng, Z., Shah, S.V., Wang, G.J., Zhang, L., *et al.* (2009). Induction of myeloid-derived suppressor cells by tumor exosomes. International Journal of Cancer Journal International du Cancer *124*, 2621-2633.

Yang, C., Ruffner, M.A., Kim, S.H., and Robbins, P.D. (2012). Plasma-derived MHC class II(+) exosomes from tumor-bearing mice suppress tumor antigen-specific immune responses. European Journal of Immunology.

Yu, S., Liu, C., Su, K., Wang, J., Liu, Y., Zhang, L., Li, C., Cong, Y., Kimberly, R., Grizzle, W.E., *et al.* (2007). Tumor exosomes inhibit differentiation of bone marrow dendritic cells. Journal of Immunology *178*, 6867-6875.

Yu, X., Harris, S.L., and Levine, A.J. (2006). The regulation of exosome secretion: a novel function of the p53 protein. Cancer Research *66*, 4795-4801.

Zhang, H.G., Liu, C., Su, K., Yu, S., Zhang, L., Zhang, S., Wang, J., Cao, X., Grizzle, W., and Kimberly, R.P. (2006). A membrane form of TNF-alpha presented by exosomes delays T cell activation-induced cell death. Journal of Immunology *176*, 7385-7393.

Zhang, X., Wang, X., Zhu, H., Kranias, E.G., Tang, Y., Peng, T., Chang, J., and Fan, G.C. (2012). Hsp20 functions as a novel cardiokine in promoting angiogenesis via activation of VEGFR2. PloS One *7*, e32765.

Zhou, Q., Li, M., Wang, X., Li, Q., Wang, T., Zhu, Q., Zhou, X., Gao, X., and Li, X. (2012). Immune-related microRNAs are abundant in breast milk exosomes. International Journal of Biological Sciences *8*, 118-123.

Zhuang, X., Xiang, X., Grizzle, W., Sun, D., Zhang, S., Axtell, R.C., Ju, S., Mu, J., Zhang, L., Steinman, L., *et al.* (2011a). Treatment of brain inflammatory diseases by delivering exosome

encapsulated anti-inflammatory drugs from the nasal region to the brain. Molecular Therapy : the Journal of the American Society of Gene Therapy *19*, 1769-1779.

Zhuang, X., Xiang, X., Grizzle, W., Sun, D., Zhang, S., Axtell, R.C., Ju, S., Mu, J., Zhang, L., Steinman, L., *et al.* (2011b). Treatment of brain inflammatory diseases by delivering exosome encapsulated anti-inflammatory drugs from the nasal region to the brain. Molecular Therapy : the Journal of the American Society of Gene Therapy *19*, 1769-1779.

Zitvogel, L., Regnault, A., Lozier, A., Wolfers, J., Flament, C., Tenza, D., Ricciardi-Castagnoli, P., Raposo, G., and Amigorena, S. (1998). Eradication of established murine tumors using a novel cell-free vaccine: dendritic cell-derived exosomes. Nature Medicine *4*, 594-600.

Zomer, A., Vendrig, T., Hopmans, E.S., van Eijndhoven, M., Middeldorp, J.M., and Pegtel, D.M. (2010). Exosomes: Fit to deliver small RNA. Communicative & Integrative Biology *3*, 447-450.